University of Zagreb

FACULTY OF SCIENCE

DEPARTMENT OF BIOLOGY

Bruno Polak

THE ROLE OF BRIDGING FIBERS IN THE ARCHITECTURE OF THE METAPHASE MITOTIC SPINDLE

DOCTORAL THESIS

Zagreb, 2019.

Sveučilište u Zagrebu

PRIRODOSLOVNO-MATEMATIČKI FAKULTET

BIOLOŠKI ODSJEK

Bruno Polak

ULOGA PREMOŠĆUJUĆIH VLAKANA U ARHITEKTURI METAFAZNOGA DIOBENOGA VRETENA

DOKTORSKI RAD

Zagreb, 2019.

This work was done in laboratory of prof. dr. sc. Iva Tolić at Ruđer Bošković Institute, Zagreb, under supervision of prof. dr. sc. Iva Tolić. As a part of Postgraduate doctoral programme of Biology, this thesis is submitted for review to Department of Biology at Faculty of Science, University of Zagreb in order to achieve the academic degree doctor of biology.

Supervisor biography

Professor Iva Tolić was born and raised in Zagreb, Croatia. She graduated from studies in molecular biology at Faculty of Science, University of Zagreb, Croatia in 1996. She achieved the academic degree doctor of biology at University of Zagreb in 2002. After this, she worked as a postdoctoral fellow in Kopenhagen and Florence. From 2005 until 2014 she worked as a Research Group Leader at Max Planck Institute of Molecular Cell Biology and Genetics in Dresden, Germany. Her research areas are mitosis, mitotic spindle mechanics, microtubules, motor proteins and other processes in the cell that rely on cytoskeletal components and motor proteins. Professor Tolić has been entrusted to lead 11 research projects, has published 75 papers in peer-reviewed journals and has recieved and acknowledged 13 awards and achievements. As an invited oral presenter she has participated more than 70 conferences and workshops. She has participated in organizing scientific meetings and is successfully promoting her scientific research in media and social networks. Now professor Tolić is a Senior Scientist at Ruđer Bošković Institute in Zagreb were she continues successfully leading relevant research projects and students towards pursuing their master and doctoral qualifications.

Acknowledgements

First of all, I would like to express my greatest gratitude to my first supervisor, Iva Tolić for an opportunity to work on this exciting project. For everything I have learnt and all the precious experience that I gained during years under her supervision. For great support, understanding and freedom do organize experimental setups.

Biggest thanks go to my family, my brother Robert, mom Vesna, dad Branko and uncle Boris. In memory of my grandma Zdenka, I am grateful for her love. Special thanks go to my love..

Huge thanks to my godparents Lav and Lidija Kalda for great laughs, advice and support.

Really amazing thanks go to best lab mates and friends that we have become, Barbara Kuzmić, Kruno Vukušić, Renata Buđa, Patrik Risteski, Juraj Simunić, Ivana Šarić, Sonja Lesjak, Jelena Martinčić, Mihaela Jagrić, Ana Milas and Luka Bačić. For great laughs, help, close colaboration and advice. With that team I would always work.

Big thanks to professor Nenad Pavin and his group, Maja Novak, Marcel Prelogović, Agneza Bosilj, Ivana Ban and Arian Ivec for great discussions and advice.

Thanks to Marieta Kralj, Marko Marjanović, Katja Ester and Igor Weber, for help with a good start with experiments in Zagreb. Thanks to Marin Barišić and Helder Maiato (Institute for Molecular Cell Biology, University of Porto, Portugal) for human U2OS cells. Thanks to Linda Wordeman for providing us with mRFP-CENP-B plasmid.

Big thanks go to all the professors at Faculty of Science in Zagreb who took part in developing my approach and mindset for the knowledge, research and passion towards science.

Last, but not least, thanks to all my beautiful friends for amazing time and memories.

University of Zagreb
Faculty of Science
Department of Biology

Doctoral thesis

The role of bridging fibers in the architecture of the metaphase mitotic spindle

Bruno Polak
Ruđer Bošković Institute

Mitosis is a fundamental process during which the genetic material is transferred to daughter cells and is orchestrated by the mitotic spindle. Between two opposite spindle poles microtubules form bundles that interact with chromosomes. Bundles that bind to kinetochores on the chromosome are called kinetochore fibers, whilst certain microtubules form antiparallel overlap bundles in the central part of the spindle. With this research localization and distribution of antiparallel overlap bundles in metaphase and the spatial organization of these bundles and kinetochore fibers possess will be investigated. By using confocal microscope whole metaphase spindles will be imaged which will enable to determine the number of overlap regions and their association with kinetochore fibers. Further work will be focused on understanding the spatial organization of the whole mitotic spindle. Used approach revealed that nearly all antiparallel fibers are linked with kinetochore fibers and that human mitotic spindle is a chiral structure.

(94 pages, 42 figures, 2 tables, 103 references, original in english)

Key words: mitosis, mitotic spindle, metaphase, microtubule, bridging fiber

Supervisor: Dr. sc. Iva Tolić, Prof.

Reviewers: Dr. sc. Inga Marijanović, Assoc. Prof.
Dr. sc. Juraj Simunić, Assist. Prof.
Dr. sc. Marin Barišić, Assoc. Prof.

Sveučilište u Zagrebu
Prirodoslovno-matematički fakultet
Biološki odsjek

Doktorski rad

Uloga premošćujućih vlakana u arhitekturi metafaznoga diobenoga vretena

Bruno Polak
Institut Ruđer Bošković

Mitoza je fundamentalan process kojim se genetička informacija prenosi na stanice kćeri, a struktura koja upravlja ovim procesom je diobeno vreteno, Između dva nasuprotna pola vretena pružaju se vlakna mikrotubula koja stvaraju interakcije sa kromosomima. Vlakna koja se vežu za kinetohore na kromosomima nazivaju se kinetohorna vlakna. Neki od ostalih svežnjeva stvaraju antiparalelne preklapajuće regije u centralnom djelu diobenog vretena. U ovom radu ispitati će se lokalizacija i zastupljenost antiparalelnih preklapajućih regija u metafazi te će se istražiti prostorna organizacija navedenih i kinethornih vlakana. Uz pomoć metode konfokalne mikroskopije snimati će se cijela vretena što će omogućiti utvrđivanje broja antiparalelnih svežnjeva, a odgovoriti će na pitanje njihove povezanosti sa kinetohornim vlaknima. Daljnji rad biti će usmjeren na razumijevanje prostorne organizacije metafaznog diobenog vretena. Uz primjenu navedenog pristupa, otkriveno je da su antiparalelna vlakna povezana sa kinetohornim vlaknima te da je diobeno vreteno u ljudskim stanicama kiralna struktura.

(94 stranice, 42 slike, 2 tablice, 103 reference, jezik izvornika: engleski)

Ključne riječi: mitoza, diobeno vreteno, metafaza, mikrotubuli, premošćujuća vlakna

Voditelj: Dr. sc. Iva Tolić, prof.

Ocjenitelji: Dr. sc. Inga Marijanović, izv. prof.
Dr. sc. Juraj Simunić, doc.
Dr. sc. Marin Barišić, izv. prof.

Contents

1 INTRODUCTION

Mitosis is a process during which duplicated chromosomes get separated and positioned into newly formed daughter cell. It is a basic process responsible for transferring genetic information to offspring and for continuation of life. The successfulness of the process relies on proper assembly of a functional micromachinery called mitotic spindle. Its main components are microtubules that form tubes and bundles with defined orientation and other proteins that interact with them. The thickest and most stable microtubule bundles in the spindle are kinetochore fibers (k-fibers). A functional spindle will assemble as the duplicated chromosomes are incorporated into the spindle with a goal to properly attach and orient these structures that contain two copies of the whole genetic information. K-fibers will form an end-on attachment with the complex protein assembly on the centromeric region of the chromosome called kinetochore. Properly attached and oriented chromosomes will in metaphase of mitosis contain two sister kinetochores attached to opposite spindle poles via two sister k-fibers. Besides k-fibers certain microtubules will form antiparallel overlap bundles in the spindle midzone [1]. These bundles contain the passive crosslinker protein called Protein Regulator of Cytokinesis 1 (PRC1) which stabilizes antiparallel interdigitating microtubules within the overlap bundles. It was recently shown that an overlap fiber links outermost k-fibers and balances forces on the periphery of the spindle. In experimental setup with laser ablation coupled to a confocal microscope, it was revealed that this bundle is associated with sister kinetochores in metaphase. This bundle was named bridging fiber and it is antiparallel as it contains passive crosslinker PRC1 [2]. Even though different aspects of metaphase have been extensively studied, it is not known what the abundance of antiparallel bundles in this phase is and what fraction contains the PRC1 protein. The new finding on bridging microtubules and their connection to peripheral k-fibers opens new questions regarding structural organization and architecture of the mitotic spindle. In order to understand the proper performance of the spindle it is important to explore how the chromosomes are incorporated in the spindle and what are the structural elements specific for the metaphase state. The question is whether other PRC1-containing fibers and what fraction of these fibers is associated with sister kinetochores in other positions throughout the whole spindle. By using a confocal microscope whole metaphase spindle in different cell lines and conditions will be imaged. This approach provides information on the distribution of bridging fibers in metaphase. The goal of the research is to describe architecture

and organization of the whole metaphase spindles. Once the fraction of bridging fibers throughout spindle is determined, the spatial organization of bundles in the spindle in metaphase will be explored. Our hypothesis is that majority of overlap fibers are linked to corresponding sister k-fibers and that these bundles possess specific spatial organization not yet observed.

The model that will be used is a human cell line U2OS (osteosarcoma, female) permanently transfected and stabilized with proteins CENP-A-GFP (kinetochore complex), mCherry-α-tubulin and photoactivatable (PA)-GFP-tubulin as well as the human cell lines HeLa (cervix cancer, female) with certain labeled proteins of interest (tubulin in microtubules, crosslinker PRC1, kinetochore protein CENP-B).

HeLa cells will be transfected by electroporation using the high-viability program. Cells will be transfected with mRFP-CENP-B plasmid to visualize kinetochores. Prior to imaging or following the transfection cells will be seeded in glass bottom microscopy dishes and imaged by using laser scanning confocal microscopes oil immersion objective heated with an objective integrated heater system. For excitation of GFP and mCherry fluorescence, a 488 and a 561 nm diode laser line are used, respectively. Z-stacks will be acquired so that the whole spindle is covered with confocal images with a 0.5 μm spacing between individual images of spindles. Measurements will be performed in ImageJ (National Institutes of Health, Bethesda, MD, USA), whilst statistical analysis will be performed in MatLab (MathWorks, Natick, USA), SciDavis (Free Software Foundation Inc., Boston, MA, USA) and R studio (R Foundation for Statistical Computing, Vienna, Austria, 2016).

First step is to image cells with labeled PRC1 protein which will be transfected with a plasmid (mRFP-CENP-B) to visualize kinetochores. This will enable to determine the number of PRC1-labeled bundles in the whole individual spindle which will then be correlated to the number of sister kinetochore pairs per spindle in HeLa cells with variable number of chromosomes. One idea is to image spindles with their long axes oriented vertically with respect to the imaging plane (vertical spindles). This experiment with a time component will provide insights into dynamics between PRC1-labeled bundle and a kinetochore in its vicinity which will give insights into their association. Labelling of endogenous PRC1 protein by using immunocytochemistry method will determine its spatiotemporal localization regardless of overexpression due to transfection for green fluorescent protein (GFP) labelling. Once these questions are answered, description will follow on how mutually connected kinetochore and bridging fibers are organized in one structural element

in the spindle. For this purpose, vertical spindles will be imaged where fluorescently tagged proteins of interest will appear as spots in one individual confocal image. In this experiment fluorescently tagged tubulin will be used (to visualize parallel microtubules in the k-fibers) as well as fluorescently tagged PRC1 (to visualize antiparallel microtubules in the bridging fibers). This will provide insights into differences and similarities in 3D organization between these bundles. Acquired images will cover whole spindle width and length which will enable us to reconstruct the spatial organization of these bundles. One additional idea is to image the spindles with their long axes oriented horizontally with respect to the imaging plane and to transform them into vertical projections using R programming language. Once the organization of these bundles is determined along the spindle long axis, next step is to find key proteins that contribute to their level of spatial organization. Since today there are commercially available drugs that specifically inhibit certain proteins in the spindle, they will be used to determine which proteins are important for the spatial architecture of the spindle. All acquired images need to be carefully analyzed by using ImageJ. Individual spots that correspond to fluorescently labelled proteins of interest can be tracked in this program and their coordinates (x, y positions) will be marked from one image to another in a set of confocal images that cover whole individual spindles. To get statistically significant results many number of cells will be imaged in each experimental setup and the results will be shown graphically.

2 OVERVIEW OF RESEARCH

2.1 THE CELL – A BUILDING BLOCK OF LIFE

A living system is characterized by the ability to catalyze metabolic processes and the ability to transfer genetic information to its offspring. Such a system is specifically organized to comprise structures that enable it to grow, develop and evolve. A single unit of life is a cell which can live as a fully functional organism or as the simplest component of a multicellular organism. The components that characterize a system as being alive are enclosed in a membrane which is also a place where communication between cell's interior and exterior takes place. From cell's membrane through cytoskeleton and organelles, nucleus and genetic material comprised within, there are hundreds of signaling pathways that orchestrate the complex life of a cell. The first person who described the cell as a basic unit of life was Robert Hook, an architect, natural philosopher and scientist. He first used the term in 1665, while looking at thin slices of cork (Figure 1a) [3]. His observations were soon extended to wood and plant tissue, as well as to fly's eye.

Possibly the most remarkable characteristic of a living organism is to create a new one by transferring copies of its genes into its offspring. The simplest way to achieve this fundamental task is to duplicate the genetic information, separate it equally and eventually to divide the cytoplasm to create two genetically identical daughter cells. In single cell organisms this is a process called mitosis and it is a form of asexual reproduction which takes place in bacteria, protists, algae, fungi and plants. Somatic cells of multicellular organisms (fungi, plants, animals) undergo mitosis to produce more cells during processes of growth and repair. Already in 1880s Walther Flemming drew in detail his observations on mitosis (Figure 1b) [4]. His study and interpretation of events in the mitosis laid foundations for further research on mitotic cell division (Figure 1c).

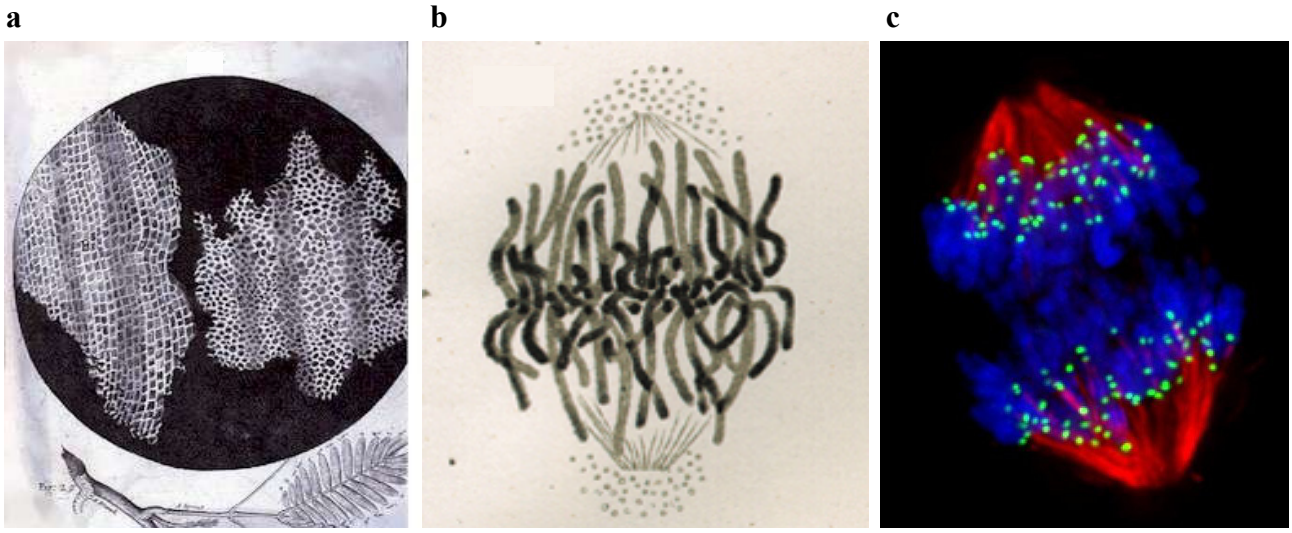

Figure 1. View on the cell and the mitotic division: a) Hook's sample of thin cork slice shows first insight into cellular organization [3]. b) Drawing of mitotic division as seen by Flemming with major components (chromosomes and microtubules) of the spindle [4]. c) Image of a HeLa cell (kinetochore protein, green; tubulin, microtubules, red; DNA, chromosomes, blue) as seen under confocal microscope. The cell is in anaphase stage of mitosis. Image is a property of Andrew McAinsh group, acquired by Phillip Auckland on API Deltavision Elite DV1 wide field microscope.

2.1.1 One day in life of a cell

A cell takes nutrients from its surrounding in a variant of feeding and in that way it grows and matures. As the cell matures it eventually becomes prepared to produce two new genetically identical daughter cells. The scenario in which the symmetric distribution of chromosomes in two daughter cells occurs is complex and intriguing. During ~24 hours, the cell is going through series of events known as the cell cycle. It is roughly divided in interphase and mitosis (M phase), (Figure 2). As interphase is a period between two mitotic divisions, during this time cell recovers from the recent division of cytoplasm, reorganizes its interior, grows and prepares for the next cycle of mitosis. It is divided in G1, S and G2 phase, during which cell doubles its mass of proteins and organelles. " G" in G1 and G2 stands for gap phase and it gives the cell time to feed, grow and to control the accuracy of ongoing events. In S phase that lasts for 10-12 hours, the cell's genetic material is being duplicated, so that it could be equally distributed to new daughter cells in M

phase. During G2 phase certain events are preparing a cells interior for division, as is for example the process of centrosome duplication. At this point it is also possible for cell to enter the, so called G0 phase, which is a resting period that can last for days, weeks or even years before the cell resumes the cell cycle [1].

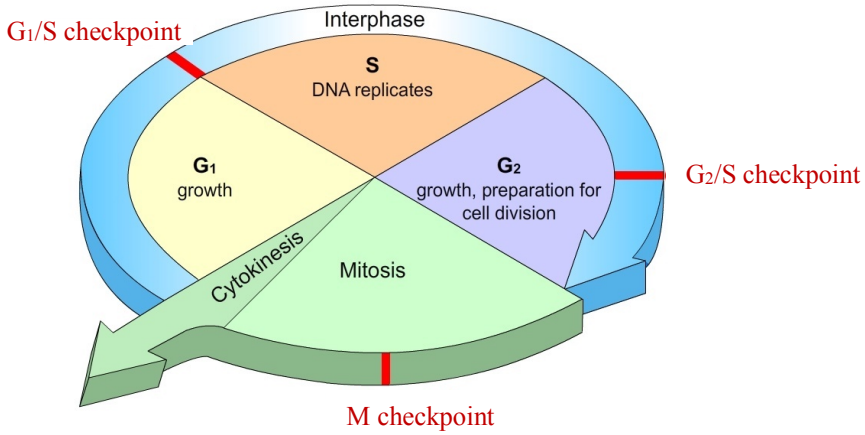

Figure 2. Scheme of a 24-hour cell cycle with pointed G1, S, G2 (interphase) and M phase (mitosis). Mitosis occupies approximately an hour of the complete cycle. Copyright 2013 Ricochet Creative Productions, LLC.

When the cell becomes ready to undergo dramatic reorganization of its interior it will proceed to the M phase. Depending on the movement of chromosomes and behavior of the mitotic spindle, it is as well divided in distinct subphases (Figure 3). The process of mitosis relies on certain complex structures that are newly assembled or disassembled on its onset while others are degraded or assembled when mitosis comes to an end. During prophase proteins called condensins regulate condensation of replicated DNA strands in the nucleus. Thus condensed into structures called chromosomes, the DNA becomes compact and its length is reduced by more than 1000-fold [5]. Duplicated DNA forms two equal halves of the chromosome called chromatids with central gap between them called centromere. Possibly the most dramatic change at the onset of mitosis is the reorganization of microtubules. In interphase these structures act as cytoskeletal components that support the cells interior and act as tracks for intracellular repositioning of proteins and organelles. As the nuclear envelope breaks down in prophase of opened mitosis, basically the entire pool of microtubules is rearranged to build up the mitotic spindle. Alternatively, in closed

mitosis the nuclear envelope stays intact as is the case in for example yeast cells. The spindle is a micromachine that comprises hundreds of proteins involved in its dynamics and stability. This structure will attach and precisely integrate condensed chromosomes and orchestrate the process towards their separation throughout mitosis until it disassembles as mitosis comes to an end. After the nuclear envelope breakdown, the mitotic spindle will begin to form between duplicated centrosomes. The main structural elements of the mitotic spindle are microtubules which form hollow polar tubes built by tubulin subunits. Prior to nuclear envelope breakdown and nucleation of spindle microtubules, the complex protein assembly called kinetochore forms at specific spots on the chromosome. It is assembled on highly condensed chromosomes at both sides of the centromeric region and is the most specific spot of interaction with microtubules of the spindle. Microtubules will interact in many different ways with the chromosomes but the goal is to achieve a specific interaction between kinetochore and the plus ends of microtubules. Once this connection is established, the active movement of chromosomes can begin. The following step of mitosis called metaphase is directed to achieve the proper orientation and alignment of attached chromosomes. Metaphase becomes stable when all chromosomes are aligned in the equatorial plane of the mitotic spindle halfway between two poles of the spindle. Here, two sister chromatids of a chromosome are held tightly bound by multisubunit protein complexes called cohesins. Once cohesins become degraded, sister chromatids can separate in a synchronized manner during the following anaphase. First, during anaphase A sister chromatids are pulled away from each other towards two poles of the spindle. Kinetochore bound microtubules shorten, and in subsequent anaphase B the distance between two spindle poles begins to increase and chromatids are pulled further away. As separating chromosomes meet the spindle poles, they already begin to de-condense marking the telophase stage of mitosis. Nuclear envelope now starts to reassemble around separated sets of chromosomes. As the fundamental part of the process is finished, the cytoplasm needs to be divided as well. On two sides of the former metaphase plate the contractile ring is formed and finally the process comes to completion as the narrowing of the contractile ring separates the cytoplasm (Figure 3) [1]. At this point, reassembled nuclear envelopes encircle daughter chromosomes and these two new cells can now begin to feed and grow until they are ready to start a new cycle of mitosis.

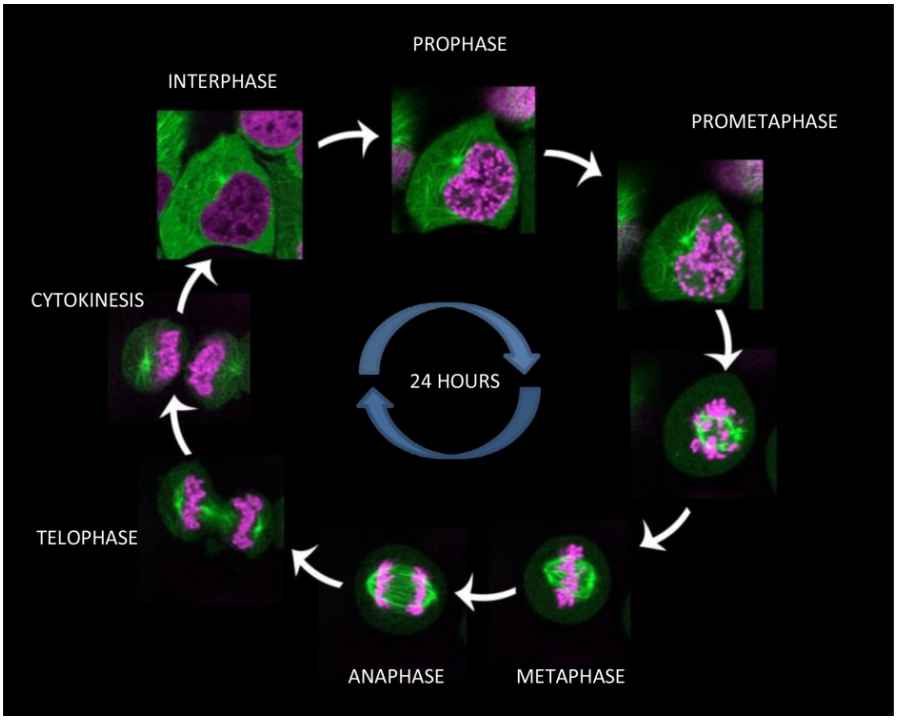

Figure 3. Live cell images summarizing mitotic stages (Zeiss LSM 710 NLO inverted laser scanning confocal microscope, Zeiss, Germany). Starting from interphase, stages in mitosis are shown in human HeLa cell (cervical cancer) expressing H2B-mCherry (chromosomes, magenta) and GFP-tubulin (microtubules, green;): condensation of chromosomes (prophase); nuclear envelope breakdown and attachment of chromosomes to microtubules of the spindle (prometaphase); alignment of chromosomes in equatorial plane of the spindle (metaphase); segregation of chromosomes (anaphase), narrowing of contractile ring (telophase); division of cytoplasms (cytokinesis).

2.1.2 Control of accuracy - cell cycle checkpoints

For the newly formed daughter cells it is crucial to carry out the same process with as less errors as possible. For the continuation of life, it is vital to ensure genetic duplication and transfer with as less unfavorable error as possible. To help with accuracy and viability, the cell has evolved a complex signaling network that regulates and controls a pause or progression through the process itself. Regulation of the cell cycle is evolutionary well preserved amongst all eukaryotic cells. In yeast cells cdc genes (cell-division-cycle genes) are crucial in passing through the control steps of the cell cycle [6]. The control steps function as a clock, which can stop so as to give time for an appropriate machinery to be fixed or to fix the encountered error. Basically, this system delays certain sequential steps of the cycle, if necessary, and is regulated by means of negative intracellular signals. At the heart of the cell cycle control system is a family of protein kinases known as cyclin dependent kinases (CDKs), which are present in a cell in constant levels but are cyclically active. By phosphorylating certain intracellular proteins, they regulate DNA replication, mitosis and cytokinesis- major events in the cell cycle [1]. CDKs are regulated by cyclins, which can bind to CDKs and activate them. Since the cyclins themselves undergo cyclic synthesis and degradation, CDKs' activity depends on the abundance of cyclins in the cell. There are 3 described checkpoints that control the accuracy of fundamental events (Figure 4). In G1 checkpoint, also known as the restriction checkpoint, a control mechanism ensures that the conditions are favorable for cell to enter the S phase. Since G1 is the first phase after cytokinesis, this control step checks how the cell is feeling and investigates when is the right time to continue the cycle. If conditions are favorable, a cell can proceed past restriction point and begin with the duplication of DNA, or it can, alternatively, enter the G0 quiescent state, thus postponing S phase. During G2 checkpoint, just finished DNA synthesis is checked for damage and errors that could have occurred during DNA replication. At this point a cell can either enter mitotic division or delay it. The final checkpoint, called the spindle checkpoint, occurs in metaphase to ensure that chromosomes are properly attached to microtubules of the mitotic spindle and aligned in the metaphase plate [7]. This checkpoint is the last barrier for chromosomes to get separated in the following anaphase. Functionality of these control steps makes the processes of chromosome segregation, cytoplasm division and production of healthy new cells the basis of continuation of life.

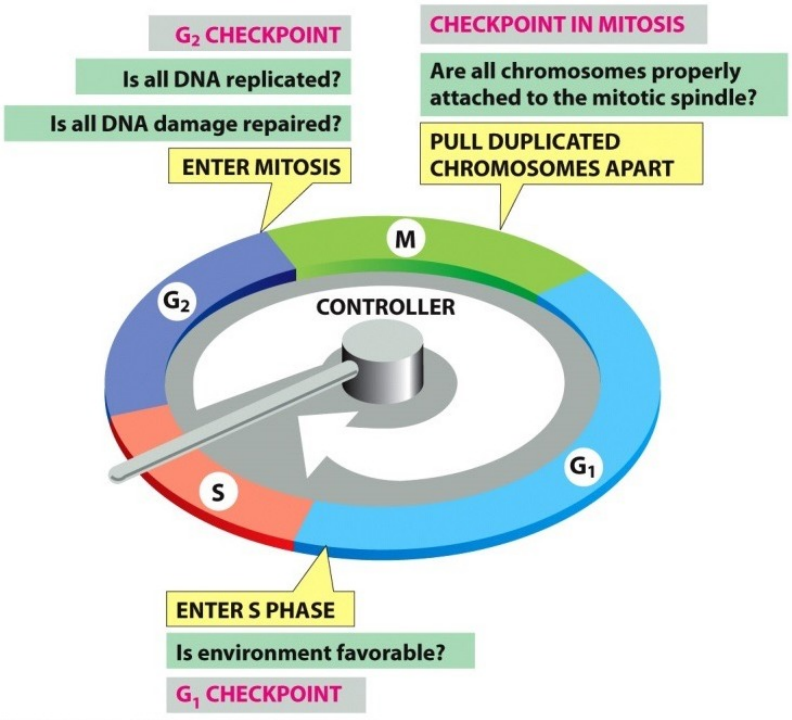

Figure 4. Restriction points of a cell cycle with pointed out precise timing of major accuracy checkpoints. G1 checkpoint makes sure that the conditions are appropriate for DNA duplication. G2 checkpoint checks whether DNA was duplicated without errors. Mitotic spindle checkpoint (checkpoint in mitosis) ensures that all chromosomes are properly attached to k-fibers and oriented in a way that they could be pulled to centers of new daughter cells at the end of mitosis [Oregonstate.edu].

2.2 BUILDING BLOCKS OF THE MITOTIC SPINDLE

Mitotic spindle is a machine, it is on a cellular level a micro-building assembled accurately with all the individual components having a precise time and place of action. Some of those will be key to stability of the spindle while at the same time others will be crucial for its dynamic behavior. These properties of the spindle are established by timely precise protein activation, recruitment and association or dissociation with the spindle.

2.2.1 Microtubule organizing centers - spindle strongholds

The main structural elements of the mitotic spindle are microtubules. They form long or short hollow polar tubes with well-defined orientation of minus and plus ends. While plus ends are free to form interactions with non-spindle elements like kinetochores of the chromosome or the cell cortex, minus ends are embedded at specific spots within the spindle. These spots are mostly microtubule organizing centers (MTOCs) which anchor microtubule minus ends. Not only do these spots act as anchors but also, they nucleate new microtubules that grow with their plus ends oriented away from the nucleation site. Main MTOCs in the spindle are centrosomes which nucleate majority of microtubules from prophase on. Centrosomes are composed of two centrioles and associated pericentriolar matrix (Figure 5a). They are duplicated during G2 phase of interphase in a process of centrosome cycle. Once duplicated, centrosomes move to opposite sides of the nucleus where they form two poles of the future spindle (Figure 5b). As the nuclear envelope breaks down in an opened mitosis they start nucleating microtubules in all directions. Microtubules that meet and interact mutually between centrosomes are the ones that will lead the formation and maturation of the spindle. Centrosomes and associated components determine the geometry of microtubules arrays throughout the cell cycle, and thus influence cell shape, polarity and motility, as well as spindle formation, chromosome segregation and cell division [8]. All centrosomes contain a structured core to which more than 50 copies of γ-tubulin ring complex (γ-TuRC) are connected [5]. Each γ-TuRC contains 13 copies of γ-isoform of tubulin that define the position of microtubule nucleation, the polar orientation of the polymer, and the lattice into which tubulin assembles [9].

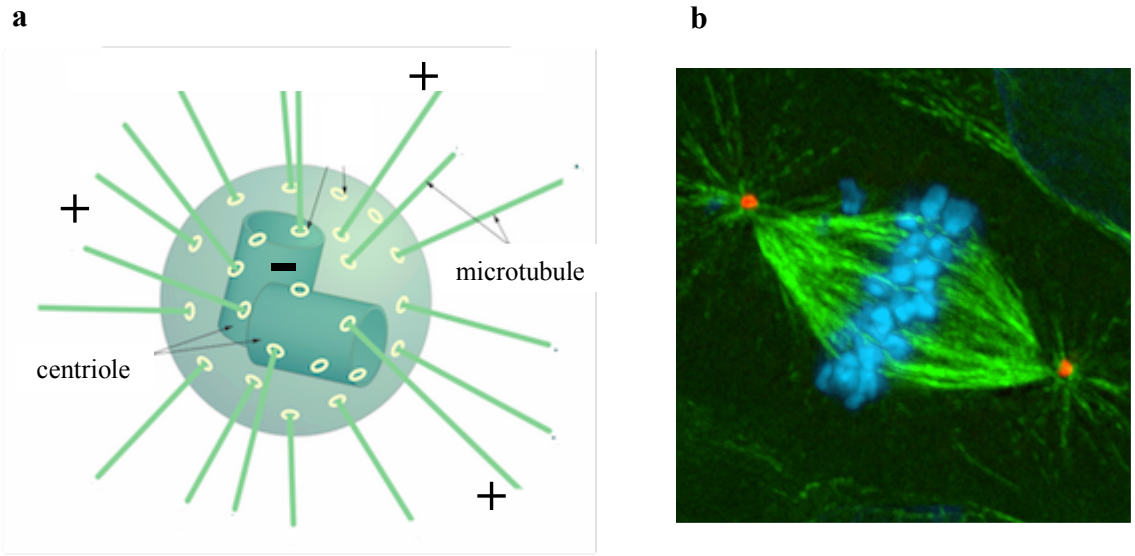

Figure 5. a) Schematic representation of a centrosome with its major components: centrioles as the central structure, light green circle as pericentriolar matrix and thin rods as newly nucleated microtubules [Study.com]. Minus and pluses represent – ends of microtubules embedded in the centrosome whilst + represents growing free ends. b) Confocal image of the mitotic cell in metaphase with centrosomes labeled red, microtubules green and chromosomes blue. Centrosomes in red represent two poles of the spindle [10].

2.2.2 Microtubules - growing versus shrinking stems

As microtubules have their beginning at described spots they will form tubes as subunits are added in a defined structural order (Figure 6a). The tubulin subunit of microtubules is a heterodimer formed from two closely related globular proteins, α and β tubulin. They are tightly bound together by non-covalent bonds thus forming microtubules as long, hollow tubes with an outer diameter of 25 nm. This cylindrical structure is built from 13 protofilaments, each composed of alternating α tubulin and β tubulin molecules [1]. Both these monomers can bind one molecule of GTP. When bound to α tubulin, GTP will never be exchanged or hydrolyzed, while β tubulin bound GTP can undergo hydrolysis to produce GDP. This hydrolysis is important for microtubule dynamics (Figure 6b). Both in interphase and mitosis microtubules often switch between phases of growth and shrinkage. This remarkable property was discovered in 1984 when Tim Mitchison and Marc Kirschner [11] deduced that microtubules switch from growth to shrinkage when they

lose their GTP caps: ”We report here that microtubules in vitro coexist in growing and shrinking populations which interconvert rather infrequently”. The dynamic instability is a general property of microtubules and may be fundamental in explaining cellular microtubule organization. As described above, they possess intrinsic polarity with their minus ends embedded in MTOC, e.g. centrosome, while the (free) plus end is more dynamic and switches fast between growth and shrinkage, a.k.a. catastrophe (Figure 6b). Microtubules grow when αβ tubulin collides with the end of a protofilament and forms a non-covalent bond. These collisions occur more frequently when the tubulin concentration is higher, and thus the growth rate increases linearly with more tubulin [12]. Microtubule ends with bound GTP are stable and polymerize, whereas ends containing GDP are unstable and depolymerize. In addition, there is a possibility for microtubules to switch from shrinkage to growth in a process known as rescue (Figure 6b). Driving these processes are a host of microtubule-associated proteins (MAPs) that make microtubules grow faster, shrink slower, undergo catastrophe more often, and so on [13]. This, so called, dynamic instability is particularly frequent within microtubule populations that build up the mitotic spindle. Microtubules of the mitotic spindle are more dynamic than ones present in interphase, with complete exchange of spindle microtubules and soluble subunits occurring within seconds [14]. Already in 1950s Shinya Inoué [15] observed that spindles are made of aligned protein fibers that exist in rapid dynamic equilibrium with a pool of unassembled subunits. He proposed that spindle fiber disassembly generates force to move chromosomes. Indeed, once the nuclear envelope breaks down in pro-metaphase, chromosomes become free to make contact with the growing microtubules via their kinetochores. These, kinetochore bound microtubules are called k-fibers and they generate forces on chromosomes throughout mitosis. During prophase, these forces direct the alignment of chromosomes to the metaphase plate and in anaphase they are directed to segregate chromosomes and pull them towards each pole of the spindle. There is also a way to modify the microtubule lattice which is important for microtubule behavior. This group of reversible alterations is called posttranslational modifications and has a role in structural variations of all newly synthesized proteins. These modifications affect protein’s functional properties and for tubulin they occur on α/β heterodimers of already polymerized stable microtubules. In this way dynamics, stability, distribution of microtubule populations in the spindle and interactions of microtubules with MAPS are finely tuned. For these variations some important modifications include polyamination, acetylation, methylation, phosphorylation and (de)tyrosination [1].

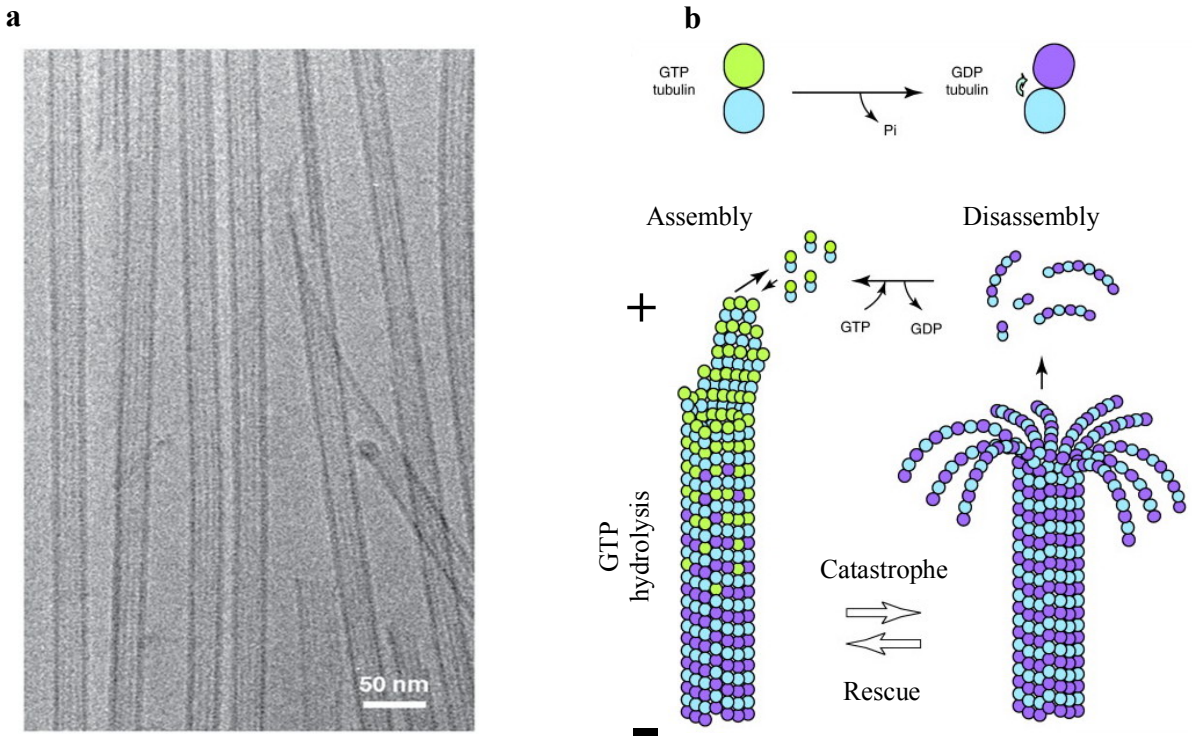

Figure 6. a) Microtubules as seen under electron microscope where their rod-like structure can be observed [18]. b) Scheme of microtubules with depicted dynamic property. Exchange of GDP/GTP tubulin can be observed as process that determines switches between growth and shrinkage [17].

2.2.3 Kinetochores - sticky links

As the spindle forms in a highly dynamic and directed manner, chromosomes have to be captured and integrated in the spindle. To ensure specific and tight interaction between chromosomes and microtubules, large sticky protein complexes called kinetochores are formed on centromeric regions of chromosomes during late prophase. Thus, one chromosome with two sister chromatids will contain two sister kinetochores on opposite sides of the centromeric region (Figure 7a). For high-fidelity chromosome segregation, kinetochores must be correctly captured by microtubules in order to begin with the anaphase onset. Transmission electron microscopy revealed the structure of the vertebrate kinetochore (Figure 7b). It appears as a trilaminar stack of plates that is situated on opposite sides of the centromeric heterochromatin of the mitotic

chromosome [18]. The properly assembled kinetochore contains two main regions. The inner one is tightly associated with the centromeric DNA and appears like a discrete heterochromatin domain throughout the cell cycle. The outer, highly dynamic plate is the site of interaction with the growing microtubules. In vertebrate cells, it contains about 20 anchoring sites for plus ends of growing microtubules of the spindle. Besides this basic function, kinetochores can also act as nucleation sites of microtubules, both on isolated mitotic human chromosomes [19] as well as in vivo [20; 21]. These kinetochore-nucleated microtubules may speed up kinetochore capture and the process of spindle assembly [22; 23]. During prometaphase, microtubules nucleated at centrosomes grow and shrink rapidly until they encounter and bind to kinetochore. Once this connection occurs on both sister kinetochores (on two sides of centromeric region), which links chromosome to opposite spindle poles, the bipolar orientation of a chromosome is established. This form of orientation is crucial for establishment of forces that will act on chromosomes throughout the following events in mitosis.

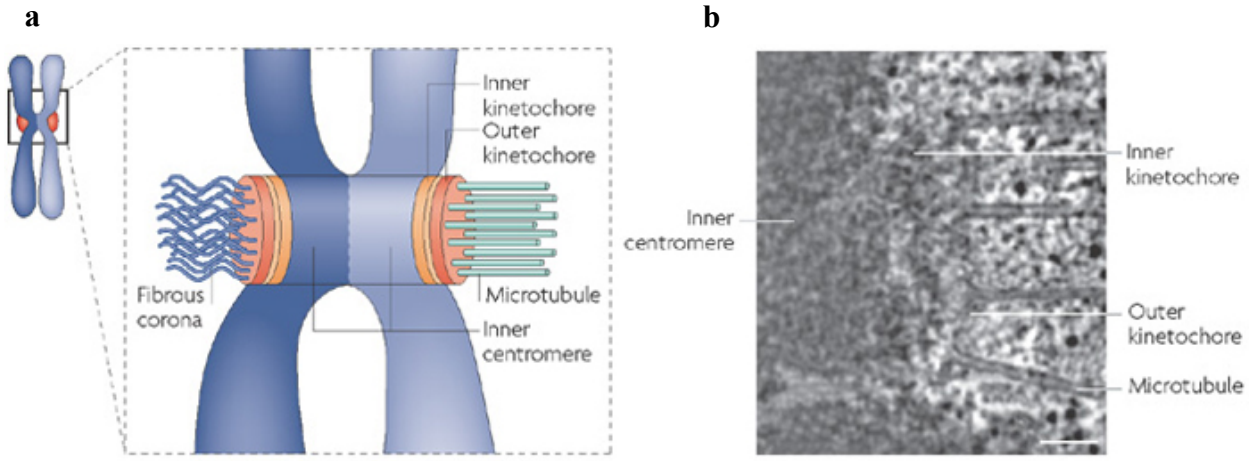

Figure 7. a) Scheme of a chromosome with two chromatids as seen in M phase of the cell cycle. Kinetochore is positioned on each side of the centromeric region with inner layer connected to chromatin fibrils and outer layer that both nucleates and binds microtubules. b) Electron microscope image of a kinetochore with shown layers and attached microtubules [24].

2.2.4 Microtubule Associated proteins - supporting players

Besides described core building elements of the spindle, its dynamic properties and stability depend heavily on microtubule associated proteins (MAPs) and motor proteins. These are the elements that tune the assembly, dynamics and stability of the spindle to direct its performance and functionality. MAPs act as supporting structural elements of microtubules and mitotic spindle as a whole. Whilst certain MAPs stabilize the assembled polymer, others mediate the interaction between individual microtubules in a bundle as well as between already established microtubule bundles. In that way they act as cross-linkers that hold microtubules in close vicinity. By precisely regulated time and place for microtubule affinity, they support the basic composition of different bundle populations in the spindle. They also mediate interaction of microtubules with other components of the spindle and other components of the cytoskeleton. Non-motor proteins promote the formation and maintenance of mitotic spindles through diverse mechanisms including the nucleation and organization of microtubules, influence on motor function, and regulation of cell cycle control. In general, these proteins are relatively large, and many are only expressed during G2/M phase of the cell cycle [25]. For example, NuMa binds microtubules directly and mechanically crosslinks microtubules at spindle poles [26]. Some non-motor cross-linking proteins like PRC1 stabilize antiparallel microtubule bundles in the spindle midzone thus maintaining overlap interdigitating regions. Others act as end-binding proteins that control microtubule dynamics and persistent microtubule growth. Further on, non-motor proteins can interact with motor proteins. In some circumstances, the interaction is direct and the non-motor protein controls the function of the motor protein [26].

2.2.4.1 Protein Regulator of Cytokinesis 1 - central stabilizer

PRC1 is a conserved non-motor cross-linking protein localized in the antiparallel overlaps of microtubules *in vitro* [27, 28, 29] and of the spindle midzone [30, 31, 32, 33, 34] where it plays an essential role in regulating its formation and cytokinesis [35]. This human CDK substrate protein was discovered in 1998 by using an *in vitro* phosphorylation screening method. With that research it was shown that its expression is finely regulated during the cell cycle with peaks of expression in mitosis. At that time, it was shown that PRC1 is phosphorylated *in vivo* in a cell cycle-regulated manner at cyclin-Cdk phosphorylation sites. Indirect immunofluorescence staining demonstrated

that PRC1 becomes associated with mitotic spindle midzone in anaphase and to contractile ring during cytokinesis. It was already then proposed that PRC1 may act as a crucial regulator involved in cytokinesis and cell cycle progression [30]. At that point Ase1 (anaphase spindle elongation 1), an orthologue of PRC1 found in budding yeast was already known [36]. A homology search of GenBank database revealed 57% similarity in their central region with no other significant sequence homology. Similarity between those two proteins led to investigation of the levels of its expression depending on the phase of the cell cycle. Synchronization experiments in HeLa cells revealed high levels of PRC1 during S to G2/M transition (mitotic entry), with dramatic decline at the entry to G1 phase (mitotic exit). Besides Ase1, orthologues of PRC1 with conserved function include SPD-1 (spindle defective 1) in *Caenorhabditis elegans* [37], Feo (Fascetto) in *Drosophila melanogaster* [38], and MAP65 (microtubule-associated protein 65) in plants [39], all of which fall in a conserved family of non-motor microtubule-associated proteins (MAPs).

Full-length PRC1 cDNA encodes a protein containing 620 amino acids with a size of 71 kDa. The NH_2-terminal region is largely α-helical with multiple coiled-coil motifs and COOH-terminal one quarter is largely composed of β sheets and turns. At the junction between these two distinct regions two Cdk phosphorylation sites are positioned at Thr-470 and Thr-481 and these two regions are clustered with two nuclear localization signals, NLSs. Central region of the sequence, comprising residues 240-440, is highly conserved among eukaryotes and is probably important for the function of PRC1. Within the protein there is also a putative consensus sequence for ubiquitination-dependent proteolysis, including two D boxes and a KEN box [30]. Truncation mutants revealed that distinct regions of the protein have distinct roles. NH_2-terminal region is required for protein's association with the cleavage furrow and midbody, whilst sequence within residues 273-486 is required for microtubule binding. This central microtubule binding domain forms two long antiparallel α-helixes connected by a low-complexity structure with β sheets and turns that probably mediate binding between PRC1 and a microtubule. This conserved microtubule binding domain has a spectrin fold also specific for several other proteins with crosslinking ability (Figure 8). Spectrin fold is the most ordered region in the PRC1-microtubule complex and makes it possible for PRC1 to distinguish parallel and antiparallel bundles. The dimerization domain has a single conformation when crosslinking two microtubules, and its structural rigidity is likely responsible for PRC1's affinity for antiparallel microtubules [40]. The linker domain has more possible conformations when PRC1 is bound to microtubules, thus enabling the initial contact with

another microtubule that can have a range of possible orientations. COOH terminus is important for the function of PRC1 in a way that changes in conformation in this region disrupt function of the midzone microtubule bundles and this as a consequence blocks cleavage [31, 41]. Thus, this region does not display any particular localization or activity but is rather important for the functionality of the rest of the protein.

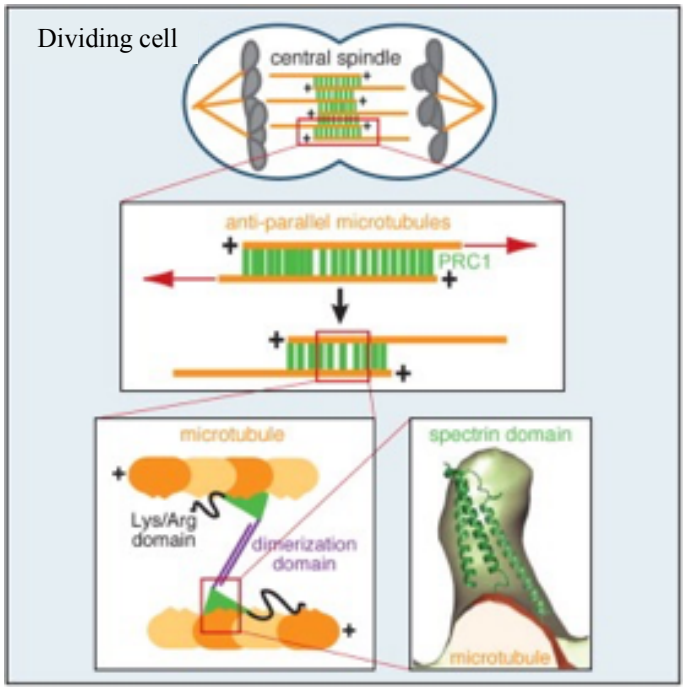

Figure 8. Schematic representation of overlap antiparallel regions crosslinked by PRC1 in a dividing cell. In zoomed region opposite orientation of crosslinked microtubules is pointed out. Scheme of a spectrin and dimerization domain and their positions with respect to the rest of the protein and attached microtubules [40].

PRC1 is required to maintain stable midzone MT bundles by binding and bundling microtubules *in vitro.* Its microtubule bundling is regulated by Cdk phosphorylation in a way that, when phosphorylated, it can bind to microtubules but cannot cross-link them. During mitosis its bundling capacity is timely regulated by (de)phosphorylation processes. Once dephosphorylated, it can cross-link microtubules and form antiparallel bundles. Phosphorylation by Cdc2/cyclin B specifically downregulates PRC1 bundling capacity in early mitosis and holds the protein in an

inactive monomeric state. Upon dephosphorylation during metaphase-to-anaphase transition, PRC1 forms oligomers and can begin to bundle antiparallel, interdigitating microtubules in order to provide stability for the midzone which is necessary for cytokinesis (Figure 9). PRC1 forms bundles of aligned microtubules where inter-microtubule linkage is made through filamentous projections at a constant angle with a value of ~38° with respect to the longitudinal microtubule axis [30, 35, 42]. Not only does PRC1 have affinity to interact with microtubules, but it also has other binding partners. *In vivo* immunoprecipitation assays revealed that its binding partner is KIF4, a chromokinesin. As will be described in further section, KIF4 is a member of microtubule-based motors that generate directional movement along microtubules. KIF4 is a motor protein that translocates PRC1 to the plus-ends of interdigitating microtubules. The domains of KIF4 that are required for interaction with PRC1 are stalk and tail domain and during metaphase-to-anaphase transition upon PRC1 dephosphorylation interaction with KIF4 is enabled. Amino-terminal half of PRC1 interacts both with PRC1 and with carboxyl-terminal half of KIF4. With this association it is made possible for PRC1 to localize to the midzone and to bundle antiparallel microtubules in late mitosis. KIF4 depletion experiments revealed that this protein is required for the assembly and stability of organized central spindle midzone and midbody [28, 32, 33]. It is with functionality of KIF4 achieved that the central spindle becomes organized and that other midzone-associated proteins concentrate into compact structures in this region which will consequently give rise to the midbody. Besides KIF4, endogenous PRC1 associates with MKLP1/CHO1 and CENP-E in cell extracts.

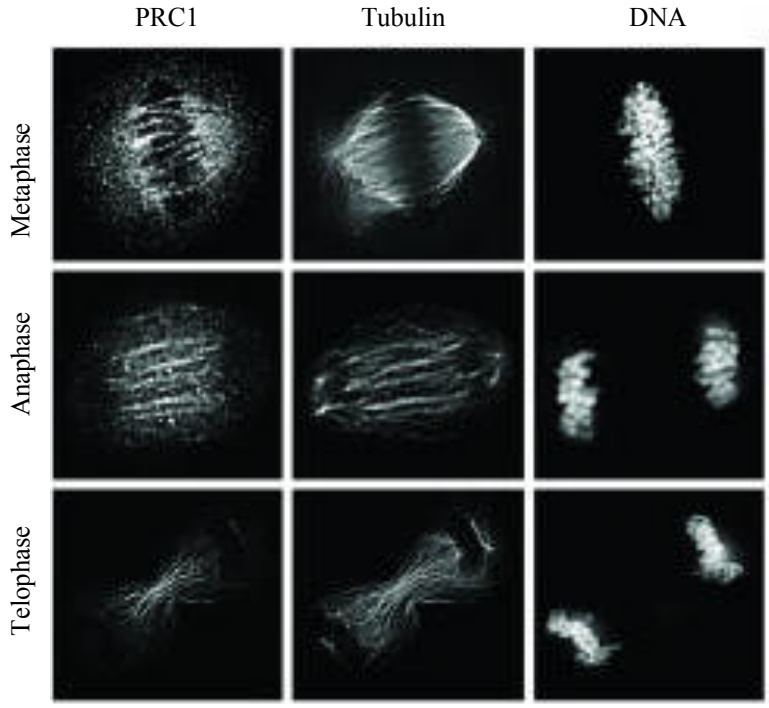

Figure 9. Confocal images of a cell with labeled PRC1, tubulin and chromosomes in metaphase, anaphase and telophase of mitosis. In metaphase PRC1 signal is localized more towards spindle center rather than the poles. In anaphase PRC1 translocates to the central spindle and to the midzone where it stays bound as the spindle grows and the contractile ring starts to contract [35].

Taken together, upon dephosphorylation PRC1 forms oligomers and associates with a motor protein Kif4 which then translocates PRC1 along the spindle to the plus-ends of antiparallel interdigitating microtubules and at this point it will allow for the antiparallel microtubules to bundle and form a midzone of the spindle. In that way organized central spindle can now serve as a platform for localization other midzone-associated proteins like centralspindlin and chromosomal passenger proteins involved in the completion of mitosis, cytokinesis. By combining structural flexibility and rigidity, PRC1 stabilizes antiparallel overlaps whilst not impeding sliding between them driven by motor proteins, like kinesin-5.

2.2.4.2 End binding proteins - points of growth

Growing microtubules accumulate at their plus ends multiple structurally unrelated factors collectively termed microtubule plus-end tracking proteins, or +TIPs. The most conserved and ubiquitous +TIPs are end binding proteins (EBs) [43] (Figure 10). They are core components of microtubule plus-end tracking protein networks. EBs are relatively small dimeric proteins which contain an N-terminal calponin homology (CH) domain, responsible for the interaction with microtubules, a linker region of unknown function, and a C-terminal coiled coil domain that extends into a four-helix bundle, required for dimer formation [44]. Through their C-terminal sequences, EBs interact with most other known +TIPs and recruit many of them to the growing microtubules ends [45]. Structural studies suggest that the EBs probably act by enhancing lateral interactions between individual protofilaments and may affect MT lattice structure [46, 47]. Mammalian cells express three members of the EB family- EB1, EB2 and EB3. It has been shown in mouse fibroblasts that EB1 is involved in formation of stable microtubules and that simultaneous depletion of EB1 and EB3 increases microtubule catastrophe frequency and disrupts persistent microtubule growth [44]. EB3 localizes throughout the cell cycle only to the plus ends of growing microtubules [48], and accumulates at the centrosome [49, 50, 51], from early prophase until the end of mitosis, concurrently with the increase of microtubule nucleation rates at the centrosome [52]. In mitosis, microtubule property to switch between growth and catastrophe becomes important for generating forces on chromosomes. This dynamic instability is, not exclusively, but still highly regulated by exchange of EBs and GTP/GDP.

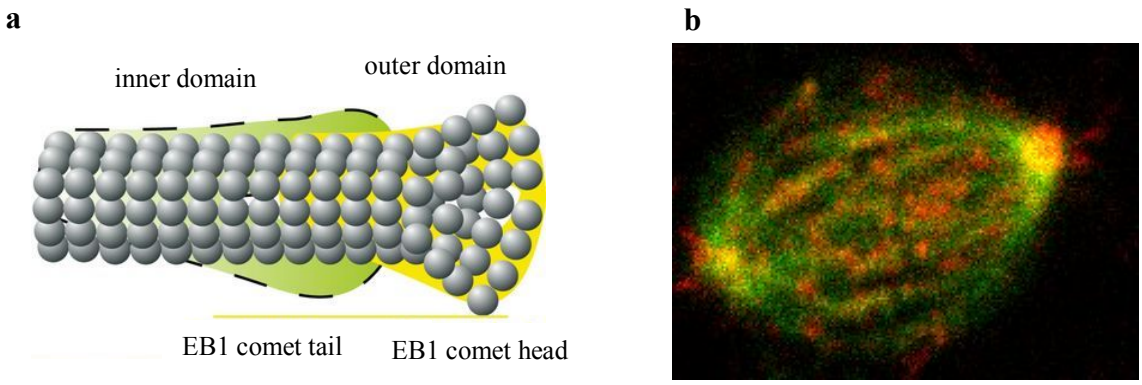

Figure 10. a) Scheme showing microtubule (gray spheres) and the + end with regions where EB1 is bound as the microtubule grows. b) U2OS cell with labeled EB3 protein (red) and tubulin labeled with SiR (green) in metaphase. Red spots define the comets that indicate growing microtubules. Yellow regions are overlay between tubulin and EB3 [53].

2.2.4.3 Motor proteins - pushing/pulling players

Motor proteins move across cytoskeleton and actively organize cell's interior. By using energy, they make traffic of all intracellular components possible. Transport inside the cell requires forces to move and position various molecular assemblies and organelles. These forces are mostly generated by motor proteins such as myosin, kinesin and dynein. To exert forces, motor proteins bind with one end to cytoskeletal filaments and with the other end to the cell cortex, a vesicle or another motor [54]. Whilst myosins are associated with contractile activity in muscle and non-muscle cells, kinesins and dyneins are microtubule motor proteins. Cytoskeletal motor proteins use structural changes in their nucleoside-triphosphate-binding sites to produce cyclic interactions with a partner protein. Further on, each cycle of binding and release must propel them forward in a single direction along a filament to a new binding site on the same filament. For such unidirectional motion, a motor protein must use the energy derived from ATP binding and hydrolysis to force a large movement in part of the protein molecule (Figure 11), [1]. The organization of microtubules into the highly ordered bipolar array of the mitotic spindle depends on activities of numerous motor and non-motor microtubule-associated proteins. Motor proteins have received significant attention because they generate force on microtubules during spindle

formation and throughout mitosis. In that way, motor proteins actively walk across microtubule fibers and direct their active movement, thus, for example, controlling the separation of mitotic spindle poles. Some of the motor proteins form oligomers that can crosslink adjacent microtubules, and in that way, they can move one microtubule relative to the other, with the direction of movement dependent on the polarity of both motor protein and microtubules. Alternatively, such motor proteins can slide antiparallel microtubules past each other in the overlap zone of the spindle. There are approximately 14 families of kinesin-related proteins. Most of them walk towards plus end of the microtubule, but in addition to this behavior, some walk towards the minus end, and some depolymerize microtubules. At the cellular level, kinesin motors perform a variety of functions during cell division and within the mitotic spindle where they help chromosomes get incorporated and segregated with the highest fidelity possible [55]. Their structure can roughly be summarized in having two heavy chains and two light chains per active motor, two globular head motor domains, and an elongated coiled-coil responsible for heavy chain dimerization. Most kinesins have a binding site in the tail for either a membrane organelle or another microtubule, thus giving them specific roles in mitotic and meiotic spindle formation and chromosome separation during cell division. The fastest kinesins can move their microtubules at about 2-3 μm/sec [1].

Dyneins are a family of minus-end-directed microtubule motors and are unrelated to kinesin superfamily. They are composed of two or three heavy chains, including motor domain, and a large and variable number of associated light chains. The dynein family has two major branches. Cytoplasmic dyneins are found in, probably all eukaryotic cells. They have a role in vesicle trafficking and in localization of the Golgi apparatus near the center of the cell. Other branch contains the axonemal dyneins which are highly specialized for the rapid and efficient sliding movements of microtubules that drive the beating of cilia and flagella, as well as of one's orchestrating mitosis. Dyneins are the largest of the known molecular motors, and they are also among the fastest with the ability to move their microtubules at the remarkable rate of 14 μm/sec [1].

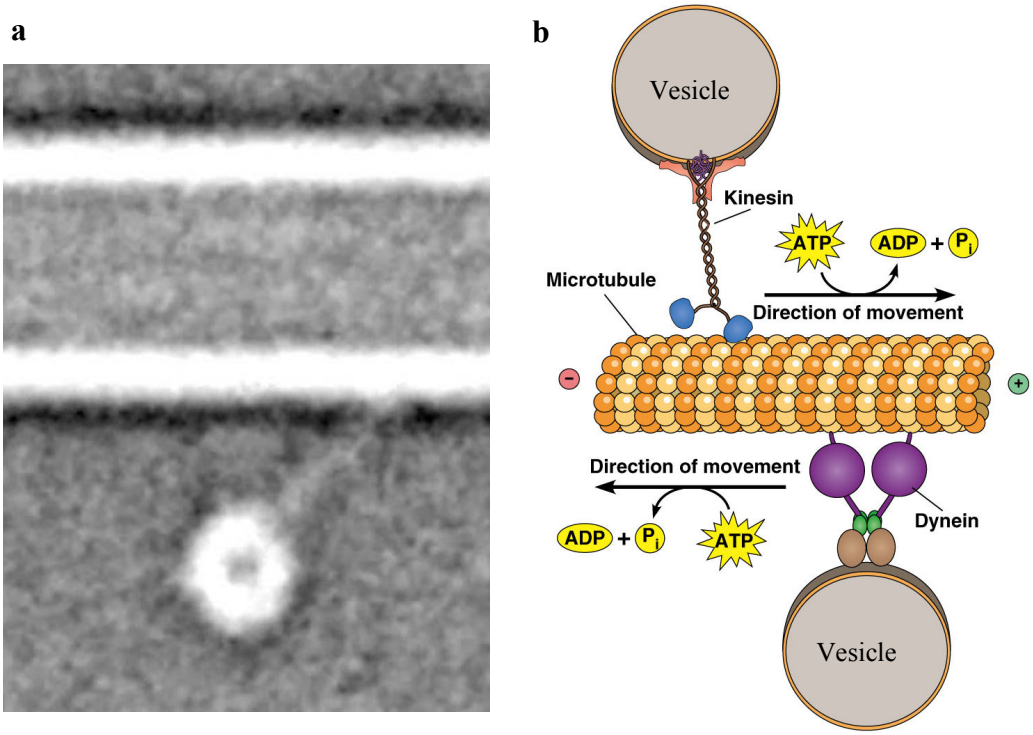

Figure 11. a) Electron microscope image of a dynein motor with head and tail domain as it was walking along the microtubule [56]. b) Scheme of a microtubule with attached motor proteins kinesin and dynein and the preferred direction of their movement where + and – indicate the orientation of microtubule (copyright 2012 Pearson Education, Inc).

2.3 FOUR STATES OF THE SPINDLE

2.3.1 Prophase - construction period

First, the spindle needs to assemble in a finely tuned and regulated manner. Once the cell is ready to yield two daughter cells and all the preparation checkpoints are passed, centrosomes will separate in a motor-dependent process that will push them to approximately opposite sides of the nucleus. As the nuclear envelope breaks down microtubules will grow rapidly from two separated centrosomes. As they grow in all directions, many will meet between the two poles and will mutually interact to form the origin of the spindle. Despite the high dynamic rate of events occurring at the centrosome, it is stable and capable of focusing parallel microtubules to form the functional pole of the spindle. This is achieved with assistance of cytoplasmic dynein which clusters parallel microtubules. Now nonmotor protein NuMa can be transported to these regions and will together with dynein tether microtubules in a way that pole structure remains robust despite dynamic instability of microtubules [58]. In order to maintain its structural integrity, it is crucial for the spindle to be able to continuously rebuild poles by reorganizing and sorting new microtubule structures [45].

To form the functional spindle, chromosomes need to be captured by growing dynamic microtubules and establish well defined positions and orientations between spindle poles. Chemically microtubules are preferentially growing in directions towards dispersed chromosomes. This is dependent on the concentration gradient of RanGTP, a member of GTPase family of proteins. RanGTP facilitates microtubule rescue, enables bipolar spindle formation and mediates microtubule-chromosome interactions. As these highly dynamic processes may seem rather random, kinetochores are already fully formed making it possible to achieve the end-on attachment with growing microtubule plus ends. By sole coincidence some chromosomes will at this point already find themselves on the way of growing microtubules between two centrosomes. These chromosomes will soon begin to form the specific interaction with microtubules. Chromosomes that are dispersed around the forming spindle need to be captured by growing microtubules and pulled closer to microtubule bundles that are forming between poles. As a microtubule grows from the centrosome in an arbitrary direction, it probes the space as it searches for kinetochores. Even

though a single microtubule probes only one direction, numerous directions will be explored eventually because numerous microtubules grow from the centrosome [26]. Plus, it was shown in yeast cells that growing microtubules pivot around the centrosome thus improving the possibility to catch a chromosome. Once kinetochore is encountered, its proper capture is achieved in a stepwise manner. First, kinetochores are captured by the lateral surface of a single microtubule that extends from either spindle pole. A captured kinetochore is then transported poleward along the microtubule [59], until the end-on connection is established (Figure 10). After the initial microtubule capture, kinetochores develop a bundle of 15-30 parallel microtubules that connect them to spindle poles. In that way a k-fiber is formed. In a mature k-fiber, tubulin heterodimers are constantly added in the kinetochore and removed from the minus ends in the pole thus promoting k-fragment elongation [25]. This form of attachment needs to be established on both sister kinetochores in order for them to become bioriented.

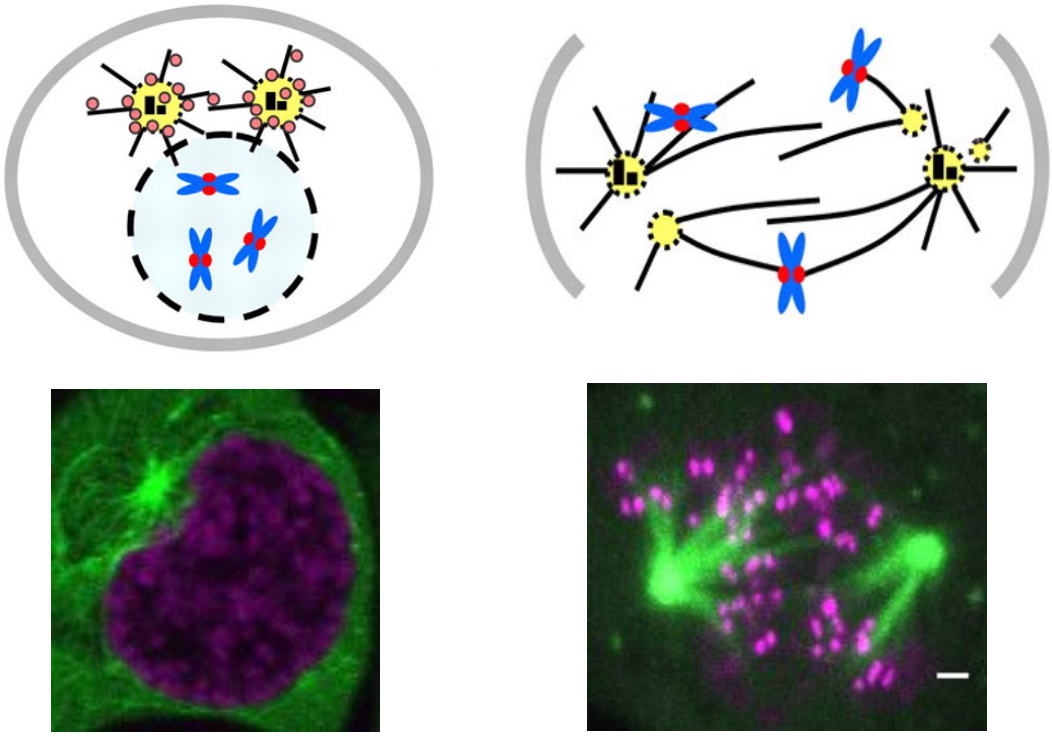

Figure 12. Top row: Scheme of prophase with two yellow spheres representing duplicated centrosomes. Black lines represent newly nucleated microtubules. Dashed black circle stands for nuclear envelope that is breaking up in prophase. Right: microtubules (black) growing in random directions and encountering chromosomes (blue). Adopted and modified from [57]. Bottom row: confocal images represent schemes above. U2OS cell (human osteosarcoma) with labeled CENP-A-GFP (kinetochore, magenta) and mCherry-tubulin (microtubules, green). Scale bar, 1 μm.

2.3.2 Metaphase - probing period

The physical stability of the spindle is reached after all the chromosomes are captured and precisely oriented. Once all chromosomes are attached by microtubules, they can be positioned halfway between spindle poles with two sister k-fibers linking them to opposite poles. Whilst k-fibers are forming, some microtubules will meet in the central part of the spindle and together form antiparallel bundles. These themselves will not form direct end-on attachment with kinetochore but rather with k-fibers as will be described below. Once all chromosomes become bioriented, they begin to oscillate in the spindle midzone. This is a specific movement of chromosomes towards opposite spindle poles with regulated switches that change the direction of their oscillations. Both microtubule attachments and dynamics at the kinetochore contribute to this process. Plus and minus end-directed motors associate with kinetochores, suggesting that motors could drive the movement of chromosomes either towards or away from the spindle equator [58]. The velocity of chromosome movement is rather constant, occurring at 2 μm/min, which is consistent with the rates of motor proteins associated with kinetochores [59]. For example, microtubule depolymerizing kinesin MCAK is important for sister kinetochore coordination during oscillations [60]. Eventually, all chromosomes actively get positioned in the equatorial plane of the spindle. Congression of the last chromosome marks the transition to the metaphase, during which oscillations are continued until anaphase. These movements are probing the chromosome's proper attachment and biorientation.

In addition to k-fibers, non-kinetochore microtubules comprise the majority of microtubules in mammalian spindles that have been studied by electron microscopy. During metaphase, they bundle together 30-50 nm apart in groups of 2-6, with antiparallel interactions apparently preferred [61]. These bundles are important for the whole spindle stability and distribution of forces between spindle poles. Their antiparallel region contains motor and non-motor cross-linking proteins. Motors contribute to antiparallel microtubule sliding, whereas passive cross-linkers take part in maintenance of the overlap integrity [25, 62]. For example, kinesin-14 and kinesin-5 are capable of sliding antiparallel spindle microtubules. Kinesin-14 is a minus end directed motor and it is believed to promote spindle shortening (inward directed force), whilst kinesin-5 probably promotes increased spindle length (outward directed force) [63]. When it comes to passive crosslinkers, PRC1 protein is the key for stability of antiparallel regions in the central spindle. PRC1 forms dimers and binds to microtubules to form cross-linkages between neighboring

interdigitating fibers [31, 64]. Its affinity to bind to microtubules is regulated by phosphorylation and dephosphorylation events precisely timed throughout mitosis [31, 65]. By combining structural flexibility and rigidity, PRC1 stabilizes antiparallel overlaps while not impeding sliding between them [40]. One such bundle of overlap microtubules which contains PRC1 links outermost sister k-fibers [2, 66, 67]. This fiber, termed "bridging fiber", balances the tension between sister kinetochores and helps the spindle to obtain a rounded shape in metaphase.

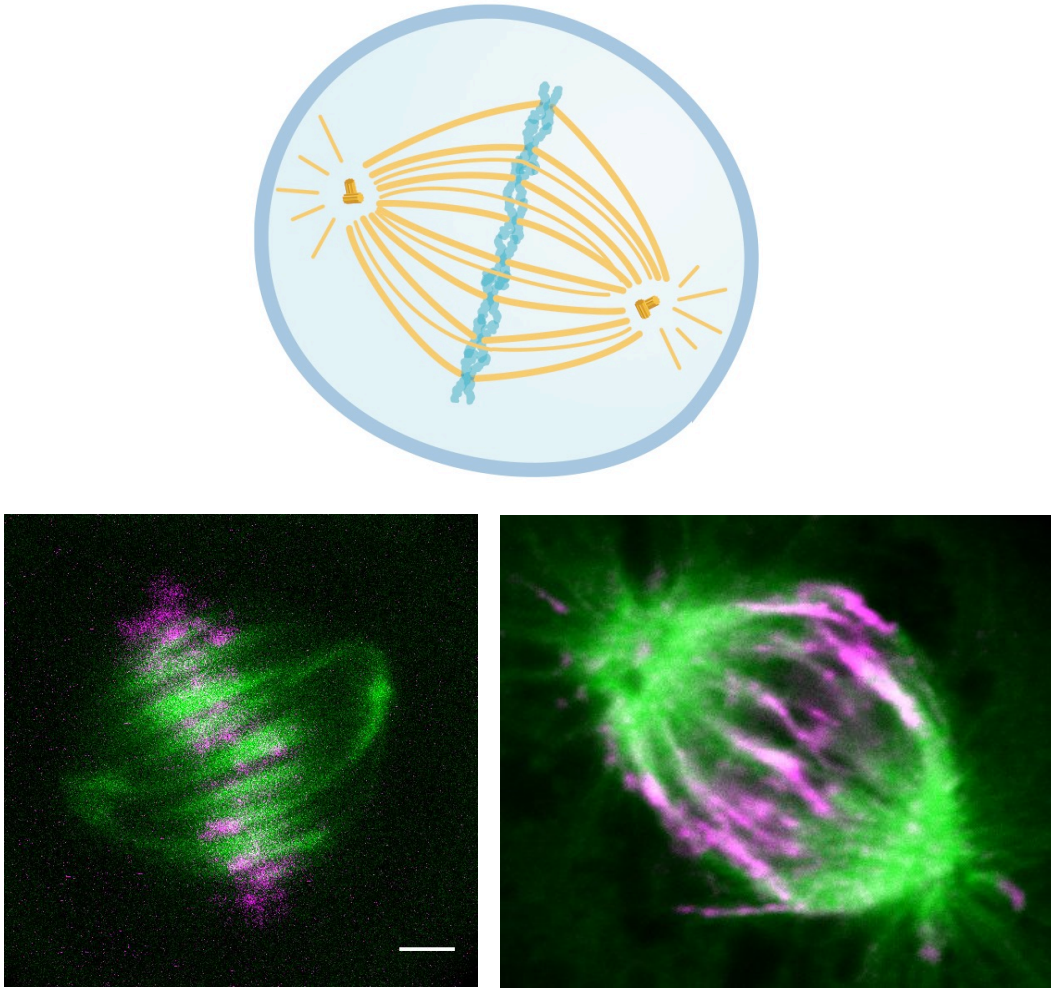

Figure 13. Top: scheme of spindle in metaphase with all formed k-fibers (thick yellow lines) and properly aligned chromosomes (blue) in the equatorial plane [wikivisually.com]. Bottom left: confocal image of a HeLa cell expressing PRC1 (green) and transiently transfected with mRFP-CENP-B (kinetochore, magenta) in metaphase. Right: HeLa cell expressing tubulin-GFP (green) immunostained against endogenous PRC1 shows its localization in metaphase. Scale bar, 2 μm.

2.3.3 Anaphase - separation period

When and if the metaphase control checkpoint is passed, chromosomes and poles of the spindle can begin to separate. This is a stage where all the chromosomes are bioriented and the cohesins that hold together the two sister chromatids can be degraded. It is with this degradation achieved that the pulling and pushing forces can separate duplicated chromosomes and transport them to the opposite spindle poles. As it is widely accepted, only in anaphase an organized central spindle midzone forms between separating chromosomes and consists of a dense network of overlapping antiparallel microtubules cross-linked by PRC1 [31, 32, 61, 65]. There are two mechanisms that contribute to separation of duplicated chromosomes, one acting at spindle poles and the other at the kinetochore. First, in anaphase A, detached sister chromatids move towards the opposite spindle poles via shortening of the attached sister k-fibers. The Pacman mechanism helps with anaphase A movement as it drives depolymerization of k-fibers at the kinetochore [68]. A synchrony of chromatid-to-pole movement is achieved by poleward flux of spindle microtubules. Poleward microtubule flux occurs due to the depolymerization of microtubule minus-ends and is driven mostly by members of the kinesin-5 family of motors which push microtubule minus-ends apart and drive sliding of antiparallel microtubules thus exerting force on the spindle poles [69]. Once separated in anaphase A, the whole spindle begins to elongate thus increasing the distance between two poles of the spindle. Even though they are two main stages occurring in anaphase, these two mechanistically distinct processes occur simultaneously in many cell types [70]. As main spots for exerting forces are kinetochores, the movement of chromosomes in anaphase seems like random swinging easily comparable with the “rag-doll” like movements. Due to this characteristic movement, the role of chromosomes during this process was interestingly compared to that of “a corpse at a funeral” as stated by Mazia. The chromosomes are the reason for the proceedings but do not take an active part in them [71]. The trigger that switches the transition from metaphase to anaphase is dependent on the anaphase promoting complex (APC). This large complex consists of 11-13 subunit proteins and its role is to tag specific proteins at this point destined for degradation. Some of these are already mentioned cohesins [72]. As the anaphase stage is successful with chromosome separation, the next stage can begin to prepare the basis for formation of two divided daughter cells.

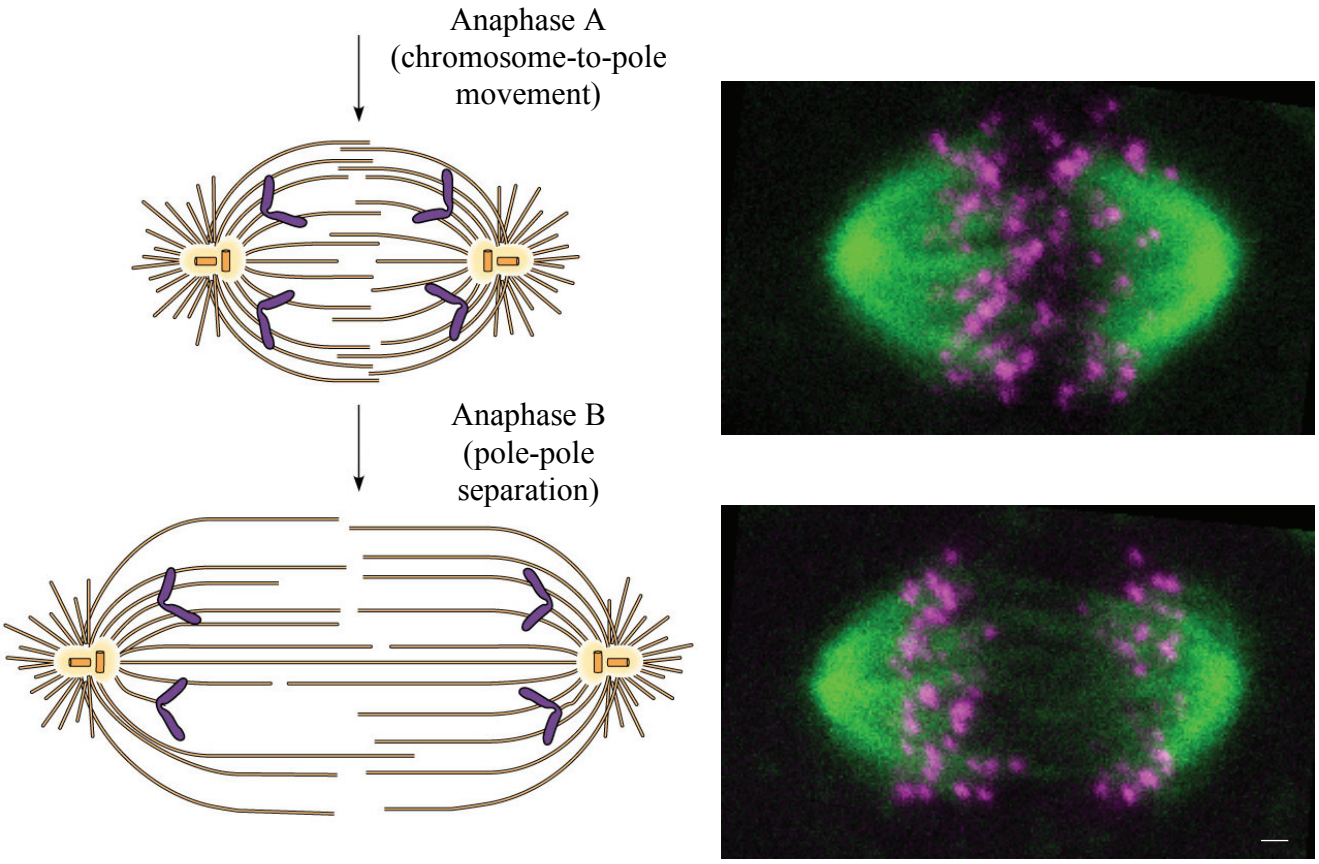

Figure 14. Left: schemes of two stages of anaphase movement. Upper scheme shows movement of chromosomes towards opposite spindle poles. Bottom scheme corresponds to movement of spindle poles further away from one another [Adopted and modified from imgbuddy.com]. Images on the right correspond to described schemes as seen under confocal microscope in U2OS cell with labeled CENP-A-GFP (kinetochore, magenta) and mCherry-tubulin (microtubules, green) in anaphase [Adopted and modified from 73]. Scale bar, 1 μm.

2.3.4 Telophase - demolition versus composition

Anaphase will pass to telophase as the central part of the spindle contracts. Now mitosis slowly comes to an end when separated chromosomes meet the spindle poles and begin to decondense. This stage of mitosis can be considered as reverse in processes occurring in prophase and prometaphase and occupies approximately 2% of the duration of the cell cycle. Telophase ongoing is primarily driven by dephosphorylation of mitotic cyclin-dependent kinase substrates. Above mentioned APC targets cyclins for proteolytic degradation. Dephosphorylation of same substrates that were phosphorylated at the beginning of mitosis drives spindle disassembly, chromosome decondensation and reassembly of nuclear envelopes. On two sides of the former metaphase plate the contractile ring is formed and it consists of filamentous actin, motor protein myosin-2 and other structural and regulatory proteins. The contractile ring is formed under the plasma membrane to which it is linked so that as it constricts, it simultaneously creates the cleavage furrow that will eventually partition the cell in two to create two new cytoplasms. (Figure 3) [1]. At this point the nuclear envelopes are fully formed around segregated chromosomes and the production of two identical cells is completed. These newly formed daughter cells can now begin to feed and grow until they are ready to begin with this same remarkable process.

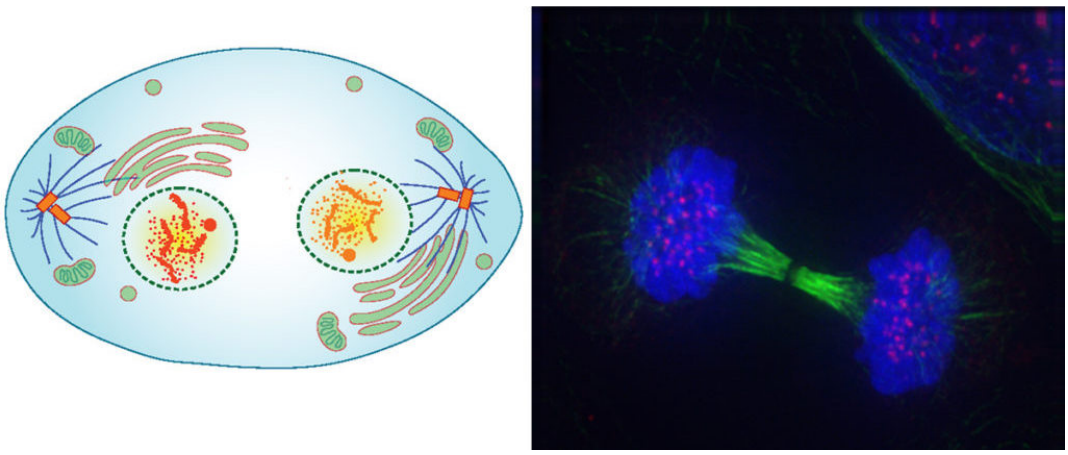

Figure 15. Left: scheme of telophase with decondensating chromosomes (red and yellow), newly assembling nuclear envelope (dashed circle), leftover microtubules (thin blue lines) as remains of the spindle and orange cylinders representing centrosomes. Confocal image of a cell in telophase with structures as stated in description of the scheme [courses.lumenlearning.com].

3 MATERIALS AND METHODS

3.1 CELL LINES

HeLa-TDS cells were permanently transfected and stabilized (courtesy of Mariola Chacon) using pEGFP-α-tubulin plasmid, which was acquired from Frank Bradke (Max Planck Institute of Neurobiology, Martinsried). HeLa-Kyoto BAC lines stably expressing PRC1-GFP [74] were courtesy of Ina Poser and Tony Hyman (MPI-CBG, Dresden). HeLa cells stably expressing EGFP-CENP-A and EGFP-centrin1 were a courtesy of Emanuele Roscioli and Andrew McAinsh (University of Warwick). Human U2OS cells, both unlabeled and permanently transfected with CENP-A-GFP, mCherry-α-tubulin, and photoactivatable (PA)-GFP-tubulin, were courtesy of Marin Barišić and Helder Maiato (Institute for Molecular Cell Biology, University of Porto, Portugal). Cells were grown in DMEM (1 g/l D-glucose, L-glutamine, pyruvate obtained from Sigma, St. Louis, MO, USA) with 50 μg/ml geneticin (Santa Cruz Biotechnology, Inc., Dallas, USA) and appropriate supplements. The cells were kept at 37°C and 5% CO_2 in a Galaxy 170 R CO_2 humidified incubator (Eppendorf, Hamburg, Germany). All used cell lines were confirmed to be mycoplasma free by using MycoAlert Mycoplasma Detection Kit (Lonza, Basel, Switzerland).

3.2 SAMPLE PREPARATION

HeLa cells were transiently transfected by electroporation using Nucleofector Kit R (Lonza, Basel, Switzerland) with the Nucleofector 2b Device (Lonza, Basel, Switzerland), using the high-viability O-005 program. Transfection protocol provided by the manufacturer was followed. Cells were transfected with mRFP-CENP-B plasmid (pMX234) provided by Linda Wordeman (University of Washington). 1×10^6 cells and 2 μg of plasmid DNA were used. Transfection of PRC1-GFP BAC line cells with mRFP-CENP-B (2.5 μg DNA) was performed 25–35 h before imaging. For labeling of microtubules with SiR-tubulin (Spirochrome AG, Stein am Rhein, Switzerland), the dye was added to cells at a final concentration of 50–100 nM, 16 h prior to imaging.

For PRC1 siRNA, 1×10^6 cells at 50–60% confluency were transfected with 200 nM targeting or control non-targeting siRNA raw constructs diluted in a Nucleofector solution R together with 2.5 μg mRFP-CENP-B plasmid. The constructs used were as follows: siGENOME SMART pool

for human PRC1 (M-019491-00-0005) and siGENOME control pool (D-001206-13-05), both from Dharmacon (Lafayette, CO, USA). To prepare samples for microscopy, following the transfection, HeLa cells were seeded and cultured in 1.5 ml DMEM medium with supplements at 37°C and 5% CO_2 on uncoated 35-mm glass coverslip dishes, No 1.5 coverglass (MatTek Corporation, Ashland, MA, USA). For experiments regarding abundance of bridging fibers, before live-cell imaging, the medium was replaced with Leibovitz's L-15 CO_2-independent medium supplemented with fetal bovine serum (FBS, Life Technologies, Carlsbad, CA, USA). For experiments with the fixed samples, cells were fixed in ice-cold methanol for 3 min, washed three times with phosphate-buffered saline (PBS, Merck, Darmstadt, Germany) with followed imaging or immunostaining.

For synchronization, cells were seeded at 40% confluency in uncoated 35-mm glass coverslip dishes, No 1.5 coverglass (MatTek Corporation, Ashland, MA, USA) with 2 ml DMEM medium with supplements. At 4 pm the day before imaging, thymidine (Sigma-Aldrich, St. Louis, MO, USA) was added at a final concentration of 2 mM. Cells were left in thymidine for 17 h, and at 9 am each dish was washed three times with warm PBS and 2 ml of fresh DMEM medium with supplements was added. At 12:30 pm, RO-3306 (Calbiochem, Merck Millipore, Billerica, MA, USA) was added at a final concentration of 9 mM. At 7 pm, the dishes were washed three times with warm PBS. Then, the cells were left in the incubator with 2 ml DMEM medium with supplements for 30 min to recover. At 7:30 pm, the medium was replaced with L-15 with appropriate supplements and 20 mM of the proteasome inhibitor MG-132 (Sigma-Aldrich, St. Louis, MO, USA) to arrest the cells in metaphase. Cells were fixed in ice-cold methanol 30 min after adding MG-132.

3.3 IMMUNOSTAINING

Unlabeled U2OS and tubulin-labeled HeLa cells were fixed in ice-cold 100% methanol for 3 min and washed. To permeabilize cell membranes, cells were incubated in Triton (0.5% in phosphate-buffered saline (PBS)) at room temperature for 25 min. To block unspecific binding of antibodies, cells were incubated in 1% normal goat serum (NGS) in PBS for 1 h at 4 °C. Cells were then incubated in 250 µl of primary antibody solution (4 µg ml^{-1} in 1% NGS in PBS) for 48 h at 4 °C. Mouse monoclonal anti-PRC1 antibody (C-1; sc-376983, Santa Cruz Biotechnology, USA) was used. After washing off the primary antibody solution, cells were incubated in 250 µl of secondary antibody solution (4 µg ml^{-1} in 2% NGS in PBS; Alexa Fluor 488 preadsorbed donkey polyclonal anti-mouse IgG, Ab150109; Abcam, Cambridge, UK) for 1 h at room temperature protected from light. After each incubation step, cells were washed three times for 5 min in PBS softly shaken at room temperature. In HeLa cells, we occasionally observed shrinkage of the spindle upon fixation; therefore, for the analysis we only chose spindles which were longer than 9 µm.

3.4 CONFOCAL MICROSCOPY FOR ABUNDANCE OF BRIDGING FIBERS

HeLa cells were imaged by using a Leica TCS SP8 X laser scanning confocal microscope with a HC PL APO 63×/1.4 oil immersion objective (Leica, Wetzlar, Germany) heated with an objective integrated heater system (Okolab, Burlingame, CA, USA). Excitation and emission lights were separated with Acousto-Optical Beam Splitter (AOBS, Leica, Wetzlar, Germany). For live-cell imaging, cells were maintained at 37°C in Okolab stage top heating chamber (Okolab, Burlingame, CA, USA). For excitation, a 488-nm line of a visible gas Argon laser and visible white light laser at 575 nm were used for GFP and mRFP/Alexa Fluor-555, respectively. GFP and mRFP/Alexa Fluor-555 emissions were detected with HyD (hybrid) detectors in ranges of 498–558 and 585–665 nm, respectively. Pinhole diameter was set to 0.8 μm. In experiments with PRC1-GFP BAC line cells (counting and coupling experiments), images were acquired at 25–35 focal planes with 0.5 μm spacing and 400 Hz unidirectional xyz scan mode. For experiments with dynamic properties in vertical spindles, live PRC1-GFP cells transiently transfected with mRFP-CENP-B were imaged at five focal planes with 0.5 μm spacing and 600 Hz unidirectional xyzt scan mode with time interval set to 13 s. In the cases when the transiently expressed mRFP-CENP-B significantly bleached during the experiment, the power of the white light laser (575 nm) was increased during the acquisition, which did not affect the measurements because the mRFP-CENP-B signal intensity was not quantified. In experiments with tubulin-GFP cells (MG132 arrested cells and siRNA experiments), images were acquired at 4–10 focal planes with 0.5 μm spacing and 400 Hz unidirectional xyz scan mode. The system was controlled with the Leica Application Suite X software (LASX, 1.8.1.13759, Leica, Wetzlar, Germany).

3.4.1 Image analysis for abundance of bridging fibers

Image processing and measurements were performed in ImageJ (National Institutes of Health, Bethesda, MD, USA). Quantification, data analysis, and scientific graphing were performed in SciDAVis (Free Software Foundation Inc., Boston, MA, USA). Cross-correlation analysis was performed in MATLAB (MathWorks, Natick, MA, USA). Figures and schemes were assembled in Adobe Illustrator CC (Adobe Systems, Mountain View, CA, USA). Statistical analysis was performed using Student's *t*-test. Data are given as mean ± s.e.m., unless otherwise indicated.

We used acquired *z*-stack images of whole spindles to quantify the number of kinetochore pairs and PRC1-labeled fibers. In spindles that were oriented with their long axis roughly parallel to the imaging plane both kinetochore pairs and PRC1-labeled fibers were observed in each *z*-slice of individual spindle. In spindles with their long axis oriented roughly perpendicular to the imaging plane, an individual PRC1-labeled bundle appeared as a bright green dot that spans about 10 *z*-slices (5 μm), whereas kinetochores were observed only in central planes that correspond to the metaphase plate area. We counted each kinetochore pair and PRC1-labeled fiber throughout the spindle minding the presence of its signal in the upper and lower *z*-plane with respect to the plane in which it had highest signal intensity.

Kinetochore pairs and PRC1-labeled fibers were defined associated if the distance between the central part of the fiber and the midpoint between centers of sister kinetochores was smaller than 0.3 μm. Spindle length was calculated as the distance between the spindle poles, whereas spindle width was calculated as the distance between the midpoints of the outermost sister kinetochores on the opposite spindle sides. The density of kinetochore pairs coupled with PRC1-labeled bundles was calculated as the number of kinetochore-PRC1 pairs in a cross section of the central part of the spindle divided by the cross-sectional area.

Trajectories of kinetochores and PRC1-labeled bundles in spindles with their long axis oriented roughly perpendicular to the imaging plane were acquired by using Low Light Tracking Tool, an ImageJ plugin [75]. Tracking of kinetochores and PRC1-labeled bundles in the *xy* plane was performed on maximum-intensity projections of up to four planes. To avoid the possible effect of trajectories being the result of the entire spindle moving as a cohesive unit, we calculated the trajectories of kinetochore pairs and of PRC1-labeled bundles with respect to the spindle's center of mass in each image. Cross-correlation was calculated with the MATLAB inbuilt function

normxcorr2, which includes normalization by dividing with the product of the local standard deviation [76]. We acquired only correlation coefficients at unshifted positions, that is, at lag = 0. In HeLa cells stably expressing tubulin-GFP that were immunostained for PRC1, we tracked a 5-pixel-thick pole-to-pole contour of tubulin-GFP signal of the sister k-fibers and the corresponding bridging fiber that spans between them. The positions of the spindle poles were estimated as the merging points of k-fibers. The bundles were tracked manually, point-by-point along the curved line, following the tubulin-GFP signal path (note that the bundles that disappeared in the *z*-direction were not tracked). We used this contour to measure intensity profiles of endogenous PRC1 in the red channel (immunostaining).

In cells expressing PRC1-GFP we tracked the pole-to-pole contour of PRC1-GFP by using approximately 30 points and measured the intensity profile in the green channel. The positions of the spindle poles were estimated as the merging points of k-fibers in the maximum-intensity projection of all *z*-slices covering the entire spindle. The mean value of the background signal present in the cytoplasm was subtracted from the intensity profiles. The length of the PRC1-labeled overlap region, L_{PRC1}, was manually determined as the width of the peak of the PRC1-GFP signal intensity in the central part of the contour. The width of the peak was defined as the distance between the positions at the base of the PRC1-GFP peak where the PRC1-GFP signal intensity is roughly equal to the mean value of the PRC1-GFP signal intensity along the contour on either side of the peak. We defined signal intensity I as the total sum of intensities in the intensity profile of a 5-pixel-thick pole-to-pole contour of PRC1-GFP signal, divided by the contour's total length, and I_{cross} as the total intensity under the peak in the intensity profile along a 5-pixel-thick line drawn transversely to the PRC1-GFP signal. The same method was used for quantification of endogenous PRC1-immunostained bundles.

The signal intensity of a cross section of a bridging fiber in cells expressing tubulin-GFP and mRFP-CENP-B was measured by drawing a 3-pixel-thick line between sister kinetochores and perpendicular to the line joining centers of the two kinetochores, whereas a cross section of the bundle consisting of a bridging fiber and a k-fiber was measured about 1 μm laterally from either kinetochore. The mean value of the background signal present in the cytoplasm was subtracted from the intensity profile.

The distance from the center was measured between the central part of the overlap fiber and the spindle long axis, perpendicular to the spindle long axis. Distance between sister kinetochores

was measured as the distance between their centers, acquired by optimizing and tracking with Low Light Tracking Tool [75].

3.5 LYSATE PREPARATION AND WESTERN BLOT ANALYSES

HeLa cells grown on six-well plates were transfected with 200 nM control siRNA (non-targeting) or PRC1 siRNA. Non-treated samples were not transfected. Following transfection and synchronization, the cells were washed with sterile PBS, and harvested by addition of RIPA buffer (Sigma, St. Louis, MO, USA) containing protease inhibitors (Complete TM; Roche, Basel, Switzerland). SDS–PAGE was performed using 12% gels and blotted onto nitrocellulose membranes (BIO-RAD, Hercules, CAL, USA). Membranes were blocked in 5% bovine serum albumin and probed using rabbit anti-PRC1 (sc-8356; Santa Cruz Biotechnology, Santa Cruz, CA, USA) or rabbit anti-GAPDH antibody (G9545; Sigma, St. Louis, MO, USA), which was used as a loading control. Bound primary antibodies were detected using peroxidase-conjugated anti-rabbit immunoglobulin G (A0545. Sigma, St. Louis, MO, USA) and Clarity ECL Western Blotting substrate (Bio-Rad, Hercules, CAL, USA). Images were acquired using the C-DiGit blot scanner (LI-COR, Bad Homburg, Germany). Images were analyzed using Image Studio software (LI-COR, Bad Homburg, Germany). Percent of PRC1 protein was calculated from Western blot band intensities of all the PRC1 isoform bands in one gel line after normalizing to the corresponding GAPDH band intensity. The data were acquired from 3 to 6 independent experiments.

3.6 CONFOCAL MICROSCOPY FOR 3D RECONSTRUCTION OF BUNDLES

HeLa and all U2OS cells were imaged using Bruker Opterra Multipoint Scanning Confocal Microscope [77] (Bruker Nano Surfaces, Middleton, WI, USA). The system was mounted on a Nikon Ti-E inverted microscope equipped with a Nikon CFI Plan Apo VC ×100/1.4 numerical aperture oil objective (Nikon, Tokyo, Japan). During imaging, cells were maintained at 37 °C in Okolab Cage Incubator (Okolab, Pozzuoli, NA, Italy). A 60 µm pinhole aperture was used and the xy-pixel size was 83 nm. For excitation of GFP and mCherry fluorescence, a 488 and a 561 nm diode laser line was used, respectively. The excitation light was separated from the emitted fluorescence by using Opterra Dichroic and Barrier Filter Set 405/488/561/640. Images were captured with an Evolve 512 Delta EMCCD Camera (Photometrics, Tucson, AZ, USA) with no binning performed. To cover the whole metaphase spindle, z-stacks were acquired at 30–60 focal planes separated by 0.5 µm with unidirectional xyz scan mode. The system was controlled with the Prairie View Imaging Software (Bruker Nano Surfaces, Middleton, WI, USA).

3.6.1 Image analysis for 3D reconstruction of bundles

Microscopy images were analyzed in Fiji Software. For the analysis of horizontal spindles, only the spindles with both poles roughly in the same plane were used to ensure that spindles are maximally vertical after the transformation into vertical orientation, which was done by using a code written in R programming language [78] in RStudio. Before the transformation, the z-stack of the spindle in a single channel was rotated in Fiji so that the spindle major axis was approximately parallel to the x-axis. Signal intensity at each pixel in a z-stack is denoted as I(i, j, k), where indices i, j denote coordinates in the imaging plane, and k denotes the number of the imaging plane of the z-stack. To transform the 3D image of the spindle into vertical orientation, we applied the transformation I'(i, j, k) = I(k, i, j), which preserves the orientation (handedness) of the coordinate system, that is, corresponds to rotation of the image without mirroring. The coordinates (i, j, k) correspond to 3D positions (x, y, z)=(i · pixel size, j · pixel

size, k · z-distance). The aberrations caused by refractive index mismatch between immersion oil and aqueous sample were taken into account by multiplying z-step size by a correction factor of 0.81 to obtain the correct z-distance. We calculated this factor as a ratio of the cell diameter in y and z direction, assuming that a mitotic cell is spherical [79]. This value is consistent with theoretical predictions for z-aberrations due to refractive index mismatch [80] and experimental measurements [81].

Bundles in 3D images of spindles oriented vertically (including transformed images of horizontal spindles and images of vertical spindles) were tracked manually using Multipoint tool in Fiji. Individual bundles were determined by moving through the z-stack. Because microtubule bundles appear as spots in a single z-image, each point was placed at the center of the signal. Moving up and down through the z-stack helped to determine this point. Each bundle was tracked through all z-planes where it appears as a single spot. In addition, positions of the spindle poles were determined as the focus point where the PRC1 signal on the microtubule bundles, which is faint in the region close to the pole, ends. Coordinates of bundles and poles from images of vertical spindles were transformed so that both poles are on the z-axis. For the analysis of helicity only the tracked points in the central part of the spindle, between 0.3 and 0.7 of the normalized spindle length, were taken into account. We used only bundles with average distance from the major axis larger than 1.35 μm.

3.7 STATISTICAL ANALYSIS AND RESULTS REPRESENTATION

Figures and schemes were assembled in Adobe Illustrator CC or CS6 (Adobe Systems, Mountain View, CA, USA) and Adobe Photoshop CS6 (Adobe Systems, Mountain View, CA, USA). Data are given as mean ± s.e.m., unless otherwise indicated. Fiji was used to scale images and adjust brightness and contrast. Data are given as mean ± s.e.m., unless otherwise stated. Significance of data was estimated by Student's t-test (two-tailed and two-sample unequal-variance). $p < 0.05$ was considered statistically significant. Values of all significant differences are given with degree of significance indicated (*$0.01 < p < 0.05$, **$0.001 < p < 0.01$, ***$p < 0.001$). The number of analyzed cells and microtubule bundles is given in the respective figure panel. For representation of results for 3D reconstruction of bundles, graphs were generated in the programming language R.

4 RESULTS AND DISCUSSION

4.1 ONE-TO-ONE ASSOCIATION BETWEEN OVERLAP FIBERS AND SISTER KINETOCHORES

Above described bridging fiber was discovered on periphery of the metaphase spindle by combining confocal fluorescence microscopy and laser ablation applied on the outermost sister k-fibers (Figure 16a). It was shown that bridging fiber contains PRC1, links outermost sister k-fibers and balances tension and compression in these regions [2], (Figure 16b).

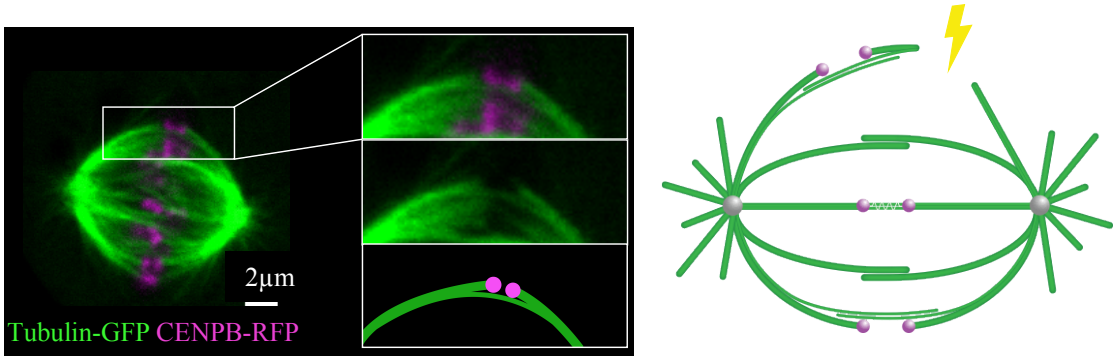

Figure 16. HeLa cell in metaphase expressing GFP-tubulin (green) transiently transfected with mRFP-CENPB (magenta) as seen under confocal microscope. Enlarged boxed region shows outermost sister k-fibers linked by a bridging fiber. Right: experimental setup with laser ablation assay that revealed association between outermost overlap bundle and sister kinetochores. Yellow lightning represents the commonly used position of the ablation and outward movement of the k-fiber and sister kinetochores as the response to the applied cutting [2].

In continuation, findings will be described that are published in 2016, in a peer-reviewed scientific journal EMBO Reports as a scientific report entitled "PRC1-labeled microtubule bundles show one-to-one association in metaphase" by authors Polak Bruno, Risteski Patrik, Lesjak Sonja and Tolić Iva M. To study the abundance of overlap microtubules that act as bridging fibers throughout the metaphase spindle, whole individual spindles were imaged. HeLa cells stably expressing PRC1-GFP from a bacterial artificial chromosome (BAC) [74] were used which enables to visualize overlap antiparallel regions in spindles. These were transiently transfected with mRFP-CENP-B to visualize kinetochores and fixed. *Z*-stacks of images that cover a whole metaphase spindle were acquired in fixed cells (Materials and Methods). Metaphase was identified by the alignment of sister kinetochores on the metaphase plate, and kinetochores were defined as sisters if the bi-orientation was estimated within individual planes. This approach enables to measure the proportions of unperturbed spindles. Spindle length determined as the distance between two spindle poles was measured to be in average 10.65 ± 0.16 μm (all results are mean ± s.e.m. unless otherwise indicated, $n = 29$). Spindle width defined as the distance between two outermost midpoints of sister kinetochores was measured to be in average 11.21 ± 0.25 μm ($n = 29$), consistent with previous measurements [2, 82] (Figure 17).

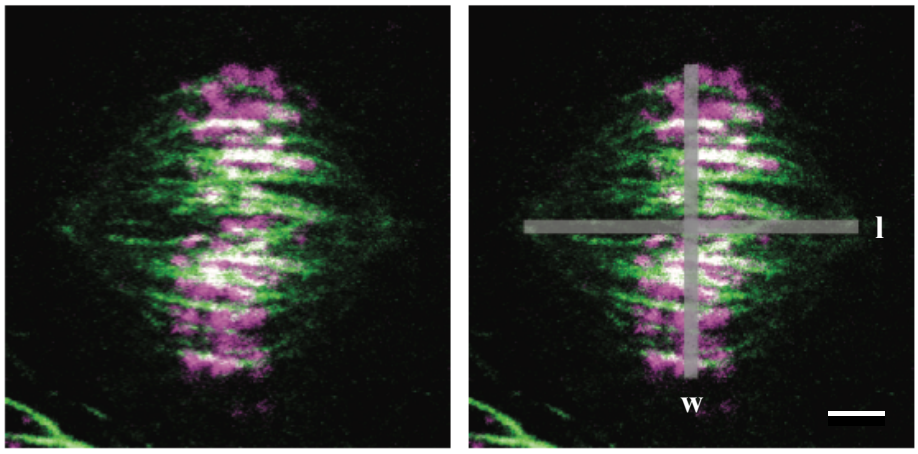

Figure 17. Spindle in a fixed HeLa cell expressing PRC1-GFP (green) and mRFP-CENP-B in maximum projection of acquired z-stack images that cover the whole metaphase spindle. Same cell is shown on the right with gray lines showing measured parameters of the metaphase spindle, l (length) and w (width). Scale bar, 2 μm.

The visualized proteins of interest provided opportunity to count the number of PRC1-labeled fibers as well as the number of sister kinetochore pairs in imaged spindles. Due to variable number of chromosomes in individual HeLa spindles [83, 84, 85], this unstable karyotype is used to determine whether the number of overlap fibers depends on the number of chromosomes per spindle. For this analysis two approaches of imaging the spindles were used. In first approach horizontal spindles were used which have their long axes connecting spindle poles oriented roughly horizontally with respect to the imaging plane (Figure 18). In this most frequent spindle orientation in the field of view, PRC1-labeled bundles appear as slightly curved lines with broader central part which gradually narrows in both directions towards opposite spindle poles. In metaphase, these bundles are present throughout the spindle, from the periphery to the central parts in the vicinity of the spindle long axis (Figure 19).

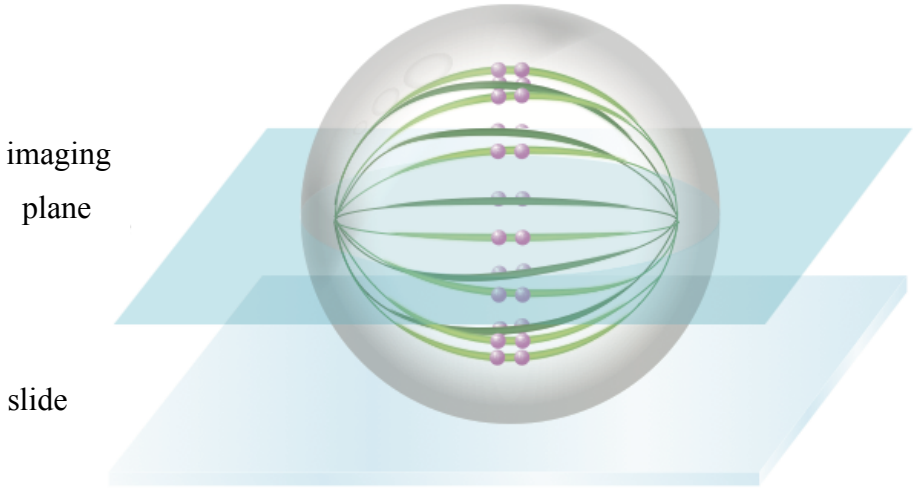

Figure 18. Scheme of metaphase spindle with its long axis oriented horizontally with respect to the imaging plane. Slide represents the bottom of the imaging dish. Imaging plane in the scheme shows orientation of individual z-stack images with 0.5 μm spacing that are acquired to cover the whole area that the spindle comprises.

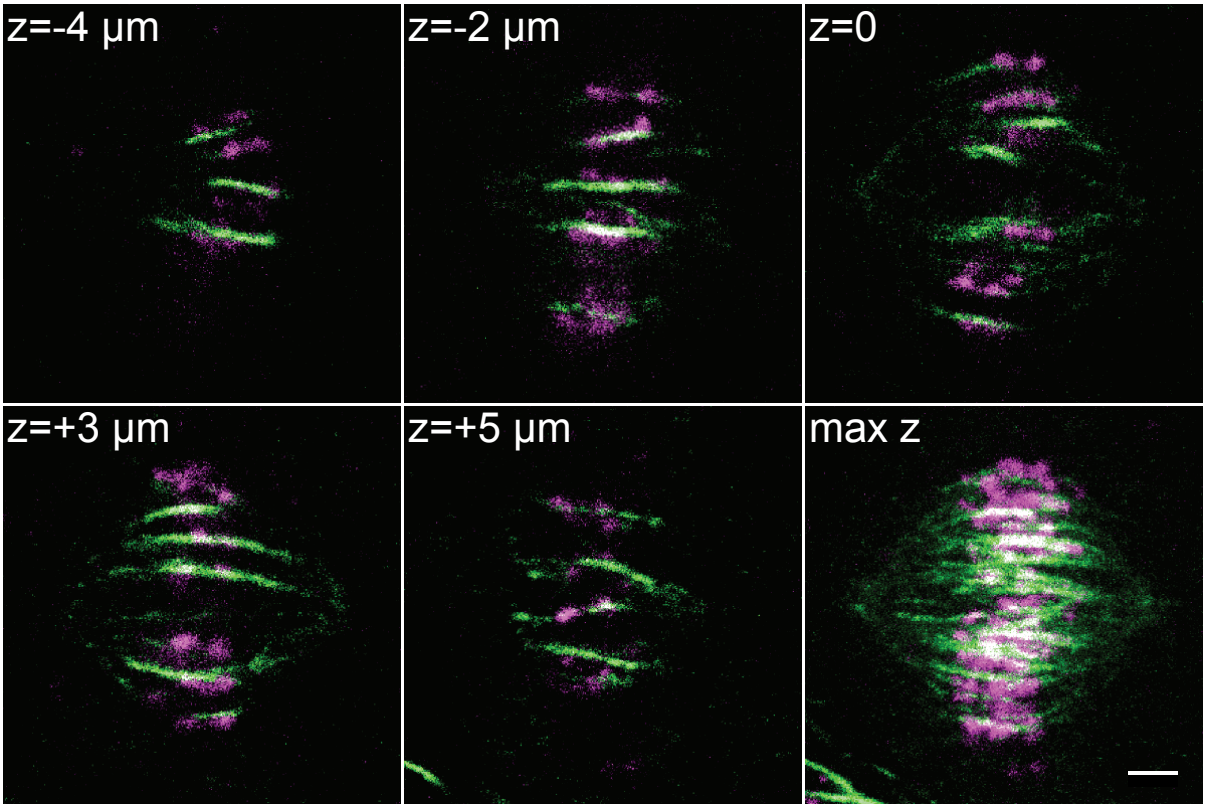

Figure 19. Spindle in a fixed HeLa cell expressing PRC1-GFP (green) and mRFP-CENP-B (magenta) oriented horizontally with respect to the imaging plane, as shown in the scheme above. Images of different z-slices (central plane of the spindle z = 0, two images below, z = 4 µm and z = 2 µm, and above, z = +3 µm and z = +5 µm), maximum projection of a z-stack (max z). Scale bar, 2 µm.

Occasionally, in the field of view spindles that are oriented with their long axes roughly perpendicular to the imaging plane can be found (Figure 20). Here, PRC1-labeled bundles appear as spots in individual imaging planes (Figure 21). It is not known what the exact reason for this orientation is, however these spindles are functional and metaphase can be determined by the number of planes in which kinetochores are present. Occasionally, these so-called vertical spindles were observed in anaphase, which implies that this orientation is not a sign of a defected spindle.

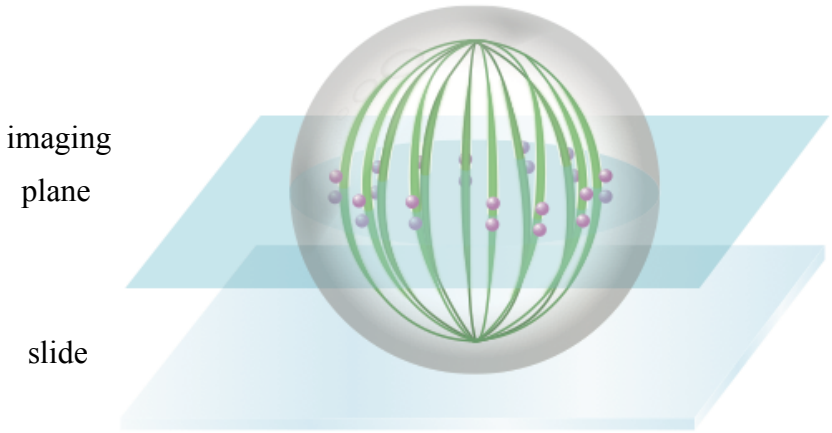

Figure 20. Scheme of metaphase spindle with its long axis oriented vertically with respect to the imaging plane. Slide represents the bottom of the imaging dish. Imaging plane in the scheme shows orientation of individual z-stack images with 0.5 µm spacing that are acquired to cover the whole area that the spindle comprises.

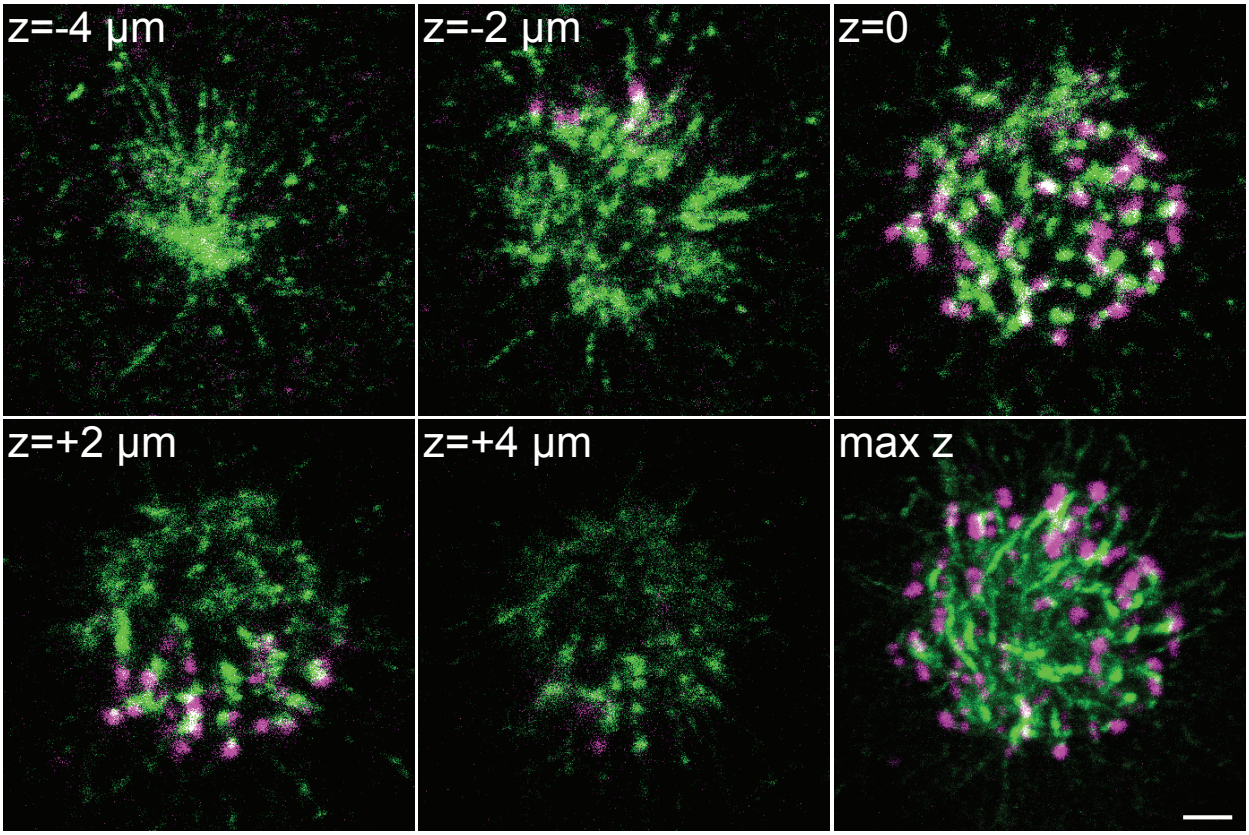

Figure 21. Spindle in a fixed HeLa cell expressing PRC1-GFP (green) and mRFP-CENP-B (magenta) oriented vertically with respect to the imaging plane, as shown in the scheme above. Images of different z-slices (central plane of the spindle z = 0, two images below, z = 4 µm and z = 2 µm, and above, z = +2 µm and z = +4 µm), maximum projection of a z-stack (max z). Scale bar, 2 µm.

These two approaches with described spindle orientations were used to count the number of PRC1-labeled bundles and sister kinetochore pairs per individual spindle. In horizontally oriented spindles, the number of PRC1-labeled bundles per spindle was 63 ± 2 and the number of kinetochore pairs was 59 ± 2 (n = 29 spindles). Even though these numbers may be somewhat underestimated due to occasional overlaying of neighboring sister kinetochores or neighboring PRC1-labeled bundles, we conclude that the mean number of PRC1-labeled bundles is roughly the same as the mean number of chromosomes. In vertically oriented spindles the average number of PRC1-labeled bundles per spindle is measured to be 75 ± 3 and the number of kinetochore pairs 72 ± 3 (n = 16 spindles). In comparison with the same analysis in horizontal spindles, these numbers here were larger due to less frequent overlaying of neighboring bundles. Importantly, here majority of kinetochores can be observed to be positioned right next to PRC1-labeled bundles. Images of vertically oriented spindles confirmed our observation in horizontally oriented spindles that the mean number of PRC1-labeled bundles is nearly the same as the number of kinetochore pairs (Figure 22).

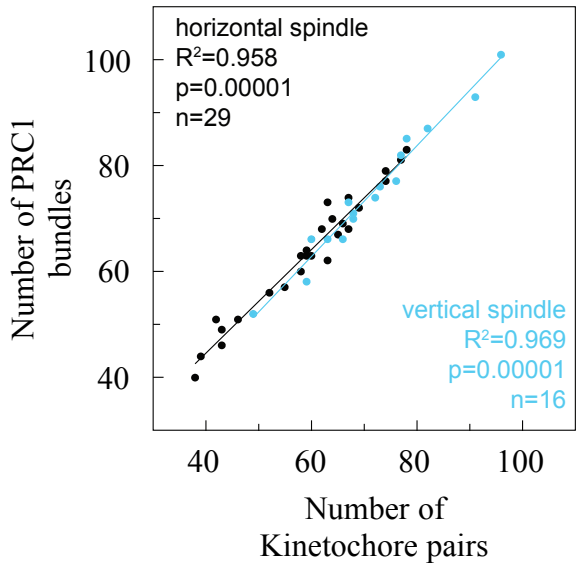

Figure 22. Correlation between the number of PRC1-labeled bundles and the number of pairs of sister kinetochores counted throughout horizontal (black) and vertical (blue) spindles of fixed HeLa cells in metaphase. Data points represent individual spindles, lines show linear fits. Data information: n, number of cells; R2, coefficient of determination; P, P-value from a t-test.

Once we knew how number of chromosomes varies from one spindle to another, we were interested to determine how the spindle changes to effectively perform its role regardless of the number of chromosomes that need to be correctly integrated and segregated. Here measured proportions of the spindle, length and width were taken into account with respect to the number of chromosomes. Whether spindle length and width vary to accommodate different numbers of overlap bundles and chromosomes was investigated. As expected, both spindle length and width increased with the number of kinetochore pairs and PRC1-labeled fibers. The increase in width was similar to the increase in length, which indicates that spindles accommodate a larger number of chromosomes by increasing their length and width to a similar extent.

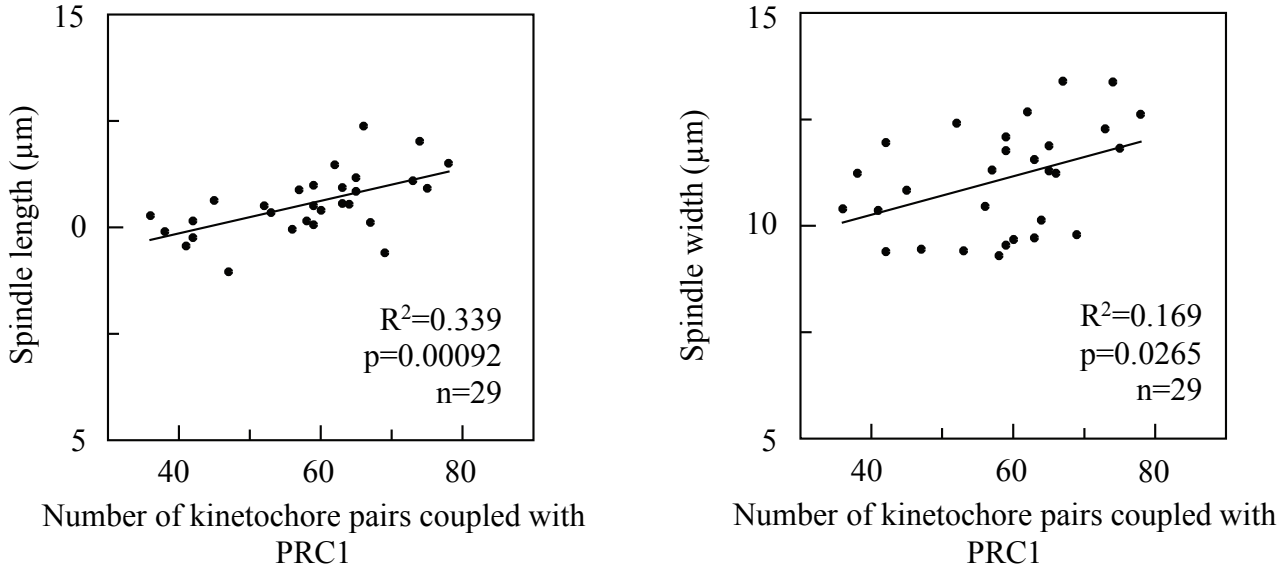

Figure 23. Spindle length and spindle width as a function of the number of kinetochore pairs coupled with PRC1-labeled bundles. Data points represent individual spindles, lines show linear fits. Data information: n, number of cells; R2, coefficient of determination; P, P-value from a t-test.

It is interesting to consider the necessity to increase spindle's length and width depending on the number of chromosomes. To examine the spatial distribution of overlap fibers in spindles with different numbers of chromosomes, the density of PRC1-labeled fibers coupled with kinetochores was measured. Density here applies to their number per unit area in the equatorial plane of vertical as well as horizontal spindles. Quantification revealed that the density does not depend significantly on the number of coupled pairs suggesting that the width of the spindle is accommodated to maintain neighboring PRC1-containing fibers at similar distances regardless of the total number of chromosomes in the spindle (Figure 24). Findings described above show that the number of chromosomes is important for the establishment of number of overlap antiparallel PRC1-containing regions.

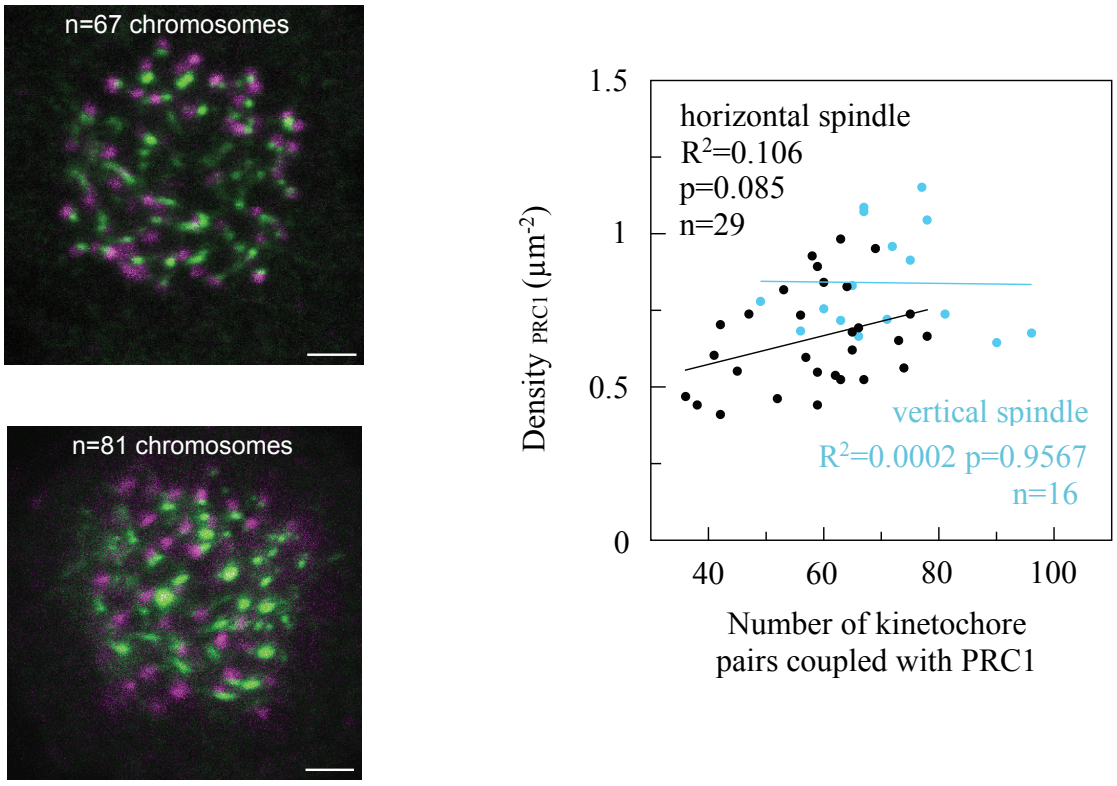

Figure 24. Left: a cross section of vertical spindles with 67 (upper) and 81 (bottom) chromosomes. On the right: number of kinetochore pairs coupled with PRC1-labeled bundles per unit area of the cross section of the central part of horizontal (black) and vertical (blue) spindles as a function of the number of kinetochore pairs coupled with PRC1-labeled bundles in the spindle. Data information: n, number of cells; R^2, coefficient of determination; P, P-value from a t-test. Scale bar, 2 µm.

4.1.1 Overlap fibers are linked to kinetochore fibers

With above described findings, we have shown that there is a strong correlation between the number of overlap bundles and chromosomes. However, this find does not provide information about the association between PRC1-labeled spots and sister kinetochore pairs. Distances between axis connecting midpoints of sister kinetochores and the corresponding bridging fiber were measured in previous work focused on the bridging fiber on the periphery of the spindle. We next set out to determine whether these components in our experiments with fixed cells show similar spatial arrangement and whether certain individual spots are positioned close to each other. Same spindles that served for quantifications above were now used to measure the distances between a PRC1-labeled bundle and the nearest kinetochore pair. A PRC1-labeled bundle and a kinetochore pair were defined as associated if the distance between them was smaller than 0.3 μm (see Materials and Methods), based on a previous measurement of this distance for outermost kinetochores [2]. We found that > 90% of PRC1-labeled fibers were positioned next to a kinetochore pair, both in horizontal and vertical spindles (n > 1,000 PRC1-labeled bundles in each approach, Figure 25). This quantification revealed that the PRC1-labeled fibers and sister kinetochores are not just randomly distributed in the transversal cross section of metaphase spindles. In vertical spindles the proximity between two differently labeled spots were even more obvious. In analyzed spindles we did not often observe random associations between three or more individual PRC1-labeled fibers and kinetochores in metaphase. Also, no distinct groups with random numbers of associated pairs were determined in fixed spindles in metaphase. On the contrary to closely positioned green and magenta pairs, analysis revealed only a small fraction of PRC1-labeled bundles and kinetochore pairs that were not mutually linked (Figure 25).

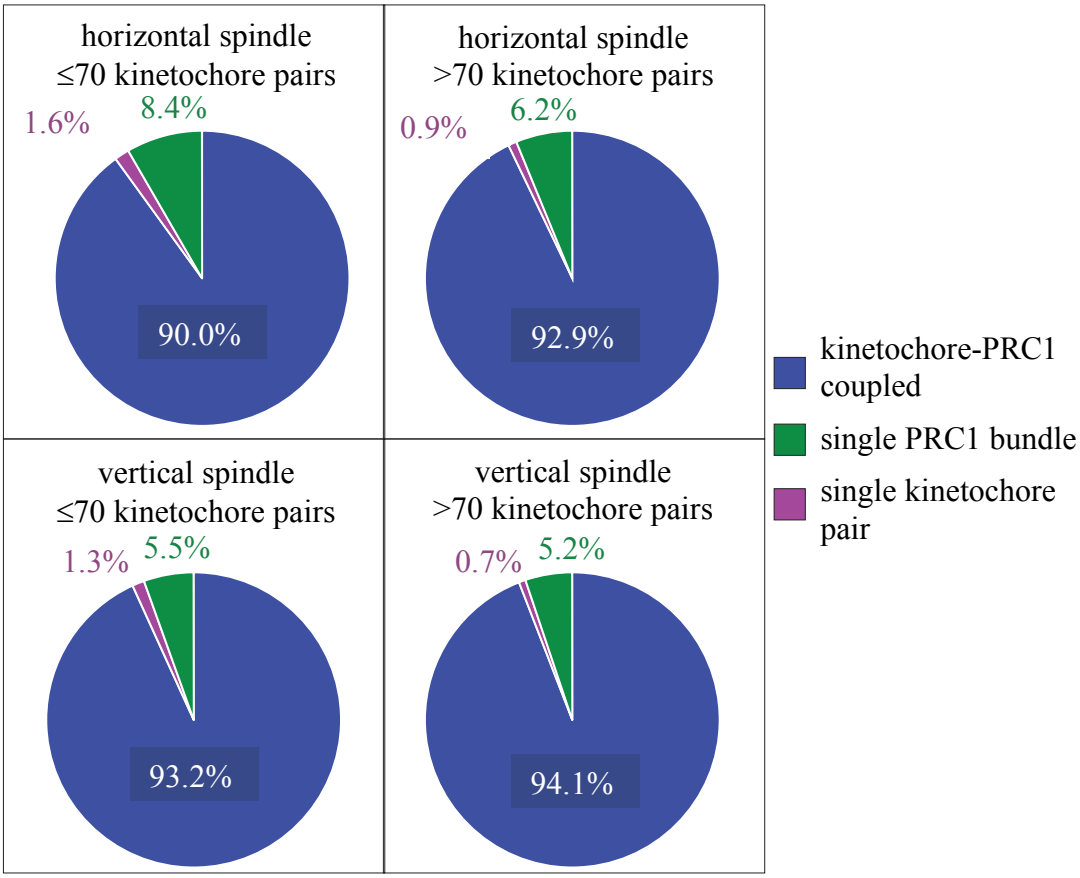

Figure 25. Pie charts showing the fraction of PRC1-labeled bundles associated with kinetochore pairs (blue), PRC1-labeled bundles not associated with kinetochores (green) and kinetochores not associated with PRC1 bundles (magenta) in horizontal (top row) and vertical spindles (bottom row) from cells with up to 70 chromosomes (left column) and more than 70 chromosomes (right column). Horizontal spindles contained a total of 1,786 kinetochore-PRC1 pairs (n = 29 cells) and vertical spindles 1,133 kinetochore-PRC1 pairs (n = 16 cells).

We wanted to further fortify this postulated association which was estimated with above described approach in static spindles. Determined pairs gave a good starting point to examine whether distances between PRC1-labeled bundles and sister kinetochores are a sign of their association. Thus, we set out to investigate how PRC1-labeled bundles and kinetochores behave in time. If they are indeed associated, imaging of vertical spindles with a time component would reveal whether closely positioned magenta (kinetochore) and green (PRC1-labeled bundle) spots show mutually dependent movements. Here, central parts around the metaphase plate were imaged

and all individual spots that correspond to PRC1 and kinetochores per spindle were tracked. The dynamics in the transversal cross section was analyzed and revealed that in the majority of the associated pairs, the PRC1-labeled bundle and the kinetochores moved along identical trajectories or moved in the same direction and passed similar distances, whereas some pairs showed movements in mutually independent directions (Figure 26a). A PRC1-labeled fiber and a kinetochore were termed associated if they moved together for at least five time frames (~1 min) (n = 274 associated and individual PRC1-labeled fibers and kinetochores from five cells). Quantification revealed 82.5 ± 2.7% (n = 226) of mutually associated fibers and kinetochores, whereas 11.7 ± 2.3% (n = 32) of PRC1-labeled fibers did not have a coupled kinetochore with which they moved along the same or similar trajectories, and 5.8 ± 0.8% (n = 16) of kinetochores were observed as free of any PRC1-labeled fiber.

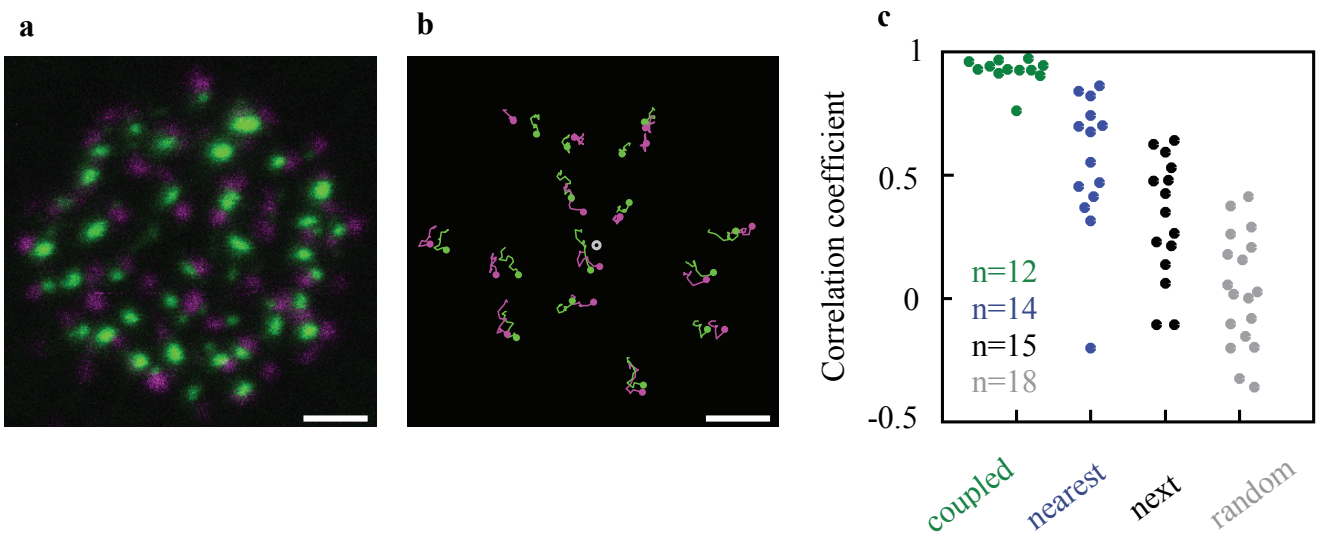

Figure 26. a) Central plane of the spindle in a live HeLa cell expressing PRC1-GFP (green) and mRFP-CENP-B (magenta) oriented vertically with respect to the imaging plane. b) Examples of trajectories, with respect to the spindle's center of the mass (white circle in the center), of individual PRC1-GFP (green) and corresponding mRFP-CENP-B (magenta) signals from the spindle in left image that moved together for at least 200 s. Dots represent starting points of trajectories, t = 0 s. Trajectories finish at t = 200 s. c) correlation coefficients between trajectories (with respect to the spindle's center of the mass) of a kinetochore pair and the trajectories of the PRC1-labeled fiber coupled with the kinetochore pair (green), the nearest neighbor PRC1-labeled fiber (blue), the next nearest neighbor (black) and a randomly chosen PRC1-labeled fiber (gray); n, the number of trajectories from three cells. Scale bar, 2 µm.

This experiment additionally gave insights into dynamic interplay between neighboring spots. Here, pairs at the periphery were chosen for analysis because those were most easily distinguished from their neighbors. Within this group, several types of behavior of neighboring PRC1-labeled fibers and kinetochores were observed. Due to the better clarity of events in this region, a stricter criterion was used for determining the interaction of PRC1-labeled fibers and kinetochores: PRC1-labeled fiber and kinetochore were termed associated if they were moving along the same or similar trajectories during the entire acquired video (~5 min). We found that 65.7 ± 4.1% of PRC1-labeled fibers and kinetochores were mutually associated. Within this group, we included the following occasional events as well: one PRC1-labeled fiber moved together with two kinetochores which do not seem to be sisters; PRC1-labeled fiber moved together with sister kinetochores until they both disappeared from the imaged planes in the *z*-direction at the same time. Other scenarios in which we term a kinetochore and PRC1-labeled fiber uncoupled (34.3 ± 4.1%) were as follows: first, the kinetochore seemed to be free of any PRC1-labeled fiber, and after a certain time, a PRC1 signal appeared and they started moving together; a kinetochore and PRC1-labeled fiber moved together and eventually separated to a distance greater than 0.3 μm; kinetochore first moved alone and at a certain time point moved to the vicinity of a neighboring PRC1 and they started moving together; a PRC1-labeled fiber merged with the neighboring bundle and they appeared as a single PRC1-labeled fiber; kinetochore moved with the PRC1 until PRC1 disappeared; kinetochore moved with the PRC1, at one point separated from it, and subsequently associated with the same bundle to continue moving together. The observed events reveal the dynamic nature of the interactions between PRC1-labeled fibers and kinetochores (Figure 27a). However, most of the time PRC1-labeled bridging fibers and kinetochores are in close proximity and move along same or similar trajectories (Figure 27b). Our described approach and results give novel insights into the organization of metaphase mitotic spindle and reveal abundance and specificity of overlap antiparallel bundles which were not observed previously.

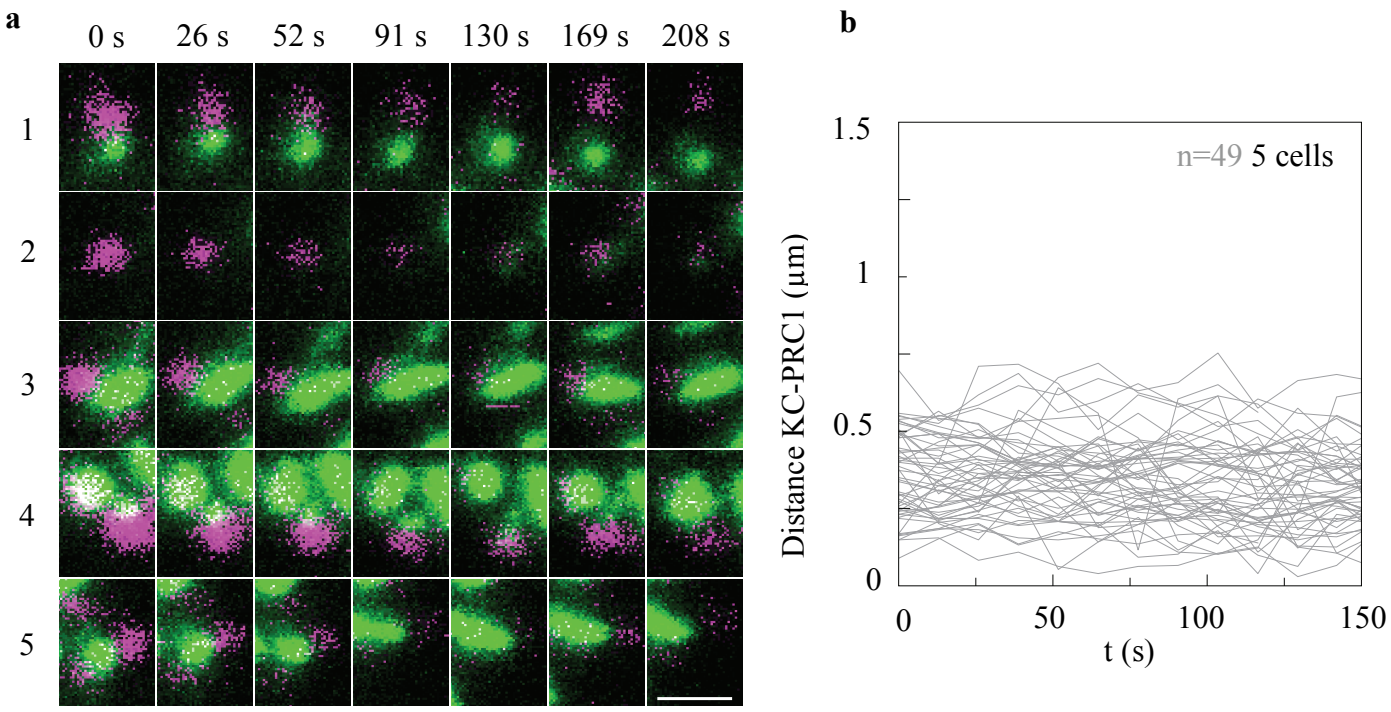

Figure 27. a) Examples of scenarios observed in dynamic interplay of PRC1-labeled bundles (green) and kinetochores (magenta) from the spindle in (A). Row 1: PRC1-labeled bundle and kinetochore move together until they separate at 130 s. Row 2: kinetochore is free of any PRC1-labeled bundle until it appears at 130 s. Row 3: kinetochore and PRC1-labeled bundle move together. Row 4: kinetochore moves with PRC1-labeled bundle which merges with neighboring bundle at 169 s. Row 5: two kinetochores move together with a single PRC1-labeled bundle. b) dynamics between PRC1-labeled bundles and corresponding kinetochores in live HeLa cells with distance between them plotted during 150 s. n, number of pairs. Scale bar, 2 µm.

4.1.2 Endogenous PRC1 distribution and perturbation of bridging fiber parameters

When PRC1 protein is overexpressed, its substantial fraction is cytosolic and localizes to brightly stained ring-shaped arrays around the interphase nucleus [31]. Thus, a cell line used here expresses PRC1-GFP but also it expresses endogenous nontagged PRC1 as well. To quantify the level of overexpression Western blot analysis was performed in cell lines used in this research. The quantification revealed 1.64 ± 0.10 times higher expression of PRC1 in PRC1-GFP tagged cell line compared with unlabeled HeLa cells (n = 6 independent experiments, P = 0.0004) while tubulin-GFP cell line showed the same expression level of PRC1 as determined in unlabeled cells (Figure 28).

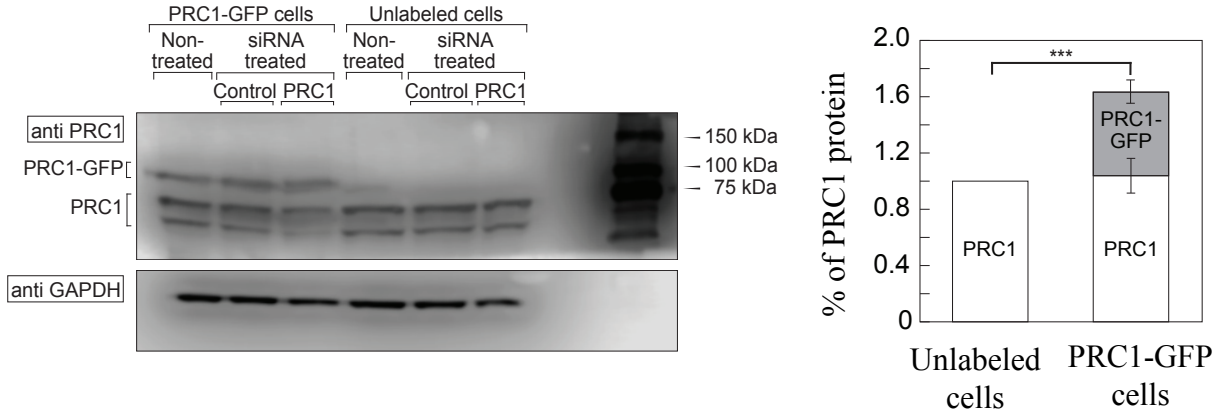

Figure 28. Western blot for PRC1 in various HeLa cell lines and conditions, as denoted in the figure. PRC1 expression in PRC1-GFP HeLa cells was 60.97 ± 10.01% higher than in unlabeled cells. Synchronized cells were lysed in lysis buffer 29 h after transfection. Cell lysates were subjected to SDS-PAGE (12% polyacrylamide), transferred on to a nitrocellulose membrane and immunoblotted with anti-PRC1 and anti-GAPDH antibodies used as a loading control. Intensities of the Western blot bands of endogenous PRC1 isoforms (61–71 kDa) and PRC1-GFP (98 kDa) were quantified as described in Materials and Methods. P-value was 0.0004.

In order to exclude the side effects of PRC1 overexpression the aim is to define the localization and distribution of endogenous PRC1 in metaphase spindles and compare it with the localization of PRC1-GFP. HeLa cells stably expressing tubulin-GFP and immunostained for PRC1 (see Materials and Methods) were used. Tubulin signal in this cell line enabled to identify the k-fibers and bridging fibers. Since we were interested in the distribution of PRC1 in a well-established metaphase, the proteasome inhibitor MG132 (see Materials and Methods) was used to ensure that the cells are arrested at this particular stage. Endogenous PRC1 was found to localize to the metaphase spindle with enrichment in its central part (Figure 29), as previously shown [2, 31]. The tubulin-GFP labeled cell line enabled to determine individual bridging fibers throughout metaphase spindles. They were determined as the tubulin-GFP signal that spans the region between two sister k-fibers. Localization of endogenous PRC1 could be precisely determined in our experiments. In cells used here 97.8 ± 0.1% of the bridging fibers were found immunostained for endogenous PRC1 (n = 46 bridges in 10 cells; Figure 29). Thus, endogenous PRC1 localizes to the bridging fibers throughout metaphase spindles. In addition to this basic interpretation, the endogenous PRC1 signal was observed to extend to the region of k-fibers (determined by tubulin-GFP signal), proximal to the estimated position of the kinetochore. This observation independently suggests that PRC1-labeled fibers are bound to sister k-fibers.

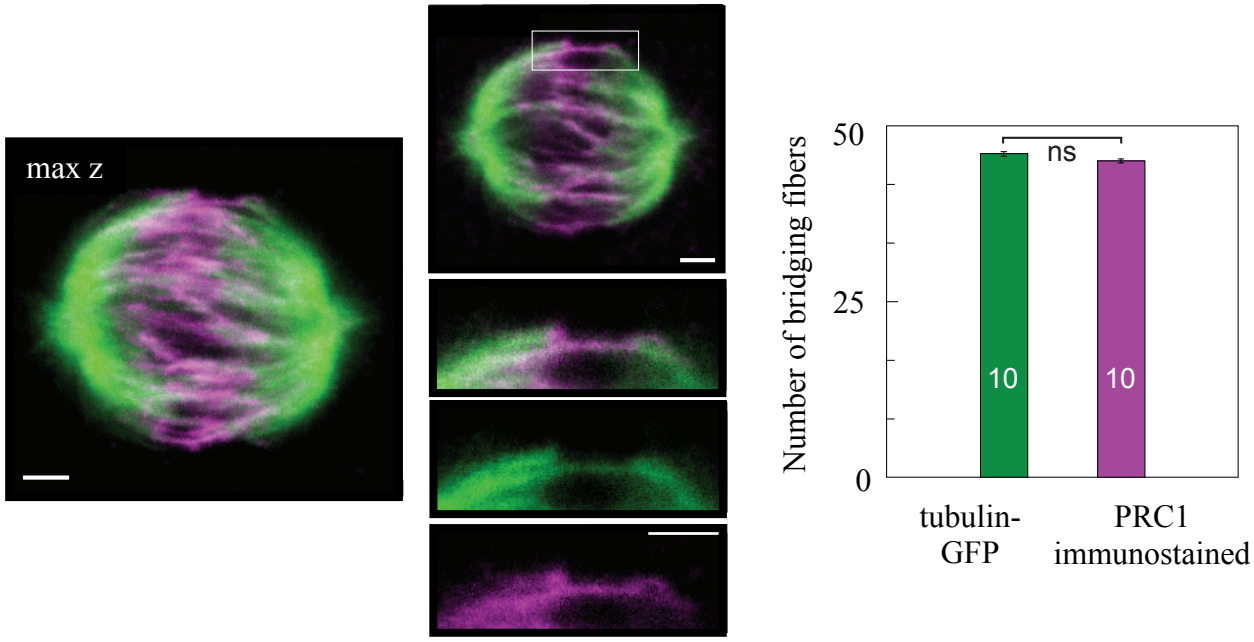

Figure 29. Left: MG132 arrested HeLa cell stably expressing tubulin-GFP (green) and immunostained for endogenous PRC1 (Alexa Fluor-555 shown in magenta) in maximum projection. Middle: one selected z-plane with enlargements of the boxed region (top: merge, middle: GFP, bottom: Alexa Fluor-555) below the first image which show the bridging fiber determined as the line connecting two ends of the sister k-fibers in green channel and localization of endogenous PRC1 (magenta). Right: Quantification of tubulin-GFP bridging fibers (green bar) immunostained for endogenous PRC1 (magenta bar). Scale bar, 2 μm.

Next, the signal of endogenous immunostained PRC1 was quantified and compared with the signal of PRC1-GFP. We tracked pole-to-pole tubulin-GFP signals of the sister k-fibers and the corresponding bridging fiber in the green channel, and measured intensity profiles of endogenous PRC1 in the red channel (Figure 30), which confirmed localization of endogenous PRC1 in the central part of the spindle (n = 15 bridges from 10 cells). Similarly, pole-to-pole intensity profiles of PRC1-labeled bundles in the cell line expressing PRC1-GFP showed localization of PRC1-GFP in the central part of the spindle (n = 50 bridges from 10 cells; Figure 30). The length of the PRC1 signal, L_{PRC1}, is defined as the width of the peak in the intensity profile. The length of the endogenous PRC1 signal was 4.95 ± 0.18 μm (n = 15 bridges from 10 cells), whereas the length of the PRC1-GFP signal was 5.49 ± 0.17 μm (n = 50 bridges from 10 cells, P = 0.10; Figure 30).

These results confirm that PRC1-GFP localizes in the same regions as endogenous PRC1. Thus, antiparallel microtubule overlaps that bind PRC1 are present in the central part of bridging fibers in metaphase spindles and extend over a well-defined region. We next wanted to know whether PRC1 signal parameters in the bridging fiber depend on the distance of the fiber from the spindle long axis because k-fibers at the periphery of the spindle are longer and more curved than those near the spindle long axis We defined two additional measures of the signal intensity: I was defined as the total intensity in the pole-to-pole intensity profile divided by the contour length of this intensity profile (Materials and Methods), and I_{cross} as the total intensity under the peak in the intensity profile acquired transversely to the PRC1 signal (Materials and Methods). L_{PRC1}, I and I_{cross} of the endogenous immunostained PRC1 was measured, as well as of PRC1-GFP in fixed and live cells throughout the spindle. In all these conditions, the parameters of the PRC1 signal did not depend on the distance from the spindle long axis. These results suggest that all bridging fibers in the spindle have a similar length of the PRC1-bound antiparallel overlap zone and a similar amount of PRC1, regardless of the length and curvature of the associated k-fibers.

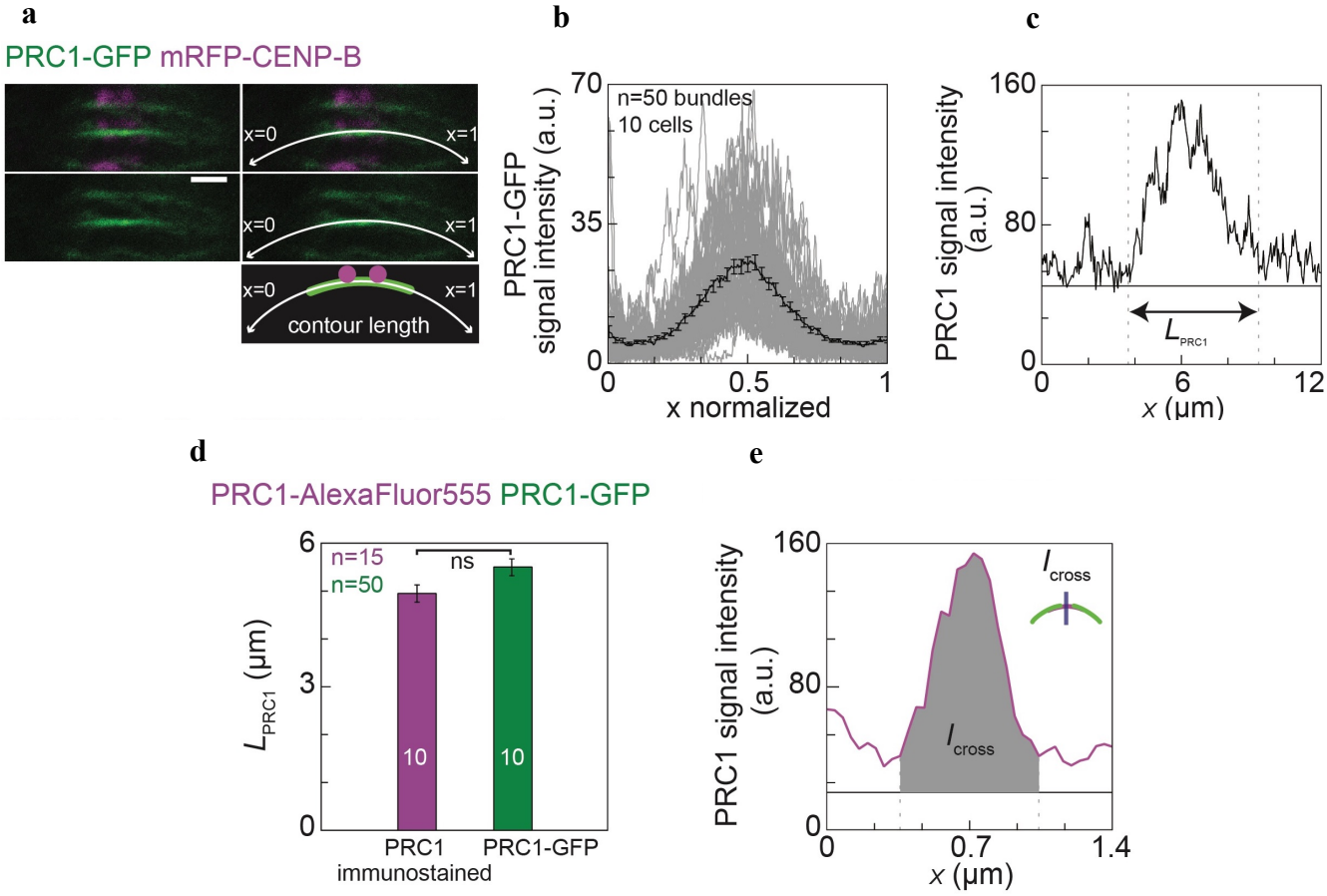

Figure 30. Starting from top left, images show selected area from a HeLa cell expressing PRC1-GFP and mRFP-CENP-B with pole-to-pole tracking (white curve) of PRC1-GFP signal (top, merge; middle, GFP; bottom, scheme). Images of the same spindle without (left) and with the tracked contour are shown. b) Graph shows normalized pole-to-pole intensity profiles of PRC1-GFP acquired in HeLa cells expressing PRC1-GFP and mRFP-CENP-B. c) Graph shows example of length measurement of the immunostained PRC1 signal (L PRC1) in HeLa cell expressing tubulin-GFP and immunostained for PRC1. d) Graph with bars shows comparison of the length L_{PRC1} between PRC1-GFP signal (green corresponds to the PRC1 fused to GFP from a PRC1-GFP cell line) and PRC1-Alexa Fluor-555 (magenta corresponds to the endogenous immunostained PRC1) (P = 0.10). e) Cross section signal intensity of the immunostained endogenous PRC1 (magenta line) from a HeLa cell expressing tubulin-GFP and immunostained for PRC1. Area under the peak is defined as I cross, measured at the position of the blue line as in scheme. Horizontal lines mark the background signal (black line), and vertical lines delimit the area (gray) where the signal was measured.Data information: numbers in bars are number of cells; n, number of bridging fibers; error bars, s.e.m.; ns, not significant difference ($P \geq 0.05$, t-test). Scale bar, 2 µm.

Previous experiments showed that knockdown of PRC1 by small interfering RNA (siRNA) reduces the thickness of the bridging fiber on the outermost part of the spindle [2]. To characterize the effect of PRC1 silencing on the whole metaphase spindle, mild PRC1 knockdown was used in order to maintain spindle integrity in HeLa cells expressing tubulin-GFP and mRFP-CENP-B (Materials and Methods). Images of cells treated with PRC1 siRNA and control siRNA were acquired 24 h after transfection. Western blot analysis showed that in unlabeled HeLa cells treated with PRC1 siRNA the amount of PRC1 was reduced by 51.10 ± 5.49% compared to control cells (n = 3 independent experiments, P = 0.0092), whereas in cells expressing tubulin-GFP the amount of PRC1 was reduced by 53.40 ± 11.76% (n = 6 independent experiments, P = 0.0478, Figure 31).

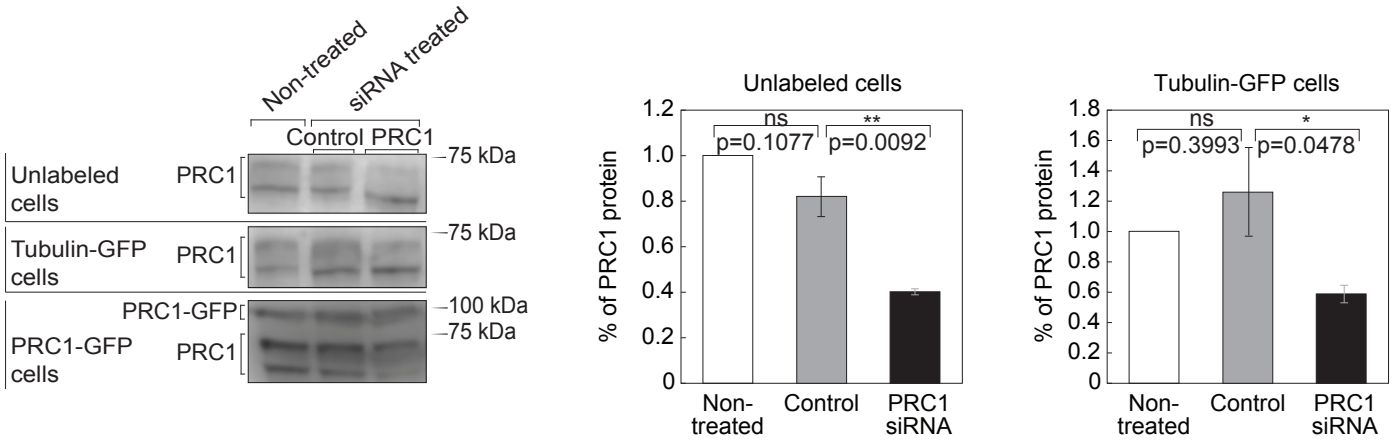

Figure 31. Western blot showing PRC1 protein from unlabeled cells, tubulin-GFP HeLa cell line, and PRC1-GFP HeLa cell line. Graphs show quantification of Western blots. Please note a decrease of the amount of PRC1 after treatment with PRC1 siRNA. HeLa cells grown on 6-well plates were transfected with 200 nM control or PRC1 siRNA. Synchronized cells were lysed in lysis buffer 29 h after transfection. Cell lysates were subjected to SDS-PAGE (12% polyacrylamide), transferred on to a nitrocellulose membrane and immunoblotted with anti-PRC1 and anti-GAPDH antibodies. Percent of PRC1 protein was calculated from Western blot band intensities measured in Image Studio Lite program after normalizing to the corresponding GAPDH band intensity. The data were acquired from three to six independent experiments. Please note that the tubulin-GFP HeLa was the least viable of the cell lines and thus the data varied. P-values are given in the graphs.

It is known that PRC1 is important for stability and integrity of overlap regions [35, 44]. The aim here is to determine how the reduced amount of PRC1 crosslinker affects the bridging microtubule bundle. Thus, signal intensities of tubulin-GFP in the bridging fiber and the k-fiber were used to determine whether the number of microtubules in the bridging fiber was changed due to reduced amount of PRC1. Following the method described in [2], we measured the signal intensity of tubulin-GFP between sister kinetochores, I_b, and across the k-fiber, laterally of kinetochore, I_{bk}. I_b is interpreted as the signal of the bridging fiber, and I_{bk} as the signal of the bundle consisting of the bridging fiber and the k-fiber together. In cells treated with control siRNA (control cells), the ratio I_b/I_{bk} was 0.44 ± 0.01 ($n = 16$ bridges in nine cells, Figure 32), consistent with previous results [2]. PRC1 knockdown reduced the ratio I_b/I_{bk} to 0.33 ± 0.01 ($n = 21$ bridges in six cells, $P = 0.0003$). The level of reduction was constant regardless of the distance of the bridging fiber from the spindle long axis. The signal intensity I_b was reduced by roughly 28% after PRC1 knockdown, which is interpreted as the reduction in the number of microtubules in the bridging fiber. On the contrary, the signal intensity $I_k = I_{bk} - I_b$, which corresponds to the number of microtubules in the k-fiber, was not affected significantly by PRC1 siRNA treatment ($P = 0.6$). Thus, our results suggest that PRC1 knockdown reduces the number of microtubules in the bridging fibers throughout the spindle.

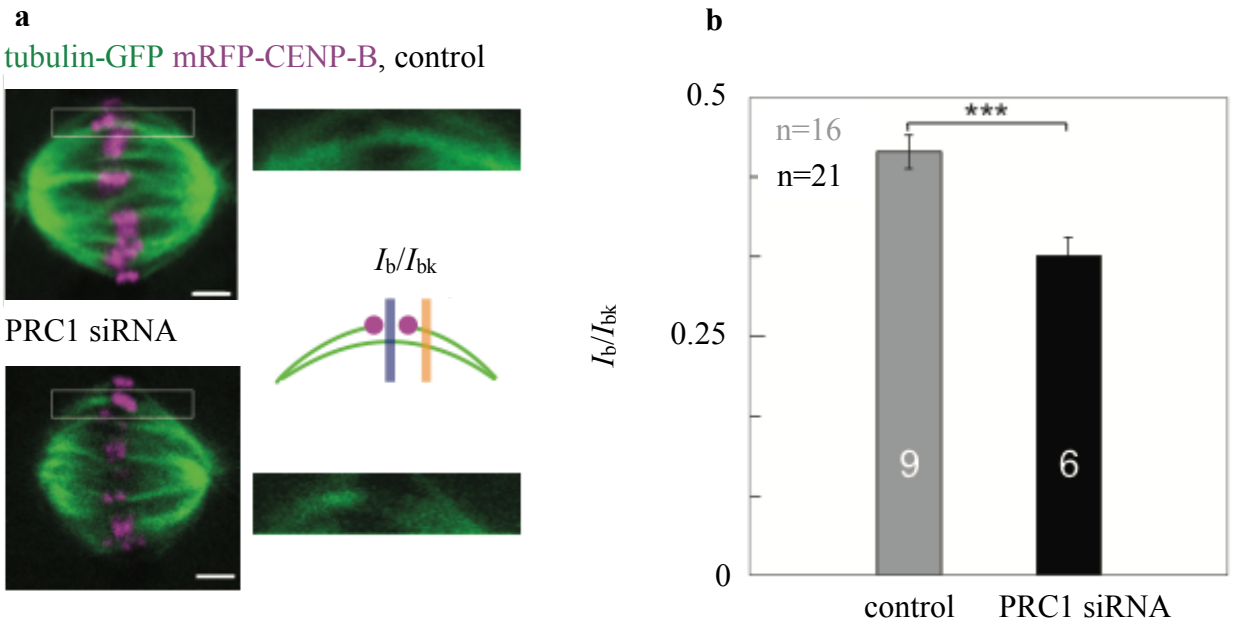

Figure 32. a) Images of HeLa cells stably expressing tubulin-GFP (green) and transiently mRFP-CENP-B (magenta) treated with control siRNA (left images) and siRNA targeting PRC1 (right images). Enlargements of the boxed region, shown to the right of the image of the whole spindle, are focused on the bridging fiber. b) Graph shows mean ratio of signal intensities of the bridging fiber (I_b, measured at the position of a blue line as in scheme) and sum of the bridging and k-fiber (I_{bk}, measured at the position of the orange line as in scheme), measured in control cells (gray bar) and PRC1 siRNA-treated cells (black bar) (P = 0.0003). Scale bar, 2 μm.

Indications for importance of bridging fiber in force balance have been described. It was shown that bridging fiber between the outermost sister k-fibers balances tension and compression within a k-fiber [2]. Since above described finding revealed that PRC1 knockdown reduces the number of microtubules in the bridging fiber, next aim is to test whether this consequence affected distances between sister kinetochores and spindle length and width. The distance between centers of sister kinetochores, d_k, was reduced from 1.00 ± 0.02 μm in control cells (n = 79 pairs of sister kinetochores in 11 cells) to 0.88 ± 0.02 μm in cells treated with PRC1 siRNA (n = 76 pairs of sister kinetochores in 10 cells, P = 0.0001, Figure 33). The distance between sister kinetochores did not depend on their distance from the spindle long axis, in both control cells and those treated with PRC1 siRNA. Spindle length and width did not change significantly after PRC1 knockdown. We

conclude that PRC1 knockdown results in a decreased distance between sister kinetochores, which we interpret as a decrease in interkinetochore tension.

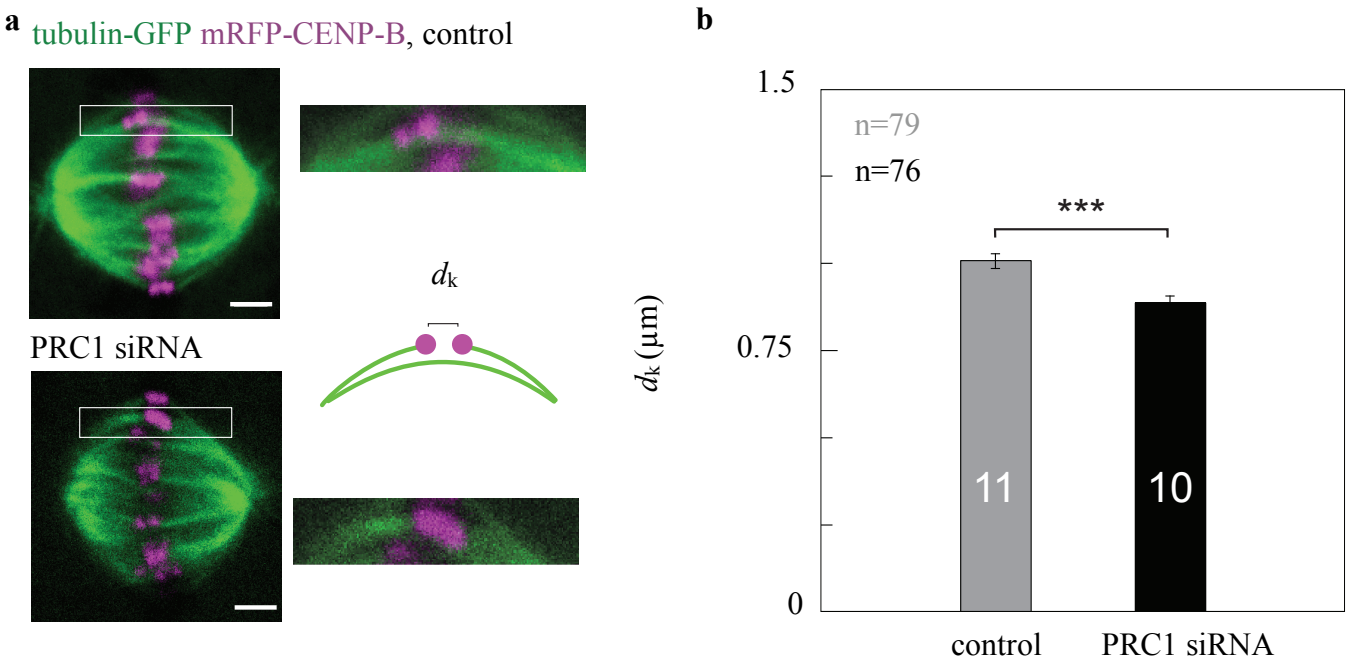

Figure 33. a) Images of HeLa cells stably expressing tubulin-GFP (green) and transiently mRFP-CENP-B (magenta) treated with control siRNA (left images) and siRNA targeting PRC1 (right images). Enlargements of the boxed region, shown to the right of the image of the whole spindle, are focused on sister kinetochores. b) Mean interkinetochore distance (d k, see scheme) measured in control cells (gray bar) and PRC1 siRNA-treated cells (black bar) (P = 0.0001). Scale bar, 2 µm.

To investigate the changes of the microtubule overlap region in the bridging fiber induced by PRC1 knockdown, HeLa cells expressing tubulin-GFP were used, and immunostained for PRC1 (Materials and Methods). An overall reduction in the PRC1 signal in the metaphase spindle was found in cells treated with PRC1 siRNA compared with control cells. In control cells, the length of immunostained PRC1 signal, L_{PRC1}, was 4.96 ± 0.08 µm (n = 29 bridges in 10 cells), which was similar to L_{PRC1} in non-treated synchronized cells described above (P = 0.95), and it did not depend on the distance from the spindle long axis. L_{PRC1} of immunostained PRC1 could not be determined in cells treated with PRC1 siRNA due to its low signal. PRC1 signal intensity, I, was found to be

reduced by 41.33 ± 1.70% (P = 0.0001), which was also independent of the distance from the spindle long axis. These data confirm the reduction in PRC1 intensity in the overlap regions due to PRC1 knockdown.

To further determine the resulting difference between overlap fibers in control and PRC1 siRNA-treated cells, HeLa cells expressing PRC1-GFP from a BAC immunostained for PRC1 were used. Western blots showed that in PRC1-GFP cell line the amount of PRC1 was reduced by 51.78 ± 5.40% in cells treated with PRC1 siRNA compared to control cells (n = 3 individual experiments, P = 0.0020). Next, signals of both immunostained PRC1 and PRC1-GFP in control and PRC1 siRNA cells were quantified as described above. Interestingly, neither the length, L_{PRC1}, of immunostained PRC1 nor the length of PRC1-GFP was altered by PRC1 knockdown. As expected, both PRC1 signal intensity, I, and the signal intensity of the cross section, I_{cross}, were reduced by PRC1 knockdown. Spindle length and width were not affected by PRC1 knockdown. Taken together, our data show that a mild knockdown of PRC1 (~50%) leads to a reduction in PRC1 signal intensity in the metaphase spindle, whereas the length of the PRC1-labeled regions remains unchanged. Now that we showed how specific antiparallel overlaps are throughout the spindle, it is interesting to consider that motor proteins localize to same areas as PRC1. Their contribution whilst they walk along antiparallel regions which are at their ends bound to sister k-fibers has been described recently [73].

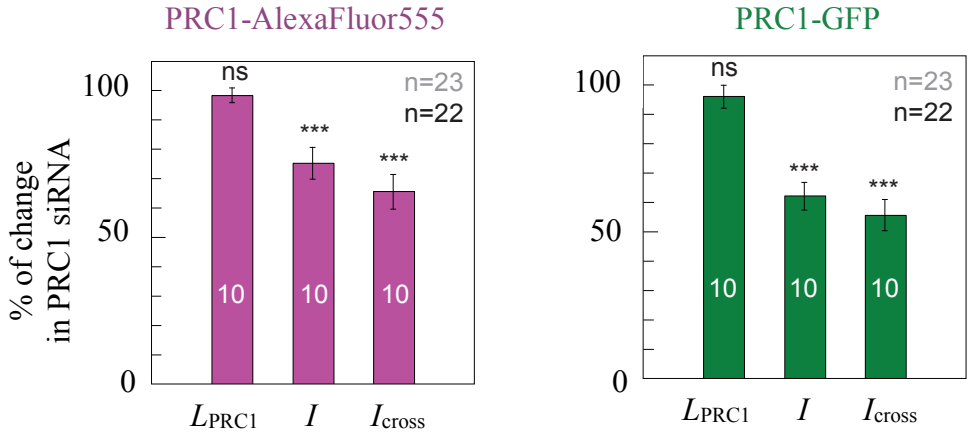

Figure 34. Graph on the left showing the length of the immunostained PRC1 signal, L_{PRC1} (P = 0.5167), signal intensity, I (P = 0.0003), and I_{cross} (P = 0.0001) in siRNA targeting PRC1 in comparison with control HeLa cells expressing PRC1-GFP and immunostained for PRC1. Graph on the right shows same quantifications as in the left but for PRC1-GFP signal.

Based on described results, it is revealed that nearly all overlap bundles in the spindle act as bridging fibers that link sister k-fibers and that each sister kinetochore pair contains a bridging fiber in metaphase.

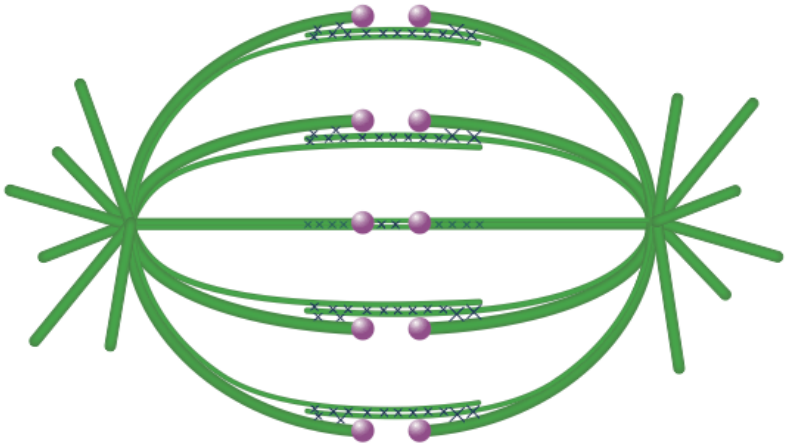

Figure 35. Scheme representing one-to-one association between PRC1-labeled bundles and sister kinetochores in metaphase.

4.2 MICROTUBULE BUNDLES POSSESS LEFT-HANDED HELICITY

Above the spindle proportions and the abundance and parameters of bridging fibers were described. Next goal is to investigate the three-dimensional (3D) organization of bridging fibers and k-fibers in metaphase. In continuation, findings will be described that are published in 2018 in a peer-reviewed scientific journal Nature Communication as an article entitled "The mitotic spindle is chiral due to torques within microtubule bundles" by authors Novak Maja, Polak Bruno, Simunić Juraj, Boban Zvonimir, Kuzmić Barbara Thomae W. Andreas, Tolić Iva M and Pavin Nenad. First, we had to determine whether the investigated bundles are continuous from vicinity of one pole all the way to the vicinity of the other pole. This precondition was confirmed by using stimulated emission depletion (STED) super-resolution microscopy in experiments performed by Juraj Simunić and Barbara Kuzmić with provided expertise from Andreas W. Thomae at Ludwig-Maximilians University of Munich. As investigating bridging fibers and k-fibers in metaphase spindle, distinct shapes that these bundles can acquire were observed. On the periphery of the horizontal spindle, that is in the two outermost groups of bundles in confocal images, the shapes resembling letter C can be observed. Bundles in the vicinity of the spindle long axis often acquire shapes resembling the letter S (Figure 36).

Hela, SiR- Tubulin, CENPA-GFP

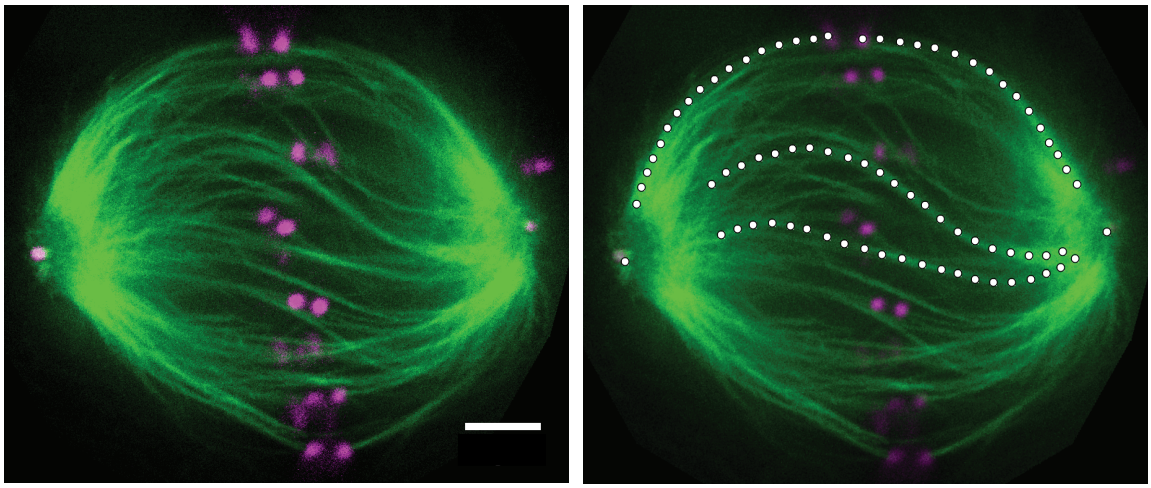

Figure 36. STED image (single z-plane) of metaphase spindle in a live HeLa cell expressing EGFP-CENP-A and EGFP-centrin1 (both shown in magenta), panel on the right shows traces of microtubule bundles superimposed on the image where we observed continuity of microtubule bundles and their different shapes in metaphase. Scale bar, 2 μm.

STED imaging provided a good insight into xy components of the bundles in one plane but the third, z component required for the 3D reconstruction is still lacking due to the resolution limit in z direction with an approximate value of 800 nm. This was a barrier that disables examination of the spatial organization of individual bundles with high precision. For this reason, vertically oriented spindles were first examined because they bypass the mentioned limitation. For detailed insight into 3D arrangement of bundles, vertically oriented spindles were used to reconstruct the spatial organization of individual bridging fibers along their length in a direction from one spindle pole to another. As already described, in these spindles optical sections are roughly perpendicular to the bundles, allowing for precise determination of the bundle position in each section and thus of the whole contour (see Methods). Fixed HeLa cells that express GFP-tagged PRC1 [30, 31] and mRFP-CENP-B determining metaphase were used. When imaged in this manner and viewed end-on along the spindle axis in the projection containing images that cover all z planes of individual spindles, the bundles reveal rosette-like appearance. If the bundles had a planar shape they would form an aster-like arrangement when viewed from this perspective (Figure 37). With this approach on perspective of vertical spindles, it is revealed that the arrows connecting bottom and top end of each bundle rotate clockwise, implying that bundles follow a left-handed helical path along the spindle axis.

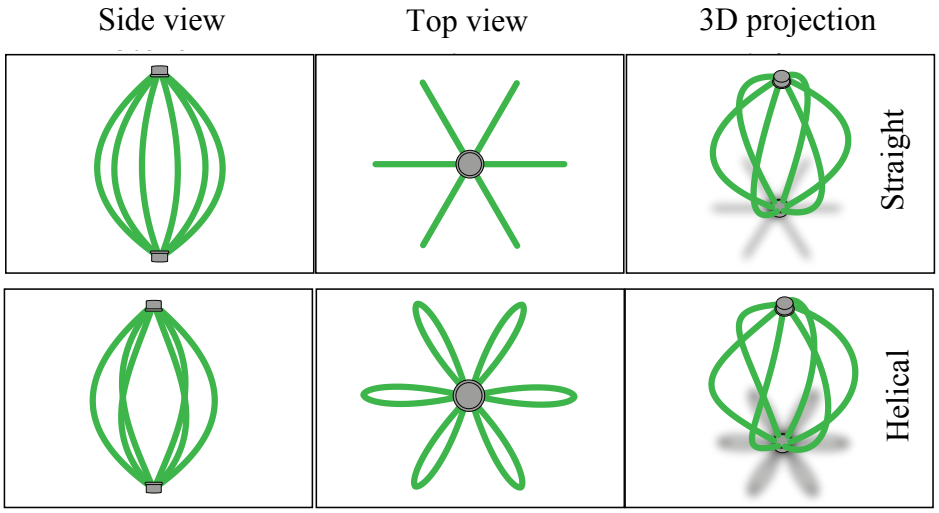

Figure 37. Schemes show spindle with either planar (top row) or helical (bottom row) spatial arrangement as viewed from different perspectives. Comparison between aster-like and rosette-like arrangement from the top view and a corresponding 3D projection. Assembled by Zvonimir Boban.

The helicity of bundles was defined as the average change in angle with height (Figure 38a), where negative numbers denote left-handed helicity. Quantification of tracked bridging bundles revealed the value of their helicity to be -2.5 ± 0.2 deg μm^{-1} (mean ± s.e.m., n = 415 bundles from 10 cells). When live cells with labeled tubulin (U2OS cells) were used, the result of the helicity of k-fibers coupled to bridging fibers was obtained with value of -1.3±0.2 deg μm^{-1}. Even though this value here is smaller, helicity was also present in these bundles as well. Since investigated bundles consist of individual microtubules, we come to conclusion that individual microtubules within the bundle twist around each other like metal wires in a steel wire rope (Figure 38b).

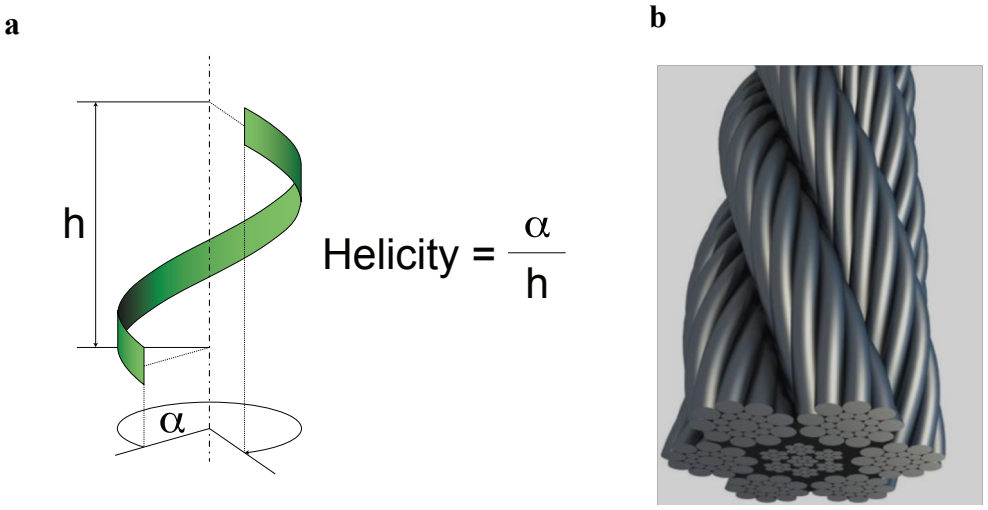

Figure 38. a) Schematic representation of the microtubule bundle helicity measurement and a steel wire rope. b) Note metal wires that twist around each other as we propose do the individual microtubules within a bundle [indiamart.com].

In order to eliminate the possible side effects of different orientation of analyzed spindles, next goal was to quantify observed helicity in horizontal spindles as well. Here, the acquired z-stacks need to be rearranged in order to obtain the slices perpendicular to the spindle axis, similar to the z-stacks of vertical spindles (Figure 39; see Methods). The method of stack rearrangement revealed that bundles in horizontal spindles possess left-handed helicity as is the case in vertical spindles (Figure 40). Here horizontal spindles had higher left-handed helicity (-3.3 ± 0.2 deg μm^{-1}, mean ± s.e.m., n = 388 bundles from 10 cells) than vertical ones (p value from a Student's t-test = 0.012 (two-tailed and two-sample unequal-variance), and the reason for this should be further investigated. To further validate helicity of bundles different conditions were used which all revealed its presence (Table 1). Even though the values vary depending on the labeling, spindle orientation, and cell lines, the bundles consistently twist in a left-handed direction and do not strongly deviate from a value of -2 deg μm^{-1} (Table 1). With conducted experiments we can confirm that the mitotic spindle is a chiral object where microtubule bundles follow a left-handed helical pattern.

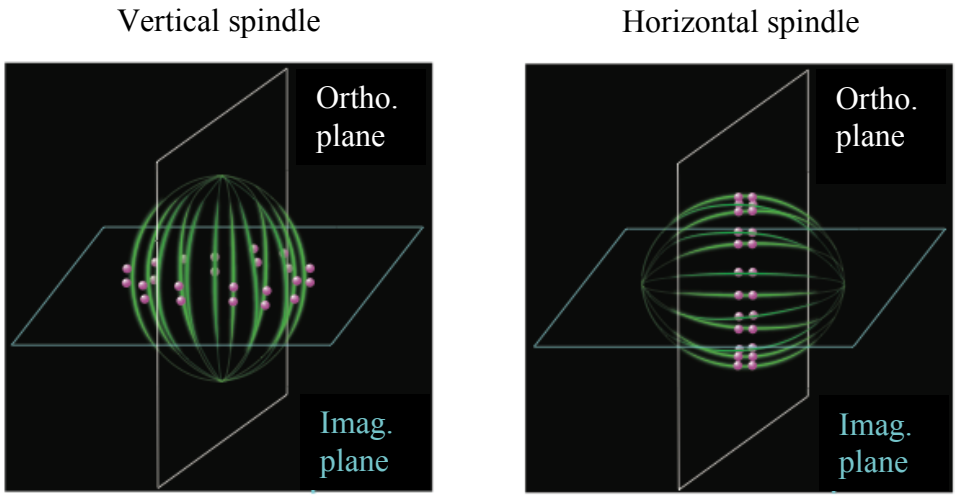

Figure 39. Imaging scheme of vertically (left) and horizontally (right) oriented spindle. White rectangles indicate the orientation of the imaging plane and the idea to rearrange the acquired z-stack into the orthogonal plane in order to obtain slices perpendicular to the imaging axis.

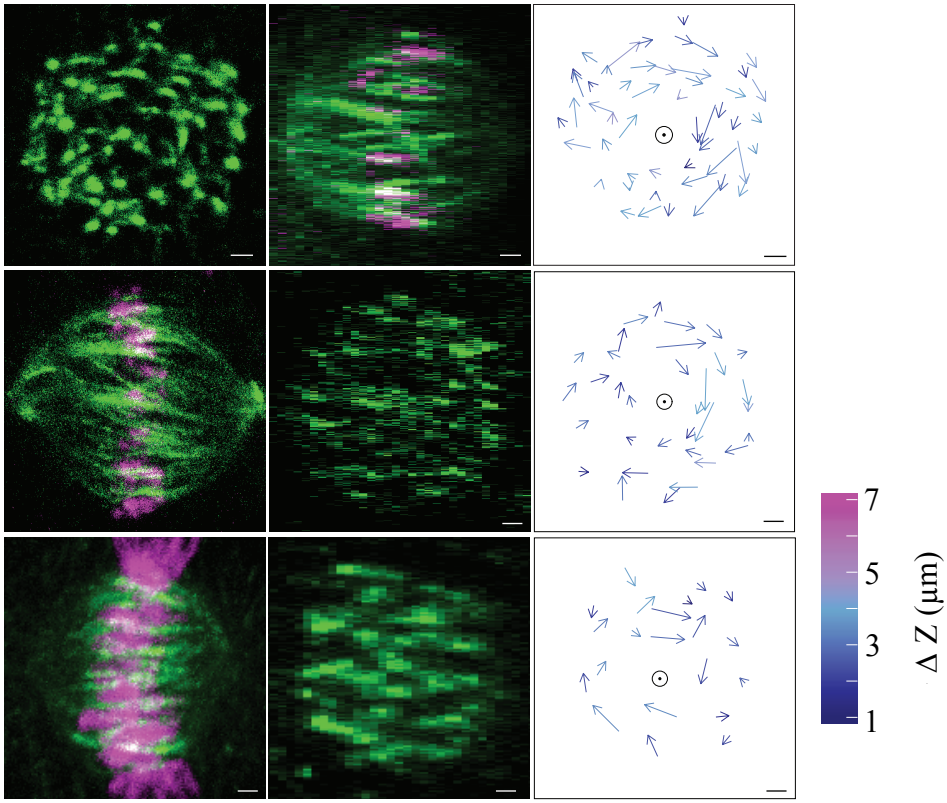

Figure 40. Imaging plane of a vertical spindle in a fixed HeLa cell expressing PRC1-GFP and mRFP-CENP-B (only PRC1-GFP is shown) (left); orthogonal plane of the same spindle (middle); arrows connecting starting and ending points of PRC1-GFP bundles traced upwards (right). Longer arrows roughly correspond to larger twist around the spindle axis (circle), colors show z-distance between starting and ending points. Scale bar, 1 μm.

Table 1. Values of bundle helicity depending on the labeling, spindle orientation, and cell lines

Cell line	Live / fixed	Spindle orientation	Helicity (deg μm^{-1}) mean ± s.e.m.	N.of cells	N. of bundles
HeLa PRC1-GFP	fixed	vertical	-2.5 ± 0.2	10	415
HeLa PRC1-GFP	fixed	horizontal	-3.3 ± 0.2	10	388
HeLa Anti-PRC1	fixed	horizontal	-3.0 ± 0.3	10	226
HeLa PRC1-GFP	live	vertical	-1.2 ± 0.1	27	918
HeLa PRC1-GFP	live	horizontal	-2.6 ± 0.2	10	218
U2OS Anti-PRC1	fixed	horizontal	-2.5 ± 0.6	10	159
U2OS mCherry-tubulin	live	vertical	-1.3 ± 0.2	20	478

As obtained data was analyzed, the question was which contributing factors cause the chirality to be established in the spindle. Certain hypothetical contributing mechanisms were examined. From our point of view, the chirality could be established as a result of forces acting within microtubule bundles in the central spindle or on the other hand causal forces can be exerted by astral microtubules that interact with the cell cortex on two opposite sides of the spindle. We first examined the contributing factors within central parts of the spindle, and motor proteins came into question since it is known that they rotate the microtubule as they walk on the microtubule lattice, as is the case for kinesin-5 [86]. The most direct effect we could achieve was by using the drug that will cause the kinesin-5 to detach from the microtubule lattice and fall off the spindle. Thus, we used S-trityl-L-cysteine (STLC), which prevents movement of kinesin-5 along the microtubule lattice by targeting its catalytic domain and inhibiting ATP-ase activity [87, 88]. The experimental setup was established as described in the Methods section. Briefly, the whole untreated spindle was imaged, then the drug was added and the same spindle was imaged again 5 and 10 minutes after the addition of the drug. STLC treatment caused the bundle traces to change from a clockwise rotation to a more random distribution. Both vertical and horizontal spindles were examined. Average values of helicity in vertical spindles were close to zero after the addition of the drug (Figure 41). In horizontal spindles STLC reduced the helicity threefold with respect to the initial values (Table 2). Mock treatments used as a control did not affect significantly the helical property of the spindles, which additionally showed that repeatedly imaging the same spindles does not intervene with our experimental setup (Figure 41). Importantly, STLC did not change spindle lengths and widths, which could affect our conclusions if happened. Based on these results, we conclude that kinesin-5 has an important role in the maintenance of the spindle chirality. To explore whether cortical pulling forces contribute to the maintenance of chirality, we used latrunculin A, an agent that depolymerizes actin cortex, thus disrupting forces exerted between astral microtubules and cell cortex [89]. Here no significant effect was observed and the helical property of bundles was preserved (Table 2). We conclude that cortical pulling forces have a minor effect on the shape of microtubule bundles within the spindle.

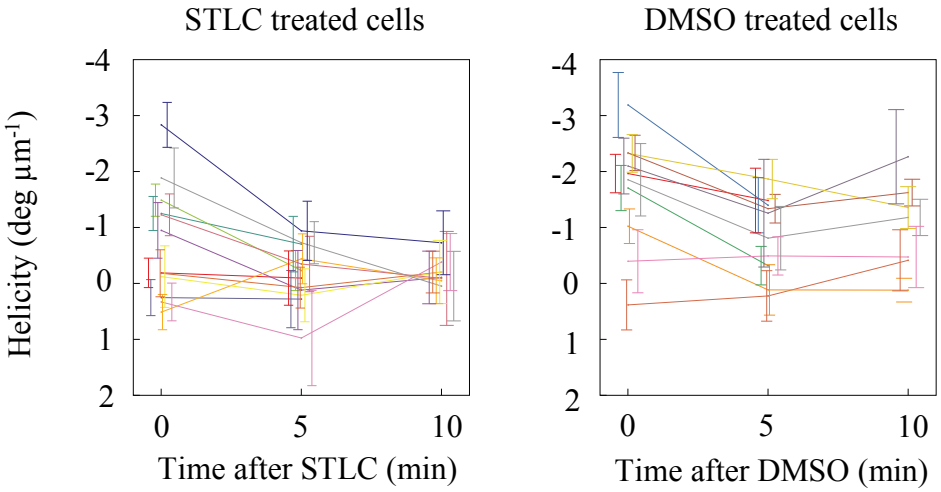

Figure 41. Helicity of vertical spindles from individual live HeLa cells expressing PRC1-GFP measured before and at 5 and 10 minutes after treatment with either STLC (left) or DMSO (solvent for STLC, control, right). Values from each cell are represented by different color and connected with lines.

Table 2. Summary of spindle helicity values from live cells treated with STLC, Latrunculin A or DMSO in different conditions.

Cell type	Treatment	Helicity (deg µm^{-1}) mean ± s.e.m.	Number of cells	Number of bundles	p-values
HeLa horizontal	None	-2.6 ± 0.2	10	218	$7{\cdot}10^{-11}$
HeLa horizontal	STLC (5-25 min)	-0.9 ± 0.2	16	317	
HeLa vertical	None (0 min)	-1.2 ± 0.1	27	918	$2{\cdot}10^{-9}$
HeLa vertical	STLC (5 min)	-0.2 ± 0.2	12	395	$2{\cdot}10^{-6}$
HeLa vertical	STLC (10 min)	-0.2 ± 0.2	8	203	
HeLa vertical	None (0 min)	-1.2 ± 0.1	27	918	0.042
HeLa vertical	DMSO (5 min)	-0.9 ± 0.2	10	337	0.33
HeLa vertical	DMSO (10 min)	-1.0 ± 0.2	7	228	
U2OS vertical	None	-1.3 ± 0.2	20	478	$3{\cdot}10^{-6}$
U2OS vertical	STLC (10 min)	0.01 ± 0.2	8	141	
HeLa horizontal	None	-2.6 ± 0.2	10	218	0.41
HeLa horizontal	Lat A (1-2 hours)	-2.4 ± 0.2	10	240	

We conclude that the chiral architecture of the spindle we described relies mainly on forces generated within microtubule bundles by proteins that interact with and walk along the microtubule lattice. Chirality is an intriguing property of the biological world present at all scales ranging from molecules to whole organisms, and with our finding the spindle can now be classified as a chiral structure as well.

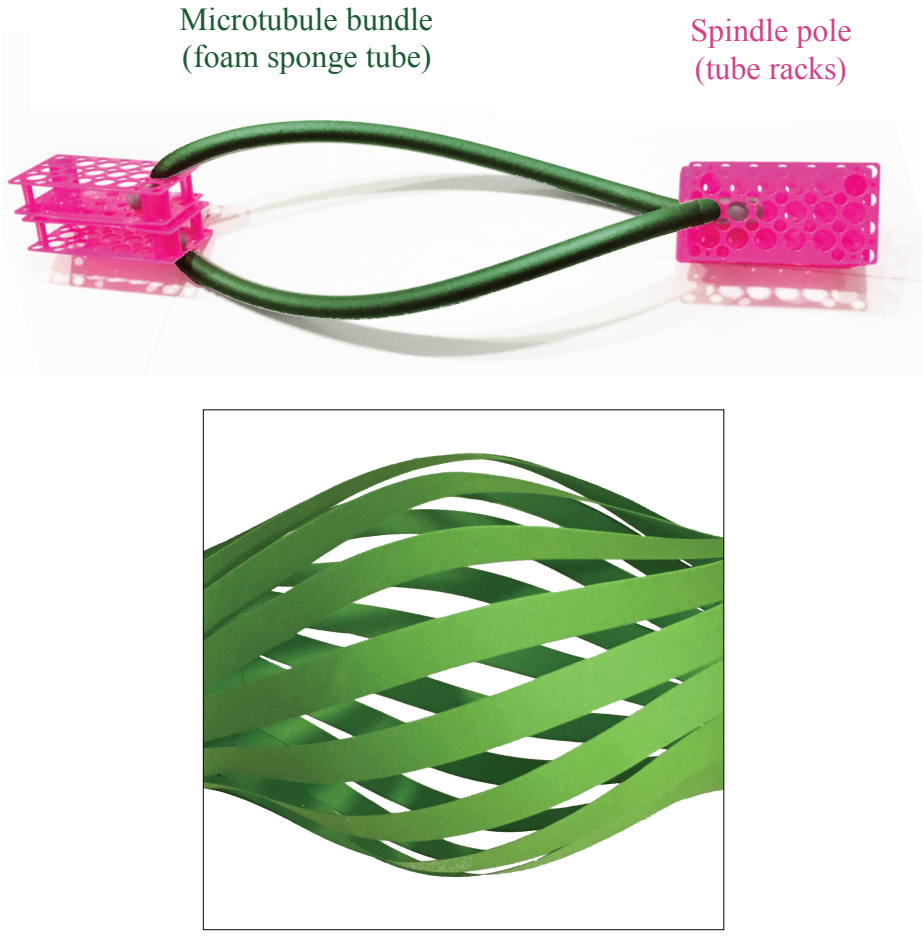

Figure 42. Scheme summarizing conclusion on spatial arrangement of microtubule bundles and the whole metaphase spindle. Helical shape of microtubule bundles (model made of foam sponge tube and tube racks) determines the chiral architecture of the metaphase spindle (paper model of a spindle).

4.3 CONCLUDING DISCUSSION

The spindle is a robust complex structure not easily accessible when it comes to studying of forces and individual structural components. To study such a complex structure, today most commonly used approach is microscopy coupled with treatment of the studied system in a way that different forms of perturbations give insights into importance of different components. Treatments can be performed on a level of one sort of protein with commonly used approaches as are for example RNA interference and/or optogenetics. Another approach is used on a level of direct mechanical perturbation applied in a specific region of interest. The example here is laser ablation coupled with simultaneous acquisition of time series on a microscope. The laser used for severing of distinct precisely determined regions is a femtosecond laser which enables application of short pulses set on specific, usually high wavelengths (above 700 nm). The description of bridging fiber on the periphery of the spindle [2] provided motivation to explore whether the revealed specific association is present in regions other than the outermost positions in the metaphase spindle. By imaging z-stacks of images that cover whole individual metaphase spindles we first found that there is a strong correlation between number of chromosomes and overlap bundles per spindle in HeLa cells with variable number of chromosomes. Dynamics in transversal cross section revealed that these closely positioned components move in pairs and often along identical trajectories. This type of interaction between overlap bundles and k-fibers throughout the spindle has not been previously observed.

When the protein of interest is expressed from a Bacterial Artificial Chromosome (BAC), it is often simultaneously overexpressed. Previous studies have shown that PRC1 exhibits a slightly different localization when overexpressed. In particular, a substantial fraction of the protein is cytosolic and localizes to brightly stained ring-shaped arrays around the interphase nucleus [31]. Immunocytochemistry performed in this work revealed that endogenous PRC1 binds to overlap regions already in well-established metaphase. Localization and affinity of PRC1 to bind to microtubules at the onset of anaphase have been widely proposed [31, 35, 61] and now we revealed that stable PRC1 containing bundles are established even earlier and are associated with individual sister k-fibers throughout the whole metaphase spindles. This crosslinker seems to be key to stabilizing and incorporating new microtubules into the bridging fiber as they grow along the existing ones as indicated by RNAi specifically targeting PRC1. If all PRC1 molecules are

already occupied between antiparallel microtubules, it seems as if no other protein can hold them tightly bound within overlap regions. The reduced distance between sister kinetochores in RNAi experiment indicates the consequential perturbation of force distribution along k-fibers in metaphase. Despite this difference, spindle length and width were preserved. According to our previously published model [2], the compression in the bridging fiber counteracts the tension at the end of the k-fiber. Thus, when both forces are reduced, the spindle shape can remain unchanged, which is in agreement with our measurements.

Motor proteins that localize to antiparallel region can exert forces that affect anaphase dynamics. Pushing forces exerted by bridging fiber are able to segregate chromosomes independently of the spindle pole and the most promising candidate motor that contributes to chromosome and pole separation is MKLP1 as shown in a recent research [73].

The chirality of the spindle is a novel organizational property not yet observed in human spindles. The exact role of the chirality in the spindle is difficult to discuss at the moment since it could solely be a property of a system with all its components making it organized in a well-defined structural order. Physical interpretation of this find was conducted in group of Nenad Pavin at Faculty of science in Zagreb, Croatia. Applied theory together with experiments suggests that the twisting moment in the microtubule bundle is around $-10\,\mathrm{pN\mu m}$ and the bending moment $140\,\mathrm{pN\mu m}$. The theory predicts that torques generate curved shapes of bundles, where the twisting component of the torque is required for the helical component of the shape [90]. This level of organization has been previously observed in yeast spindles, which consist of a single rod-shaped microtubule bundle [91, 92]. We speculate that kinesin-5 turns antiparallel microtubules around each other while sliding them apart, which generates torque in the microtubule bundles and consequently their helical shape. Moreover, given that kinesin-5 is localized mainly close to the spindle pole [93], it may have a role in the generation of torque at the pole. Alternatively, linear forces acting on microtubules may lead to torsion due to a helical arrangement of tubulin subunits in the microtubule [94, 95]. However, in our experiments with kinesin-5 inactivation spindle length did not change, suggesting that linear forces did not change, thus the observed change in spindle chirality is most likely due to torque exerted by this motor. Finally, in addition to kinesin-5, other mitotic motors, such as kinesin-14, kinesin-8, and dynein [96, 97, 98], may be involved in the generation of torque.

Taken together, research conducted on whole metaphase human spindles revealed existence of stable overlap bundles already in metaphase which are bridging sister k-fibers and balancing force distribution in such elastic elements that span between two opposite spindle poles. Length of the overlap antiparallel region in these bundles is more finely tuned than their thickness and reduction of number of microtubules in the bridging fiber reduces tension exerted on kinetochores. Individual bundles, both parallel (k-fibers) and antiparallel (bridging fibers) possess left-handed helicity in metaphase which results in a chiral organization of the spindle as a whole. For human metaphase spindles this is a newly described property of spatial organization not previously observed.

5 CONCLUSIONS

Spindle is a complex micromachinery involved in a basic process of transferring the genetic information to offspring. Experimental setups developed to study such a structure are various with approaches and are unique with specific questions in the focus. With described approach our goal was to investigate the organization of this remarkable structure as a whole. Imaging the area that comprises the entire spindle in the cytoplasm provided insights into fine levels of bundle organization in metaphase. First, we showed that nearly all overlap microtubules are linked to sister k-fibers. After the discovery of bridging fiber between the outermost k-fibers, this is the first time that all overlap microtubules were given such a specific property that is present throughout the metaphase mitotic spindle. All of these bundles are antiparallel, contain crosslinker PRC1 and link each pair of sister k-fibers in metaphase. Dynamics in the transversal cross section area around the metaphase plate revealed that PRC1 and kinetochores are not completely independent elements but rather spend most of the time moving together in pairs. For example, this approach can in future provide basis for experimental setups in determining the bridging fiber that corresponds to a specific chromosome in the spindle. As a continuation of described one-to-one association between PRC1-labeled bundles and sister kinetochores, novel insights into spatial organization of these bundles were provided with this research. By closely examining individual antiparallel bundles, it is shown that they possess a helical structure, a feature not previously described in human spindle. In metaphase of unperturbed spindles this property is present in majority of individual bundles, thus resulting in the chiral organization of the spindle as a whole. Individual microtubules twist around each other within a bundle which leads to the rotation of the bundle cross-section along its length. By examining the tubulin-labeled bundles, we confirm that this is a general architectural property of the spindle, not limited to specific populations of microtubules. At the moment we can say that motor proteins contribute to the generation of helical shapes of microtubule fibers. In near future, it will be interesting to define the stage of mitosis at which chirality of the spindle appears, and to reveal what aspects of mitotic division rely on this architectural property.

6 REFERENCES

1. Alberts B, Johnson A, Lewis J, Raff M, Roberts K, Walter P: Molecular biology of the cell, Garland Science, Taylor & Francis Group, 2002
2. Kajtez J, Solomatina A, Novak M, Polak B, Vukusic K, Rudiger J, Cojoc G, Milas A, Sumanovac IS, Risteski P, Tavano F, Klemm AH, Roscioli E, Welburn J, Cimini D, Glunčić M, Pavin N, Tolić IM: Overlap microtubules link sister k-fibres and balance the forces on bi-oriented kinetochores. Nat Commun 7: 10298, 2016
3. Hook R: Micrographia, The Royal Society, London, 1665
4. Paweletz N, Walther Flemming: pioneer of mitosis research. Nat Rev Mol Cell Biol, 2(1): 72-75, 2001
5. McIntosh JR, Molodtsov MI, Ataullakhanov FI: Biophysics of mitosis, Q Rev Biophys, 45(2): 147-207, 2012
6. Hartwell LH, Culotti J, Reid B: Genetic control of the cell-division cycle in yeast. I. Detection of mutants, Proc Natl Acad Sci U S A, 66(2): 352-359, 1970
7. Murray A: Cell cycle checkpoints, Curr Opin Biol, 6(6): 872-876, 1994
8. Nigg EA, Stearns T: The centrosome cycle: centriole biogenesis, duplication and inherent asymmetries, 13(10): 1154-1160, 2011
9. Wiese C, Zheng Y: Microtubule nucleation: gamma-tubulin and beyond, Journal of Cell Science, 119(20): 4143-4153, 2006
10. Vleugel M, Kok M, Dogterom M: Understanding force-generating microtubule systems through in vitro reconstitution, Cell Adhesion & Migration, 10 00-00, 10.1080/19336918.2016.1241923, 2016
11. Mitchison T, Kirschner ML: Dynamic instability of microtubule growth, Nature, 312(5991): 237-242, 1984
12. Walker RA, O'Brien ET, Pryer NK, Soboeiro MF, Voter WA, Erickson, HP, Salmon, ED: Dynamic instability of individual microtubules analyzed by video light microscopy: rate constants and transition frequences, J Cell Biol, 107(4): 1437-1448, 1988
13. Brouhard GJ: Dynamic instability 30 years later: complexities in microtubule growth and catastrophe, Mol Biol Cell, 26(7): 1207-1210, 2015

14. Salmon ED, Leslie RJ, Saxton WM, Karow ML, McIntosh JR: Spindle microtubule dynamics in sea urchin embryos: analysis using a fluorescein-labeled tubulin and measurements of fluorescence redistribution after laser photobleaching, J Cell Biol, 99(6): 2165-2174, 1984
15. Inoue S: Polarization optical studies of the mitotic spindle. I. The demonstration of spindle fibers in living cells, Chromosoma, 5(5): 487-500, 1953
16. Amos LA, Hirose K: Studying the Structure of Microtubules by Electron Microscopy. In: Zhou J. (eds) Microtubule Protocols. Methods in Molecular Medicine™, vol 137. Humana Press, 2007
17. Al-Bassam J, Chang F: Regulation of microtubule dynamics by TOG-domain proteins XMAP215/Dis1 and CLASP, Trends Cell Biol, 21(10): 604-614, 2011
18. Brinkley BR, Stubblefield E: The fine structure of the kinetochore of a mammalian cell in vitro, Chromosoma, 19(1): 28-43, 1966
19. Telzer BR, Moses MJ, Rosenbaum JL: Assembly of microtubules onto kinetochores of isolated mitotic chromosomes of HeLa cells, Proc Natl Acad Sci U S A, 72(10): 4023-7, 1975
20. Witt PL, Ris H, Borisy GG, Origin of kinetochore microtubules in Chinese hamster ovary cells, Chromosoma, 81(3): 483-505, 1980
21. De Brabander M, Geuens G, De Mey J, Joniau M: Nucleated assembly of mitotic microtubules in living PTK2 cells after release from nocodazole treatment, Cell Motil, 1(4): 469–483, 1981
22. Tulu US, Fagerstrom C, Ferenz NP, Wadsworth P: Molecular requirements for kinetochore-associated microtubule formation in mammalian cells, Curr Biol, 16(5): 536–541, 2006
23. Maiato H, Rieder CL, Khodjakov A: Kinetochore-driven formation of kinetochore fibers contributes to spindle assembly during animal mitosis, J Cell Biol, 167(5): 831–840, 2004
24. O'Connor C: Chromosome segregation in mitosis: The role of centromeres, Nature Education, 1(1):28, 2008
25. Manning AL, Compton DA: Structural and regulatory roles of nonmotor spindle proteins, Curr Opin Cell Biol, 20(1): 101-106, 2008

26. Merdes A, Heald R, Samejima K, Earnshaw WC, Cleveland DW: Formation of spindle poles by dynein/dynactin-dependent transport of NuMA, J Cell Biol, 149(4): 851-862, 2000
27. Bieling P, Telley IA, Surrey T: A minimal midzone protein module controls formation and length of antiparallel microtubule overlaps, Cell, 142(3): 420 – 432, 2010
28. Subramanian R, Ti SC, Tan L, Darst SA, Kapoor TM: Marking and measuring single microtubules by PRC1 and kinesin-4, Cell, 154(2): 377 – 390, 2013
29. Kapitein LC, Janson ME, van den Wildenberg SM, Hoogenraad CC, Schmidt CF, Peterman EJ: Microtubule-driven multimerization recruits ase1p onto overlapping microtubules, Curr Biol, 18(21):1713-1717, 2008
30. Jiang W, Jimenez G, Wells NJ, Hope TJ, Wahl GM, Hunter T, Fukunaga R: PRC1: a human mitotic spindle-associated CDK substrate protein required for cytokinesis, Mol Cell, 2(6): 877 – 885, 1998
31. Mollinari C, Kleman JP, Jiang W, Schoehn G, Hunter T, Margolis RL: PRC1 is a microtubule binding and bundling protein essential to maintain the mitotic spindle midzone, J Cell Biol, 157(7): 1175 – 1186, 2002
32. Kurasawa Y, Earnshaw WC, Mochizuki Y, Dohmae N, Todokoro K: Essential roles of KIF4 and its binding partner PRC1 in organized central spindle midzone formation, EMBO J, 23(16): 3237 – 3248, 2004
33. Zhu C, Jiang W: Cell cycle-dependent translocation of PRC1 on the spindle by Kif4 is essential for midzone formation and cytokinesis, Proc Natl Acad Sci USA, 102(2): 343 – 348, 2005
34. Pellman D, Bagget M, Tu YH, Fink GR, Tu H: Two microtubuleassociated proteins required for anaphase spindle movement in Saccharomyces cerevisiae. J Cell Biol, 130(6): 1373 – 1385, 1995
35. Zhu C, Lau E, Schwarzenbacher R, Bossy-Wetzel E, Jiang W: Spatiotemporal control of spindle midzone formation by PRC1 in human cells, Proc Natl Acad Sci USA, 103(16): 6196 – 6201, 2006
36. Janson ME, Loughlin R, Loiodice I, Fu C, Brunner D, Nedelec FJ, Tran PT: Crosslinkers and motors organize dynamic microtubules to form stable bipolar arrays in fission yeast, Cell, 128(2): 357 – 368, 2007

37. Verbrugghe KJ, White JG: SPD-1 is required for the formation of the spindle midzone but is not essential for the completion of cytokinesis in C. elegans embryos, Curr Biol, 14(19): 1755 – 1760, 2004
38. Verni F, Somma MP, Gunsalus KC, Bonaccorsi S, Belloni G, Goldberg ML, Gatti M: Feo, the Drosophila homolog of PRC1, is required for central-spindle formation and cytokinesis, Curr Biol, 14(17): 1569 – 1575, 2004
39. Smertenko A, Saleh N, Igarashi H, Mori H, Hauser-Hahn I, Jiang CJ, Sonobe S, Lloyd CW, Hussey PJ: A new class of microtubule-associated proteins in plants, Nat Cell Biol, 2(10): 750 – 753, 2000
40. Subramanian R, Wilson-Kubalek EM, Arthur CP, Bick MJ, Campbell EA, Darst SA, Milligan RA, Kapoor TM: Insights into antiparallel microtubule crosslinking by PRC1, a conserved nonmotor microtubule binding protein, Cell, 142(3): 433 – 443, 2010
41. Kellogg EH, Howes S, Ti S, Ramírez-Aportela E, Kapoor TM, Chacón P, Nogalesa E: Near-atomic cryo-EM structure of PRC1 bound to the microtubule, Proc Natl Acad Sci USA, 113(34): 9430-9439, 2016
42. Fu C, Yan F, Wu F, Wu Q, Whittaker J, Hu H, Hu R, Yao X: Mitotic phosphorylation of PRC1 at Thr470 is required for PRC1 oligomerization and proper central spindle organization, Cell Res, 17(5): 449-457, 2007
43. Tirnauer JS, Bierer BE: EB1 proteins regulate microtubule dynamics, cell polarity, and chromosome stability, J Cell Biol, 149(4): 761-766, 2000
44. Komarova Y, De Groot CO, Grigoriev I, Gouveia SM, Munteanu EL, Schober JM, Honnappa S, Buey RM, Hoogenraad CC, Dogterom M, Borisy GG, Steinmetz MO, Akhmanova A: Mammalian end binding proteins control persistent microtubule growth, J Cell Biol, 184(5): 691-706, 2009
45. Akhmanova A, Steinmetz MO: Tracking the ends: a dynamic protein network controls the fate of microtubule tips, Nat Rev Mol Cell Biol, 9(4): 309-322, 2008
46. Sandblad L, Busch KE, Tittmann P, Gross H, Brunner D, Hoenger A: The Schizosaccharomyces pombe EB1 homolog Mal3p binds and stabilizes the microtubule lattice seam, Cell, 127(7): 1415-1424, 2006

47. des Georges A, Katsuki M, Drummond DR, Osei M, Cross RA, Amos LA: Mal3, the Schizosaccharomyces pombe homolog of EB1, changes the microtubule lattice, Nat Struct Mol Biol, 15(10): 1102-1108, 2008
48. Vitre B, Coquelle FM, Heichette C, Garnier C, Chrétien D, Arnal I: EB1 regulates microtubule dynamics and tubulin sheet closure in vitro, Nat Cell Biol, 10(4): 415-421, 2008
49. Mimori-Kiyosue Y, Shiina N, Tsukita S: The dynamic behavior of the APC-binding protein EB1 on the distal ends of microtubules, Curr Biol, 10(14): 865-868
50. Berrueta L, Kraeft SK, Tirnauer JS, Schuyler SC, Chen LB, Hill DE, Pellman D, Bierer BE: The adenomatous polyposis coli-binding protein EB1 is associated with cytoplasmic and spindle microtubules, Proc Natl Acad Sci U S A, 95(18): 10596-10601, 1998
51. Morrison EE, Askham JM: EB 1 immunofluorescence reveals an increase in growing astral microtubule length and number during anaphase in NRK-52E cells, Eur J Cell Biol, 80(12): 749-753, 2001
52. Piehl M, Tulu US, Wadsworth P, Cassimeris L: Centrosome maturation: measurement of microtubule nucleation throughout the cell cycle by using GFP-tagged EB1, Proc Natl Acad Sci U S A, 101(6): 1584-1588, 2004
53. Tamura N, Draviam VM: Microtubule plus-ends within a mitotic cell are 'moving platforms' with anchoring, signalling and force-coupling roles, Open Biology, 2(11): 120132, 2012
54. Pavin N, Tolić-Nørrelykke IM: Dynein, microtubule and cargo: a ménage à trois, Biochem Soc Trans, 41(6): 1731-1735, 2013
55. Wordeman L: How kinesin motor proteins drive mitotic spindle function: Lessons from molecular assays, Semin Cell Dev Biol, 21(3): 260-268, 2010
56. Imai H, Shima T, Sutoh K, Walker ML, Knight PJ, Kon T, Burgess SA: Direct observation shows superposition and large scale flexibility within cytoplasmic dynein motors moving along microtubules, Nat Commun, 6: 8179, 2015
57. Kim K, Rhee K: The pericentriolar satellite protein CEP90 is crucial for integrity of the mitotic spindle pole, J Cell Sci, 124(Pt 3):338 –347, 2011
58. Pfarr CM, Coue M, Grissom PM, Hays TS, Porter ME, McIntosh JR: Cytoplasmic dynein is localized to kinetochores during mitosis, Nature, 345(6272): 263-265, 1990

59. Kim Y, Heuser JE, Waterman CM, Cleveland DW: CENPE combines a slow, processive motor and a flexible coiled coil to produce an essential motile kinetochore tether, J Cell Biol, 181(3): 411–419, 2008
60. Wordeman L, Wagenbach M, von Dassow G: MCAK facilitates chromosome movement by promoting kinetochore microtubule turnover, J Cell Biol, 179(5): 869-879, 2007
61. Mastronarde DN, McDonald KL, Ding R, McIntosh JR: Interpolar spindle microtubules in PTK cells, J Cell Biol, 123(6 Pt 1): 1475 – 1489, 1993
62. Glotzer M: The 3Ms of central spindle assembly: microtubules, motors and MAPs, Nat Rev Mol Cell Biol, 10(1): 9 – 20, 2009
63. Gatlin JC, Bloom K: Microtubule motors in eukaryotic spindle assembly and maintenance, Semin Cell Dev Biol, 21(3): 248-254, 2010
64. Neef R, Gruneberg U, Kopajtich R, Li X, Nigg EA, Sillje H, Barr FA: Choice of Plk1 docking partners during mitosis and cytokinesis is controlled by the activation state of Cdk1, Nat Cell Biol, 9(4): 436 – 444, 2007
65. Hu CK, Ozlu N, Coughlin M, Steen JJ, Mitchison TJ: Plk1 negatively regulates PRC1 to prevent premature midzone formation before cytokinesis, Mol Biol Cell, 23(14): 2702 – 2711, 2012
66. Milas A, Tolic IM: Relaxation of interkinetochore tension after severing of a k-fiber depends on the length of the k-fiber stub, Matters, doi: 10.19185/matters.201603000025, 2016
67. Tolic IM, Pavin N: Bridging the gap between sister kinetochores, Cell Cycle, 15(9): 1169 – 1170, 2016
68. Asbury CL: Anaphase A: Disassembling microtubules move chromosomes toward spindle poles, Biology (Basel), 6(1): 15, 2017
69. Scholey JM, Civelekoglu-Scholey G, Brust-Mascher I: Anaphase B, Biology (Basel), 5(4), 2016
70. Ganem NJ, Upton K, Compton DA: Efficient mitosis in human cells lacking poleward microtubule flux, Curr. Biol, 15(20):1827–1832, 2005
71. Mazia D: Mitosis and the physiology of cell division, The Cell, Volume 3: Meiosis and Mitosis, 77-412, 1961

72. Kernan J, Bonacci T, Emanuele MJ: Who guards the guardian? Mechanisms that restrain APC/C during the cell cycle, Biochim Biophys Acta Mol Cell Res, 1865(12): 1924-1933, 2018
73. Vukusic K, Buđa R, Bosilj A, Milas A, Pavin N, Tolić, IM: Microtubule sliding within the bridging fiber pushes kinetochore fibers apart to segregate chromosomes, Dev Cell 43(1), 11–23, 2017
74. Poser I, Sarov M, Hutchins JR, Heriche JK, Toyoda Y, Pozniakovsky A, Weigl D, Nitzsche A, Hegemann B, Bird AW: BAC TransgeneOmics: a high-throughput method for exploration of protein function in mammals, Nat Methods, 5(5): 409 – 415, 2008
75. Krull A, Steinborn A, Ananthanarayanan V, Ramunno-Johnson D, Petersohn U, Tolic-Norrelykke IM: A divide and conquer strategy for the maximum likelihood localization of low intensity objects, Opt Express, 22(1): 210 – 228, 2014
76. Lewis JP: Fast normalized cross-correlation, Vision Interface, 10: 120 – 123, 1995
77. Buđa R, Vukušić K, Tolić IM: Dissection and characterization of microtubule bundles in the mitotic spindle using femtosecond laser ablation, Methods Cell Biol, 139:81–101, 2017
78. R Core Team. R: A Language and Environment for Statistical Computing (R Foundation for Statistical Computing, Vienna, Austria), 2016
79. Lancaster OM, Le Berre M, Dimitracopoulos A, Bonazzi D, Zlotek-Zlotkiewicz E, Picone R, Duke T, Piel M, Baum B: Mitotic rounding alters cell geometry to ensure efficient bipolar spindle formation, Dev Cell, 25(3), 270–283, 2013
80. Hell, SW, Reiner G, Cremer C, Stelzer EHK: Aberrations in confocal fluorescence microscopy induced by mismatches in refractive index, J Microsc, 169(3), 391–405, 1993
81. Besseling, TH, Jose J, Van Blaaderen A: Methods to calibrate and scale axial distances in confocal microscopy as a function of refractive index, J Microsc, 257(2), 142–150, 2015
82. Hori A, Morand A, Ikebe C, Frith D, Snijders AP, Toda T: The conserved Wdr8-hMsd1/SSX2IP complex localises to the centrosome and ensures proper spindle length and orientation, Biochem Biophys Res Commun, 468(1-2): 39 – 45, 2015
83. Landry JJ, Pyl PT, Rausch T, Zichner T, Tekkedil MM, Stutz AM, Jauch A, Aiyar RS, Pau G, Delhomme N: The genomic and transcriptomic landscape of a HeLa cell line. G3 (Bethesda) 3(8): 1213 – 1224, 2013

84. Adey A, Burton JN, Kitzman JO, Hiatt JB, Lewis AP, Martin BK, Qiu R, Lee C, Shendure J: The haplotype-resolved genome and epigenome of the aneuploid HeLa cancer cell line, Nature, 500(7461): 207 – 211, 2013
85. Ruess D, Ye LZ, Grond-Ginsbach C: HeLa D98/aH-2 studied by chromosome painting and conventional cytogenetical techniques, Chromosoma, 102(7): 473 – 477, 1993
86. Yajima, J, Mizutani K, Nishizaka T: A torque component present in mitotic kinesin Eg5 revealed by three-dimensional tracking, Nat Struct Mol Biol, 15(10), 1119–1121, 2008
87. DeBonis S, Skoufias DA, Lebeau L, Lopez R, Robin G, Margolis RL, Wade RH, Kozielski F: In vitro screening for inhibitors of the human mitotic kinesin Eg5 with antimitotic and antitumor activities, Mol Cancer Ther, 3(9), 1079–1090, 2004
88. Skoufias DA, DeBonis S, Saoudi Y, Lebeau L, Crevel I, Cross R, Wade RH, Hackney D, Kozielski F: S-trityl-L-cysteine is a reversible, tight binding inhibitor of the human kinesin Eg5 that specifically blocks mitotic progression, J Biol Chem, 281(26), 17559–17569, 2006
89. Spector I, Shochet NR, Kashman Y, Groweiss A: Latrunculins: novel marine toxins that disrupt microfilament organization in cultured cells, Science, 219(4584), 493–495, 1983
90. Novak M, Polak B, Simunić J, Boban Z, Kuzmić B, Thomae AW, Tolić IM, Pavin N: The mitotic spindle is chiral due to torques within microtubule bundles, Nat commun, 9(1), 3571, 2018
91. Winey M, Mamay CL, O'Toole ET, Mastronarde DN, Giddings TH, McDonald KL, McIntosh JR: Three-dimensional ultrastructural analysis of the Saccharomyces cerevisiae mitotic spindle, J Cell Biol, 129(6), 1601–1615, 1995
92. Ding R, McDonald KL, McIntosh JR: Three-dimensional reconstruction and analysis of mitotic spindles from the yeast, Schizosaccharomyces pombe, J Cell Biol, 120(1), 141–151, 1993
93. Iwakiri Y, Kamakura S, Hayase J, Sumimoto H: Interaction of NuMA protein with the kinesin Eg5: its possible role in bipolar spindle assembly and chromosome alignment, Biochem J, 451(2), 195–204, 2013
94. Erickson HP: Microtubule surface lattice and subunit structure and observations on reassembly, J Cell Biol, 60(1), 153–167, 1974

95. Feng Y, Mitran S: Data-driven reduced-order model of microtubule mechanics, Cytoskeleton (Hoboken), 75(2), 45–60, 2018
96. Walker RA, Salmon ED, Endow SA: The Drosophila claret segregation protein is a minus-end directed motor molecule, Nature, 347(6295), 780–782, 1990
97. Bormuth V, Nitzche B, Ruhnow F, Rammner B, Howard J, Diez S: The highly processive kinesin-8, Kip3, switches microtubule protofilaments with a bias toward the left, Biophys J, 103(1), L4–L6, 2012
98. Can S, Dewitt MA, Yildiz A: Bidirectional helical motility of cytoplasmic dynein around microtubules, eLife, 3: e03205, 2014

Web sources

1. http://oregonstate.edu/instruction/bi314/fall11/cellcycle.html
2. http://study.com/academy/lesson/centriole-definition-structure-function.html
3. http://wikivisually.com/wiki/File:Metaaphase.svg
4. http://imgbuddy.com/cell-division-anaphase.asp
5. http://courses.lumenlearning.com/wmopen-biology1/the-steps-of-mitosis
6. http://www.indiamart.com/proddetail/steel-wire-ropes-15376507988.html

7 BIOGRAPHY

Bruno Polak was born on August 1, 1986 in Zagreb. He graduated from the Department of Biology at the Faculty of Science in Zagreb in 2015. During the studies, as a member of the Association of Biology Students (BIUS), he attended field studies on biodiversity and as a demonstrator participated in the practical part of the Zoology and Plant Physiology courses. Since 2015 he has been working in the Biophysics Laboratory at the Ruđer Bošković Institute (IRB) as an Associate on the Project (ERC) under the mentorship of prof. dr. sc. Iva Tolić. He was enrolled in the Postgraduate Study of Biology at the Faculty of Science in Zagreb. He was participating in research on biophysics of the cell, studying the architecture of the spindle and spatial organization of the microtubule bundles. During his work at the IRB, he participated in five international conferences ("Central European Genome Stability and Dynamics Meeting", 2016, Zagreb (presentation), 2016 ASCB Annual Meeting, San Francisco (poster), Gordon Research Conferences 2016 "Muscle & Molecular Motors ", Mount Snow, (poster), EMBL Symposia 2016" Microtubules: From Atoms to Complex Systems ", Heidelberg (poster)," Cold Spring Harbor Laboratory Symposium on Quantitative Biology, Chromosome Segregation & Structure ", 2017 Spring Harbor (poster)) and 1 workshop (ESF workshop - "Dynamics of the Cytoskeleton", Zagreb, Croatia (poster)). So far, he has published 3 papers in international scientific journals. In 2019 he received “2018 Branimir Jernej Foundation Award”- annual award for a publication in the fields of molecular biology, neurosciences and biomedicine published in 2018.

Publications:

1. Kajtez, J. *, Solomatina, A. *, Novak, M. *, Polak, B., Vukušić, K., Rudiger, J., Cojoc, G., Milas, A., Šumanovac Šestak, I., Risteski, P., Tavano, F., Klemm, A. H., Roscioli, E., Welburn, J., Cimini, D., Glunčić, M., Pavin, N., Tolić, I. M. (2016). Overlap microtubules link sister k-fibers and balance the forces on bi-oriented kinetochores. Nat. Commun. 7, 10298;

2. Polak, B. *, Risteski, P. *, Lesjak, S., and Tolić, I.M. (2017). PRC1-labeled microtubule bundles and kinetochore pairs show one-to-one association in metaphase. EMBO Rep. 18, 217-230;

3. Novak, M. *, Polak, B. *, Simunić, J. *, Boban, Z. *, Kuzmić, B. *, Thomae, A., Tolić, I.M., Pavin, N. (2018). The mitotic spindle is chiral due to torques within microtubule bundles. Nat Commun, 9 (1): 3571

*These authors contributed equally